C.P. No. 899

C.P. No. 899

MINISTRY OF AVIATION

AERONAUTICAL RESEARCH COUNCIL

CURRENT PAPERS

The Spectral Energy Balance in a Turbulent Mixing Layer

By

P. Bradshaw and D. H. Ferriss

LONDON: HER MAJESTY'S STATIONERY OFFICE

1967

Price 13s. 6d. net

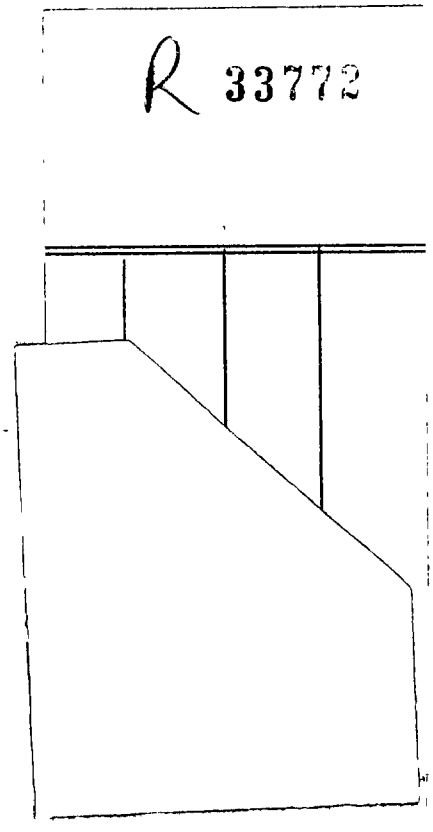
R 33772

C.P. No. 899*

March, 1965

The Spectral Energy Balance in a Turbulent Mixing Layer

- By -
P. Bradshaw and D. H. Ferriss

Measurements are presented of the spectral density of contributions to the turbulent energy balance as a function of longitudinal wave number. The energy transfer through the spectrum has been deduced, taking advantage of the apparent smallness of the pressure diffusion, and some of its components have been measured directly: transfer in the direction of decreasing wave number occurs in some parts of the flow because of the influence of the large eddies, which dominate several of the processes observed. The overall energy balance is also discussed.

List of Contents

1./

*Replaces N.P.L. Aero Report 1144 - A.R.C. 26 743

1. Introduction

The study of the turbulent energy balance is logically the next stage in the investigation of a turbulent flow after making the measurements of intensities, spectra and correlations which help to form one's basic ideas about the structure of the flow. The particular value of such a study is in formulating and testing hypotheses about the relation between the turbulent shear stress and the velocity field. It is well known, for instance, that the Prandtl mixing length relation can be given physical meaning, under highly restricted circumstances, by considering the energy-balance equation[1], and can be improved by an allowance for the effects of energy diffusion[2]. However, the ordinary energy-balance equation, relating production, dissipation, diffusion and advection, makes no use of any information about the eddy structure that one may have gleaned from the correlation measurements mentioned above, nor does it tell one very much more about the eddy structure. In this paper we have attempted to remedy these defects by considering the energy-balance equation for a given wave number and at a given position in the flow: we call this the "spectral energy balance". The overall energy balance expresses conservation of energy in a unit volume in physical space: the spectral energy balance expresses conservation of energy in a unit volume in physical space, for a given unit volume in wave number space. Roughly speaking, the terms in this equation are the spectral densities of the terms in the overall energy-balance equation together with extra terms representing energy transfer to the given wave number from all other wave numbers. As used in this paper "energy transfer" means transfer into a volume in wave-number space and <u>not</u> across a surface. Extra terms also arise because typical length and wave-number scales change in the x_1 direction, leading to a redistribution of energy among different wave numbers: they will be ignored in the discussion (though <u>not</u> in the calculations).

In isotropic turbulence, the spectral energy balance reduces to

$$(-\text{ rate of decay}) \;=\; \text{gain by energy transfer} - \text{dissipation} \qquad \ldots(1)$$

which can be further simplified, using the condition of isotropy, by integrating over the surface of a sphere of radius k in three-dimensional wave-number space (see Fig. 1) to get the energy balance for a given wave-number magnitude. This is the well-known equation[3]

$$\frac{\partial E(k)}{\partial t} \;=\; T(k) - 2\nu k^2 E(k) \qquad \ldots(2)$$

which is related to the Fourier transform of the von Kármán-Howarth equation for the velocity correlations. Various theoretical forms for the energy transfer rate $T(k)$ have been put forward and comparisons with experiment have been made by several workers, the most recent being Uberoi[4] who deduced $T(k)$ by difference from direct measurements of $E(k_1)$ behind a grid, deriving $E(k)$ as $-\frac{1}{2}k(\partial/\partial k_1)E(k_1)$. We have not been able to make any measurements in the locally-isotropic range in the present experiment because of the smallness of the spatial scales, so that we cannot make comparisons with the theoretical predictions for $T(k)$.

In shear flow, the anisotropy of the energy-containing turbulence makes a wave-number-magnitude spectrum less suitable, and it is far easier

experimentally/

experimentally to consider a one-dimensional spectrum (equal to the three-dimensional spectrum integrated over all values of the other two wave-number components), obtainable as the Fourier transform of correlations with separations in one co-ordinate direction only. We have chosen the longitudinal spectrum, partly because the well-defined "large eddies" in the mixing layer[5] are strongly periodic in the stream direction and partly because it is possible to represent the longitudinal wave-number spectrum of some of the less important terms by the frequency spectrum without gross error (in the present experiment we have done this only for some of the spatial diffusion terms). It does not seem to be profitable to consider a spectral energy balance entirely in terms of frequency.

We have measured the true wave-number spectra of the production and advection terms, and three of the nine energy-transfer terms, in the quasi-plane mixing layer of a 2 in. diameter jet at a Reynolds number $U_m x/\nu$ of 7×10^5 (U_m = 336 ft/sec, x = 4 in.): it was shown in Ref. 5 that the effects of axisymmetry are negligible at this distance from the nozzle and that the flow is to a good approximation self-preserving. The experimental arrangements were the same as in Ref. 5 and are more fully described in the unpublished version of that paper, NPL Aero Report 1054 (1963). The difficulties encountered in measuring the triple correlations are discussed in Appendix II.

We have not tried to measure the pressure-velocity spectra, which contribute to spatial diffusion and to interchange of energy between the velocity components but not to energy transfer from one wave number to another, at least in an incompressible fluid. We have not been able to measure the dissipation, but it is worth noting that, at a sufficiently high Reynolds number for the energy-containing and dissipating ranges of wave number not to overlap appreciably, the dissipation is nearly equal to the energy transfer through a one-dimensional wave number at the upper end of the energy-containing range. The dissipation could thus be deduced from a complete set of energy-transfer spectra without measuring correlations at sufficiently small separations to obtain the microscales: this would be unutterably tedious but it is possible with present-day hot-wire techniques, which is more than can be said for microscale measurements in a small-scale mixing layer.

The standard account of spectral representations of turbulence is Batchelor's (Ref. 3, Chapter 2 and part of Chapter 3). A less rigorous account which gives more of the practical details is that of Lumley and Panofsky[6], and a useful summary of elementary results for random processes is given by Goodman[7]. Treatises on communication theory, Brownian motion and so on provide some background material but care is needed to distinguish those results that are valid only for processes with normal (Gaussian) probability distributions.

2. The Overall Energy-Balance Equation

2.1 Description

The equation is obtained[8] by taking the momentum (Navier-Stokes) equation for the component of velocity in the x_i direction, multiplying by u_i averaging, assuming that the density is constant, and summing over $i = 1, 2, 3$. We also multiply by two to clear fractions: some authors omit this step. The equation can be divided into two parts, one expressing the balance of energy in the mean flow, which is not particularly informative in the present case, and one for the turbulent energy balance. The terms in the

latter,/

latter, which add up to zero (see Fig. 2(b)), and which are by custom taken as positive for loss of energy and negative for gain of energy, are

(i) the advection

$$U_1 \frac{\partial \overline{u_i^2}}{\partial x_1} + U_2 \frac{\partial \overline{u_i^2}}{\partial x_2}, \quad \text{or} \quad \left(\frac{U_2}{U_m} - \eta \frac{U_1}{U_m} \right) \frac{d\overline{u_i^2}/U_m^2}{d\eta}$$

in dimensionless, self-preserving form (see Notation: terms are summed over all values of implicitly repeated suffices) which is the net rate at which the mean flow convects turbulent energy out of a unit volume fixed in space: in most parts of the mixing layer the two terms are of the same sign and the same order of magnitude.

(ii) the production

$$2\,\overline{u_1 u_2} \left(\frac{\partial U_1}{\partial x_2} + \frac{\partial U_2}{\partial x_1} \right) + 2(\overline{u_1^2} - \overline{u_2^2}) \frac{\partial U_1}{\partial x_1}$$

$$\text{or} \quad \left[2 \frac{\overline{u_1 u_2}}{U_m^2} - 2\eta \frac{(\overline{u_1^2} - \overline{u_2^2})}{U_m^2} \right] \frac{dU_1/U_m}{d\eta} \quad \text{approximately.}$$

The first term is usually much the larger: if one considers the "energy equation" for the three components of the intensity separately before summing over i, it appears that this term contributes only to $\overline{u_1^2}$, but this is not a useful piece of information because pressure-velocity products $2\,\overline{p\,\partial u_i/\partial x_i}$ (whose sum is zero) immediately redistribute the energy. The production occurs because of the net extension of vortex lines and sheets by the mean velocity gradient, or, to take another point of view, by the working of mean velocity gradients against Reynolds stresses.

(iii) the diffusion

$$\frac{\partial}{\partial x_1} \left(2 \frac{\overline{pu_1}}{\rho} + \overline{u_i^2 u_1} \right) + \frac{\partial}{\partial x_2} \left(2 \frac{\overline{pu_2}}{\rho} + \overline{u_i^2 u_2} \right)$$

$$\text{or} \quad \frac{1}{U_m^3} \frac{d}{d\eta} \left(2 \frac{\overline{pu_2}}{\rho} + \overline{u_i^2 u_2} \right) - \eta \frac{d}{d\eta} \left(2 \frac{\overline{pu_1}}{\rho} + \overline{u_i^2 u_1} \right)$$

which is the rate at which energy is transferred to the other parts of the flow by pressure forces and by the velocity fluctuations themselves, $\overline{u_i^2 u_2}$ representing the transport of u_i^2 kinetic energy by u_2 fluctuations. The two terms in each pair of round brackets are of the same order of magnitude: triple velocity products can be measured by ordinary hot-wire techniques, but little progress has been made in measuring pressure fluctuations within the flow. The two derivatives with respect to η are of the same order of

magnitude/

magnitude but the factor η is small compared with unity, so that the first group of terms, representing diffusion in the x_2 direction, is much the larger. Its integral across the shear layer is zero: this is a useful check of experimental values obtained as the difference between the other terms in the energy balance.

(iv) the viscous term

$$2\nu \overline{\frac{u_i \partial^2 u_i}{\partial x_j^2}} = 2\nu \overline{\left(\frac{\partial u_i}{\partial x_j}\right)^2} \cdot [1 + O(1/Re)] = \epsilon[1 + O(1/Re)]$$

where ϵ is the dissipation, or rate of conversion of turbulent energy into heat (see p.29 of Ref. 8). The three-dimensional spectrum of $\overline{\left(\frac{\partial u_i}{\partial x_j}\right)^2}$ is k_j^2 times the spectrum of u_i^2 so that dissipation occurs in the smallest eddies. It is extremely difficult to measure $\overline{\left(\frac{\partial u_i}{\partial x_j}\right)^2}$ which must be obtained as $\left[\frac{\partial^2}{\partial r_j^2} \overline{(u_i(x)\, u_i(x + r_j))}\right]_{r_j=0}$ (see Section 3.3)

An overall energy balance for the mixing layer was derived by Townsend[8] from the measurement of Liepmann and Laufer[9]. The advection term was calculated by assuming that $\overline{u_3^2} = \frac{1}{2}(\overline{u_1^2} + \overline{u_2^2})$. The dissipation was obtained from measurements of $\frac{d^2}{dr^2} R_{11}(o,r,o)$ which showed that the microscale was constant from about $\eta = -0{\cdot}07$ to $\eta = 0{\cdot}06$: it was assumed that the microscale was constant right across the layer. The value of dissipation obtained seems to be too small, because the diffusion term (obtained by difference) does not integrate to zero: actually the advection term plotted in Ref. 8 appears to have the wrong sign in the outer part of the layer (the intensity should <u>increase</u> downstream along all streamlines except at $\eta = 0$) but the difference does not account for the discrepancy in the diffusion term.

We have been unable to measure the dissipation or even to see if the microscale is plausibly constant right across the layer, because of the very small scale of the flow: the length $2\pi(\nu^3/\epsilon)^{1/4}$, which is of the order of the wavelength of the smallest dissipating eddies, is only 0·002 in. near $\eta = 0$ at $x = 4$ in. This is about a tenth of the length of the hot wires, and corresponds to a frequency of 1 Mc/s which is about 20 times the limit of the anemometers. The dissipation rate is of the order of 10^6 times that in Uberoi's experiment on grid turbulence, and is as high as 20 percent of the maximum dissipation near the wall in a boundary layer with a free-stream velocity equal to U_m. Attempts in a larger-scale mixing layer in a makeshift open-jet tunnel merely exchanged inadequate spatial resolution for excessive integrating time. We have therefore been forced to use Liepmann and Laufer's measurements, increased by a factor determined by requiring the diffusion

(difference)/

(difference) term to integrate to zero. The dissipation is very nearly proportional to $(q^2)^{3/2}$ or $\tau^{3/2}$ except at the extreme edges of the flow, indicating that the dissipation length parameter is roughly constant across the flow. In the present experiment we have found that the sum of the frequency spectral densities of the three intensity components, $\phi_{ii}(\omega x/U_c)$, measured at $\omega x/U_c = 300$ and normalized by the mean square intensities (and supposed to be representative of $\overline{(\partial u_i/\partial x_1)^2}/\overline{u_i^2}$) rises from 54 units at $\eta = 0{\cdot}1$ to 82 units at $\eta = -0{\cdot}05$: nearer the inner edge of the layer where the fluctuations become irrotational the value decreases again. This result may be affected by the frequency response of the apparatus and it is doubtful if the spectral density at $\omega x/U_c = 300$ has much relation to the spectral density in the dissipating range at roughly ten times this frequency, so that the best course seems to be to use Laufer's data.

The only other major difficulty, which for various reasons held up this work for several months, was our inability to measure the U_2 (radial) component of mean velocity with any assurance of accuracy, a most infuriating snag in view of the comparative simplicity of the measurements. A plausible U_2-component profile, measured with a linearized X-probe was given in NPL Aero Report 1054, but it differed more than might have been expected from the theoretical profile obtained from the continuity equation on the assumption of exact self-preservation, so that we decided to repeat the measurement. However, we found that a spurious positive U_2 component was induced at the wires by the asymmetrical passage of the shear flow over the probe body, the streamlines being more highly curved on the side where the mean velocity was least. Exactly the same considerations account for the "displacement effect" of pitot tubes. We finally decided to use the theoretical profile to calculate the advection.

2.2 Results

The resulting energy balance is shown in Fig. 2(b). The rate of energy loss by diffusion near the centre of the layer is now somewhat smaller than the dissipation instead of being twice the dissipation as in Liepmann and Laufer's work, although the distribution of diffusion across the layer is still not known very accurately because of the approximations made in deriving the dissipation. We have measured $\overline{u_2^3}$ and $\overline{u_1^2 u_2}$ directly: the diffusion by triple correlations estimated by assuming $\overline{u_3^2 u_2} = \overline{u_2^3}$, is shown for comparison in Fig. 2(c). In view of the various approximations made in obtaining the energy balance, the most that one ought to say is that the pressure-velocity diffusion is fairly small compared with the triple-correlation diffusion, or $\overline{pu_2}/\rho\ \overline{q^2 u_2} \ll 1$.

This is a most interesting conclusion, for which one would like to have stronger evidence. Unfortunately, there are no reliable measurements of pressure-velocity correlations at a point in turbulent shear flow, but it is possible to make an indirect estimate of their magnitude which supports the above conclusion. Wooldridge and Willmarth[10] showed that the correlation coefficient between the pressure fluctuation at the surface beneath a boundary layer and the u_2 fluctuation within the flow was small compared with the correlation coefficient between p and $\partial u_2/\partial t$: cursory measurements in the near field of a jet[5] support this, and if the same is true for measurements of p

and/

and u_2 at the same point, then, since $\overline{p\,\partial u_2/\partial t}/\sqrt{\overline{p^2}.\overline{(\partial u_2/\partial t)^2}} < 1$ necessarily, $\overline{pu_2}/\sqrt{\overline{p^2}.\overline{u_2^2}} \ll 1$. It is known that $\sqrt{\overline{p^2}}/\rho\,\overline{q^2}$ is nearly unity in the boundary layer and in a wall jet (comparing the pressure fluctuation measurements of Lilley and Hodgson[11] with the turbulence measurements of Bradshaw and Gee[12]), so it is probably near unity in a mixing layer, or even less because of the absence of a wall. Since $\overline{q^2u_2}/\overline{q^2}\sqrt{\overline{u_2^2}}$ is of order unity in the mixing layer, it follows that $\overline{pu_2}/\rho\,\overline{q^2u_2} \ll 1$ to the same order that $\overline{pu_2}/\sqrt{\overline{p^2}.\overline{u_2^2}} \ll 1$.

The longitudinal diffusion, $\dfrac{\partial}{\partial x_1}(2\,\overline{pu_1}/\rho + \overline{q^2u_1})$, (Fig. 2(d)) is much smaller than the lateral diffusion, but the fact that it is even noticeable near the edges of the flow implies that the boundary-layer approximation is not very accurate in such a rapidly-spreading flow as the mixing layer.

The new energy balance data presented here are qualitatively the same as Liepmann and Laufer's and do not warrant much extra comment. The ratio of diffusion to dissipation in the central region is still extremely high and constitutes a useful argument against believers in local energy equilibrium of turbulent flows. The presence of large advection and diffusion terms at large negative η, where the production and dissipation are negligible, is even more noticeable here than at the high-velocity edge of a boundary layer or wake. This implies that the irrotational field near the edges of the flow is more intense, compared with the turbulence proper, than in other flows, because the strong, large eddies produce strong, large-scale irrotational fluctuations which penetrate well outside the fully-turbulent region. This argument does not conflict with the suggestions above that the pressure fluctuations within the turbulent flow are no larger, compared with the mean-square intensity, than in other types of shear layer.

3. The Spectral Energy-Balance Equation

This equation is derived from the Navier-Stokes equations in Appendix I and written out, almost in full, at the end of that Appendix. It is also derived, but not discussed, by Hinze[13]. The terms which correspond to the advection, production, diffusion and dissipation need no further explanation.

The usual convention for the sign of the energy transfer $T_{\ell ii}(k)$ is that it is positive when energy is entering the wave number interval k, $k + dk$ (see equations (1) and (2)). Thus, $T_{\ell ii}(k)$ is normally negative in the energy-containing range and positive in the dissipating range. The physical significance of the triple correlation

$$\overline{[u_\ell(\underset{\sim}{x}) - u_\ell(\underset{\sim}{x} + \underset{\sim}{r})]\,u_i(\underset{\sim}{x}).u_i(\underset{\sim}{x} + \underset{\sim}{r})}$$

from which $T_{\ell ii}(k)$ is derived, may be explained as the net rate of extension, of vortex lines and sheets contributing to the u_i covariance with separation $\underset{\sim}{r}$ (eddies larger than r), by a change in u_ℓ over the distance r. This extension (or contraction) is responsible for a transfer of energy from a given value of $\underset{\sim}{k}$ to higher or lower values. If $\underset{\sim}{r} = r_1$, $\underset{\sim}{k} = k_1$.

When/

When $\ell = 1$, the one-dimensional Fourier transform of $\frac{\partial}{\partial r_1}\overline{(u_1 - u_1')u_i u_i'}$ with respect to r_1 converts the operator $\partial/\partial r_1$ into a factor ik_1 (where symbol i denotes $\sqrt{-1}$ in contrast to suffix i) so that the spectral density T_{1ii} is simply k_1 times the Fourier sine transform of $\overline{(u_1 - u_1')u_i u_i'}$. When $\ell = 2$ or 3, however, the derivatives with respect to r_ℓ have to be obtained directly by measuring the correlation at a number of values of r_2 near $r_2 = 0$, for each of a range of values of r_1, which represents an unacceptable amount of work. In general, T_{2ii} and T_{3ii} are non-zero at zero wave number.

The experimental results for the spectral energy balance are shown in Figs. 4 - 6 and tabulated in Table 1. Further graphs and tables of the raw data are available from the authors. Some of the spectral densities are negative: although ordinary energy spectra are necessarily positive, these are energy flux spectra which can have either sign. Because of this, we have plotted $k_1 \phi(k_1)$ against $\log k_1$ instead of $\log \phi$ against $\log k_1$: this shows up the high-wave-number end of the spectra and has the additional advantage that equal areas represent equal contributions to the spectra, since $\phi(k_1)dk_1 = k_1 \phi(k_1)\, d(\log k_1)$. The energy spectrum is plotted logarithmically in Fig. 7 to aid in the identification of the different wave-number ranges. In the discussion below we shall use "diffusion", "production", etc., as abbreviations for "density of longitudinal wave-number spectrum of diffusion, production, etc.".

3.1 Production

Production spectra - or at least $\overline{u_1 u_2}$ spectra - have been measured previously by many workers, and the $u_1 u_2$ spectra in the mixing layer were discussed in Ref. 5. The most noticeable feature is the peak in the spectrum at the large-eddy wave number. Actually the peak in the wave-number spectrum is less pronounced than the peak in the frequency spectrum, which suggests that the large eddy frequency is more nearly constant than the large eddy wavelength, but inhomogeneity of the flow may be partly responsible, because there is a considerable difference between the $\overline{u_1 u_2}$ correlations with upstream and downstream separations. There is also a considerable difference between the $\overline{u_1 u_2}$ and $\overline{u_2 u_1}$ correlations, which is closely connected with the existence of large eddies in the form of mixing jets, either ingoing or outgoing. We have constructed arguments in favour of either direction, of which the slightly more plausible contradicts the deduction in Ref. 5 that the jets move outwards, but neither argument is very satisfactory.

3.2 Diffusion

In discussing the triple spectra representing diffusion it is necessary to distinguish between diffusion of the energy of a given group of eddies and diffusion by a given group of eddies. Let us consider

(i)/

(i) the (instantaneous) amplitude of u_i-component fluctuations with wave numbers between k and $k + dk$.

This is written as $\exp(ikr)\, dZ_i(k)$ which may be regarded[3] as a suitable extension of the Fourier representation $a \cos \omega t + b \sin \omega t$: we will abbreviate this to $u_i(k)$. It is the output of a "wave number filter" of bandwidth dk and centre frequency k.

(ii) the mean energy of $u_i(k)$.

This is $\overline{\exp(ikr)\, dZ_i(k) \,.\, \exp(-ikr)\, dZ_i(-k)} = \overline{[u_i(k)]^2}$ $= \overline{dZ_i(k)\, dZ_i(-k)} \doteq \overline{u_i^2}\, \phi_{ii}(k)$. The minus sign may be regarded as a mathematical device to obtain the modulus $a^2 + b^2$: $dZ_i^*(k) = dZ_i(-k)$.

(iii) the fluctuating "energy", with wave numbers between k' and $k' = dk'$, to which $u_i(k)$ contributes.

This is $\exp(ik'r)\, dZ_i(k)\, dZ_i(k' - k)$. (ii) is formally the mean of the integral of this over all k': this is the same as the integral of the mean, and the mean is zero unless $k' = 0$.

We may now distinguish between

(iv) the diffusion, by u_ℓ fluctuations, of the integral of (iii).

This is the "spectral density of diffusion" that appears in the energy balance at wave number k, and can be derived rigorously as the Fourier transform of $\dfrac{\partial}{\partial x_\ell} \overline{u_i(\underset{\sim}{x})\, u_\ell(\underset{\sim}{x})\, u_i(\underset{\sim}{x} + r_i)}$ (see Appendix I). The mean product of (iii) with $u_\ell(k'')$ is zero unless $k'' = k'$, when it is $\overline{dZ_i(k)\, dZ_i(k' - k)\, dZ_\ell(-k')}$, so that the final mean product is $\overline{dZ_i(k) \int_{k'} dZ_i(k' - k)\, dZ_\ell(-k')}$.

This may be written as $\overline{[\exp(ikr)\, dZ_i(k)] \left[\exp(-ikr) \int_{k'} dZ_i(k'-k) dZ_\ell(-k') \right]}$.

The second term in square brackets is seen, by analogy with (iii), to be the fluctuating product, with wave numbers between k and dk, of $u_i(k''')$ and $u_\ell(k'''')$, integrated over all k''' and k'''' (subject to the requirement $k''' + k'''' = k$). Thus it is the result of multiplying u_i by u_ℓ and then filtering out wave number k, so the mean product may be written $\overline{u_i(k)\, u_i u_\ell(k)}$, and the spectral density of diffusion is $\dfrac{\partial}{\partial x_\ell} \overline{(u_i(k)\, u_i u_\ell(k)}$ if the shape of the spectrum does not alter very quickly across the layer.

and/

and

(v) the diffusion, by $u_\ell(k)$, of the energy of u_i component fluctuations.

This can only be $\frac{\partial}{\partial x_\ell}\left(\overline{u_\ell(k)\, u_i^2(k)}\right)$: it is diffusion by a chosen group of eddies, as opposed to (iv) which is diffusion of a chosen group of eddies. When $i = \ell$ (iv) and (v) become the same and represent self-diffusion of a chosen group of eddies.

As is pointed out on pp.107-110 of Ref. 8, turbulent diffusion may be thought of as the sum of several processes. First there is diffusion by pressure forces, $\partial \overline{pu_i}/\partial x_i$, about which we know very little but which seems to be fairly small in the mixing layer. The main part of the energy diffusion in the mixing layer is apparently "bulk convection" by the large eddies, with some contribution from "gradient diffusion" at the lower wave numbers. These can be contrasted as respectively convection of small eddies by larger eddies and diffusion of larger eddies by small eddies, and compared with the diffusion of momentum, which is necessarily an interaction between different velocity components at the same wave number. Momentum diffusion is expected to decrease at high wave numbers, rather more quickly than the intensity does, because small eddies are less affected by the mean velocity gradient than larger eddies: by the simple arguments usually advanced in favour of local isotropy of the smallest eddies, we expect $R_{12}(k) \propto 1/k$ approximately. The measurements of Sandborn and Braun[14] exhibit this property but the results of Ref. 5 for the mixing layer are not sufficiently reliable at the higher wave numbers for any definite conclusion to be drawn. Gradient diffusion is expected to decrease even more quickly than this because the effective diffusivity depends in some way on the total intensity of all eddies with wave numbers smaller than k, (like the "effective viscosity" in Heisenberg's expression[3] for the spectral energy transfer), but in general bulk convection will decrease no faster than the intensity. The bulk convection in the high-intensity region of the mixing layer is extremely large and the diffusion exceeds the production for $k_1 x > 50$ approximately. The implications of this for the principle of local isotropy are discussed below. The diffusion of the very large eddies has to be regarded as gradient diffusion but is still effected chiefly by the large eddies. Since the large eddies are so intense the diffusion at very low wave numbers can exceed the production, leading to negative rates of energy transfer in the high-intensity region of the shear layer.

We can define the spectral equivalent of what Townsend calls the "bulk convection velocity" $\mathcal{V} \equiv \overline{u_i^2 u_2}/\overline{u_i^2}$, as $\mathcal{V}(k) \equiv \overline{u_i^2 u_2}\ \phi_{i2i}/\overline{u_i^2}\ \phi_{ii}$: this is not a spectral density in the ordinary sense and the symbol $\mathcal{V}(k)$ is merely a conventional sign. $\mathcal{V}(k)$ is to be regarded as the "propensity-to-be-diffused" of u_i eddies of wave number k, and not as a measure of the bulk convection velocity of u_2 eddies of wave number k.

The most interesting thing about the experimental results is that although the production spectrum has a noticeable peak at the large-eddy wave number (except in the outer part of the layer) the turbulent diffusion spectrum and $\mathcal{V}(k)$ do not: in fact $\mathcal{V}(k)$ (Fig. 10) has a minimum near the large eddy wave number except at $\eta = 0{\cdot}1$ where the large eddies have almost

disappeared/

disappeared from the intensity spectrum. We cannot say whether the same applies to the pressure diffusion but as $\frac{\partial}{\partial x_2}\overline{pu_2} \ll \frac{\partial}{\partial x_2}\overline{q^2 u_2}$ it is safe to conclude that the energy of the large eddies is not very strongly diffused. This is to be expected, because the large eddies are strongly periodic in the x_1 direction and, although it is convenient to think of them as outward-going "jets" followed by a larger-scale backflow this is more a model of the process of diffusion by the large eddies than a model of the large eddy motion itself, which is more like a lightly-damped wave: the large eddies are therefore rather coherent structures.

The large eddies are, it appears, responsible for much of the diffusion of the smaller-scale energy-containing eddies. We have not been able to define a quantity analogous to $\mathcal{V}(k)$ which would represent the "power-to-diffuse" of eddies of a given wave number, but the power of the large eddies to diffuse can be seen qualitatively from the measurements of $\overline{u_1^2(k)\, u_2(k)}$ in Fig. 9. This is an example of diffusion of type (v) - see beginning of this section - which represents the diffusion of u_1-component energy by u_2 fluctuations of wave number k: the peak at the large-eddy wave number is pronounced at $\eta = -0{\cdot}05$ and $0{\cdot}05$, but not at $\eta = 0$, where the mean square value $\overline{u_1^2 u_2}$ is nearly zero, or at $\eta = 0{\cdot}1$, where the large eddies have died out. $\overline{u_2^2(k)\, u_2(k)}$ belongs both to type (iv) and type (v) and represents self-diffusion of u_2 fluctuations: it has a slight peak at the large eddy wave number at $\eta = -0{\cdot}05$ only, so that even the u_2 component of the large eddies is not greatly diffused.

At $\eta = -0{\cdot}05$, the gain by diffusion is by far the largest term in the energy balance at low wave numbers. This is because $(\partial/\partial\eta)(\overline{u_1^2 u_2})$ is very large in this region and the u_1^2 spectrum contains a lot of energy at low wave numbers. $(\partial/\partial\eta)\,\overline{u_2^3}$ is much smaller. The approximation of $\overline{u_3^2 u_2}$ by $\overline{u_2^3}$ is likely to be least accurate in this region but a correction would, if anything, further increase the diffusion at low wave numbers. At $\eta = 0{\cdot}1$, on the other hand, the diffusion is much the largest term in the energy balance at high wave numbers, being chiefly composed of u_2-component energy: possibly the $\overline{u_3^2 u_2}$ term would again dominate nearer the outer boundary of the turbulent flow.

3.3 Dissipation and local isotropy

In Appendix I it is shown that if the dissipating eddies are isotropic the one-dimensional spectral density of dissipation at wave numbers much less than about $0{\cdot}2\left(\frac{\epsilon}{\nu^3}\right)^{1/4}$ is $4{\cdot}5\,(\nu\epsilon)^{3/4}$. It is necessary, therefore, to distinguish between the true one-dimensional spectrum $2\nu \iint k^2\, \Phi(\underset{\sim}{k})\, dk_2\, dk_3$, the wave-number-magnitude spectrum $2\nu\, k^2\, E(k)$, and the one-dimensional spectrum $15\nu\, k_1^2\, \phi_{11}(k_1) \equiv 15\nu\, k_1^2 \iint \Phi(\underset{\sim}{k})\, dk_2\, dk_3$ which is commonly used in discussion of experimental results but which is not the true dissipation spectrum although

it/

it integrates to the correct value if the dissipating eddies are isotropic so that $\epsilon = 15\nu\,\overline{(\partial u_1/\partial x_1)^2}$. Since in isotropic turbulence $E(k) = \frac{1}{2}k^3 \frac{d}{dk}\left[\frac{1}{k_1}\frac{d\phi_{11}}{dk_1}\right]_{k_1=k}$ - the factor $\frac{1}{2}$ appearing because ϕ_{11} is defined for positive wave numbers only - then if $\phi_{11}(k_1) = k_1^{-n}$, $E(k) = \frac{n(n+2)}{2}k^{-n}$: n normally increases to high values at high k_1, so $E(k)$ peaks at a very much higher value than $\phi_{11}(k_1)$ and the representation of the dissipation spectrum by $2\nu k_1^2\phi_{11}(k_1)$ gives a very pessimistic estimate of the separation between the production and dissipation ranges. In the present experiment $k_1^2\phi_{11}(k_1)$ reaches a maximum at $k_1 x \sim 300$ whereas Uberoi's results for the "universal" spectrum indicate that $k^2E(k)$ should reach a maximum at $k_1 x \sim 2500$.

We can use Uberoi's results for the "universal" dissipation spectrum, together with a wave-number-magnitude spectrum of production in the mixing layer (calculated on the basis of isotropy to give an order-of-magnitude answer) to show that the production is 100 times as large as the dissipation at a wave-number magnitude $kx = 100$ but that since the production is falling very rapidly the two become equal at $kx \simeq 250$ or $k(\nu^3/\epsilon)^{1/4} \simeq 0{\cdot}02$, where the dissipation is still less than a tenth of its maximum value. It follows that the production and dissipation ranges do not overlap significantly: it is of course obvious from the Reynolds number independence of the flow ($\nu_e/\nu \gg 1$) that there is not much dissipation in the energy-producing range. Actually, since $\nu_e/\nu \equiv \overline{u_1u_2}/\nu\,(\partial u_1/\partial x_2)$ and production $\simeq$ dissipation, $\nu_e/\nu \simeq (\overline{u_1u_2})^2/\nu\epsilon$. Putting $\epsilon = (\overline{q^2})^{\frac{3}{2}}/L_\epsilon$ and $\overline{u_1u_2} = 0{\cdot}15\,\overline{q^2}$, an almost universal value, we have $\nu_e/\nu = 0{\cdot}15\,(\overline{q^2})^{\frac{1}{2}}L_\epsilon/\nu$. Alternatively, if $\epsilon = 5\nu\,\overline{q^2}/\lambda^2$, $\frac{\nu_e}{\nu} = 0{\cdot}0045\left[\frac{(\overline{q^2})^{\frac{1}{2}}\lambda}{\nu}\right]^2$, where λ is the microscale $[\overline{u_1^2}/\overline{(\partial u_1/\partial x_1)^2}]^{\frac{1}{2}}$. Now $(\overline{q^2})^{\frac{1}{2}}L_\epsilon/\nu$ is essentially the same as the Reynolds number $u\ell/\nu$ used by Batchelor[3] in his discussion of the Kolmogorov equilibrium theory. His condition for the existence of an equilibrium range is $k_o \ll (\epsilon/\nu^3)^{\frac{1}{4}}$ where k_o is the centroid of the intensity spectrum and $(\epsilon/\nu^3)^{\frac{1}{4}}$ is the wave number at which viscous and inertial forces become comparable. This condition, which is weaker by about a factor of 5 than the condition $k_o \ll k_\epsilon$ where k_ϵ is the centroid of the dissipation spectrum, can be written as $\left(\frac{u\ell}{\nu}\right)^{3/4} \gg 1$. Therefore $k_o \ll k_\epsilon$, which is the condition for local equilibrium or "universality" of most of the dissipation spectrum, reduces to $(\nu_e/\nu)^{\frac{3}{4}} \gg 1$ very nearly. Batchelor's condition for the existence of an appreciable inertial subrange is $\left(\frac{u\ell}{\nu}\right)^{3/8} \gg 1$ or

2/

$2\left(\frac{\nu_e}{\nu}\right)^{3/8} >> 1$. Stewart and Townsend[15] derive as the condition for an inertial subrange that the decay rate (or production) at a wave-number magnitude of $0{\cdot}1\ (\epsilon/\nu^3)^{\frac{1}{4}}$ shall be less than 1/10 of the dissipation at the same wave number. This replaces ">>" by "> 100 ×". For purposes of comparison with other flows we note that in the outer region of a boundary layer $U_1\delta_1/\nu_e \simeq 75$ so that $\nu_e/\nu = \frac{1}{75}\frac{U_1\delta_1}{\nu}$ and that in the region of maximum production in any turbulent wall layer, at $u_\tau y/\nu \simeq 12$, $\nu_e/\nu = 1$ by definition. Thus

	$(\nu_e/\nu)^{\frac{3}{4}}$ or $\frac{1}{5}\left(\frac{u\ell}{\nu}\right)^{\frac{3}{4}}$	$2(\nu_e/\nu)^{\frac{3}{8}}$ or $\left(\frac{u\ell}{\nu}\right)^{\frac{3}{8}}$
Present experiment	200	30
Uberoi[4] (grid turbulence)	8	6
Grant[16] (tidal channel)	$0[4 \times 10^4]$	0[400]
Boundary layer at $U_1\delta_1/\nu = 10^4$	40	13
Wall layer at $u_\tau y/\nu = 12$	1	2
Wake[8] at $\frac{U_1 d}{\nu} = 8400$	47	14

It follows that Grant's is the only experiment in which an inertial range exists, that the only experiment on laboratory scale in which the dissipation is at all accurately isotropic is the present one*, and that Laufer's estimate of dissipation in the wall layer based on the assumption that some of the derivatives are related as in isotropic turbulence is likely to be very inaccurate (in fact the energy balance results shown in Fig. 9.13 of Ref. 8 imply a pressure-velocity correlation coefficient $\overline{pu_2}/(\overline{p^2}.\overline{u_2^2})^{\frac{1}{2}}$ of 2·5 at $u_\tau y/\nu = 10$ which is absurd). The most thorough investigation of local isotropy is Townsend's[8,17] study in the wake at $U_1 d/\nu = 8400$: he showed that the derivatives $\overline{(\partial u_i/\partial x_1)^2}$ and their flatness factors were isotropically related to within about 15 percent except near the extreme edges of the flow. However it can be seen from Fig. 7.20 of Ref. 8 that the diffusion in the wake (obtained by difference) fails to integrate to zero, indicating that if the production and advection were correctly measured the dissipation (evaluated on the assumption of isotropy) is too low by roughly 20 percent. Also, the experimental "verifications" of the well-known prediction $\phi \sim k^{-5/3}$ for the inertial range are seen to be worthless (except of course for Grant's): Sandborn

and/

---

*except for an experiment in a circular jet by Gibson (J.Fluid Mech.15, 161(1963)) in which only spectra were measured

and Braun point out that in a typical spectrum the exponent n takes all values between 0 and 7, and it was remarked in Ref. 5 that $n \simeq 5/3$ in the mixing layer where $R_{12}(k) \equiv \phi_{12}/(\phi_{11}\phi_{22})^{\frac{1}{2}}$ is still near its maximum value. The various observations that $R_{12}(k)$ tends to zero at high k do not guarantee that the energy spectrum becomes isotropic at such wave numbers, because the energy transfer spectrum only becomes isotropic some time after the production goes to zero. An additional complication occurs in flows such as the mixing layer where diffusion and advection are appreciable because both these terms go to zero at high wave number no more quickly than the intensity (see Section 3.2) and therefore much more slowly than the production. The effect on the energy-balance spectrum at high wave numbers is to add a term proportional to the spectral density of intensity. Since the diffusion integrated across the shear layer is zero it follows that the predictions of the Kolmozorov theory for the inertial subrange could only be fulfilled as an average across the layer, although there is no immediate reason to suppose that diffusion causes any difference between the spectral densities of the three intensity components. The effect of energy loss by diffusion in the dissipation range of wave numbers is very small: if we assume that the loss of energy is $\frac{\partial}{\partial x_2}\overline{q^2 u_2}\, E(k)$ - which gives the correct result for the overall diffusion - then the ratio of this to the maximum dissipation $2\nu k^2 E(k)$ at $k = 0{\cdot}2(\epsilon/\nu^3)^{\frac{3}{4}}$ is $20\ \nu/U_m x$ near $\eta = 0$ in the mixing layer.

Consideration of the energy-balance spectrum is of some help in understanding the phenomenon of "spottiness" of dissipation (see Ref. 3, pp.184-186, and Ref. 18). $\partial u/\partial t$ and the higher derivatives (that is, the high-frequency fluctuations) seem to have almost an "on-off" character, being heavily modulated at frequencies low compared with those that contribute most to the derivative, and this seems somehow contrary to Kolmogorov's hypothesis that the motion in the equilibrium range, which includes the dissipation range, is determined statistically by the dissipation rate and the viscosity. However (as Landau seems to have realized without the stimulus of the experimental results) the short-term average energy transfer across a wave number, k', say, at the bottom of the equilibrium range must, since it is an integral over all lower wave numbers, fluctuate with a spectrum which has an appreciable density at all wave numbers from zero up to the limit imposed artificially by whatever we choose as a "short-term average", presumably a distance of the order of 1000/k'. Thus the averaging distance needed to obtain a mean value of the dissipation is the same as the averaging distance needed to obtain a mean spectral density of the largest energy-containing eddies: this is a difficulty common to all attempts to obtain short-term averages of random processes, and occurs in exactly the same form in atmospheric turbulence. Even the artificial "large-eddy-plus-isotropic" model, which we have used for the mixing layer, implies that the dissipation rate at a point in space will vary according to the phase of the large eddy at that point. Kraichnan[19] has recently remarked that an Eulerian representation is much inferior to a Lagrangian representation for considering the effect of the larger eddies on the small eddies: unfortunately it is not at present possible to derive much useful quantitative information from a Lagrangian representation. Oboukhov[18] has calculated the (small) modification to Kolmogorov's form for the correlation and spectrum consequent on the assumption of a logarithmically-normal probability distribution for the dissipation averaged in x-space over a sphere of diameter equal to the correlation separation (the simplest possible three-dimensional average).

Physically,/

Physically, it seems that dissipation occurs most strongly in regions of x-space where the velocity gradients in the energy-containing structure are greatest. (These regions would be true vortex lines and sheets if it were not for the diffusive action of viscosity.) It follows once more that a mean value of dissipation can only be obtained by averaging over a distance (or volume) typical of the energy-containing eddies.

It may be noted that the close association between patches of high dissipation and eddies of high intensity implies that each group of small eddies is convected at the same speed as the energy-containing eddy that is its spectral ancestor. Therefore we must not invoke local isotropy to "prove" that the small eddies are convected at the speed of the fluid.

3.4 Energy transfer

The difference term in the spectral energy balance (Fig. 6) is the sum of the pressure diffusion and the energy transfer: since the overall pressure diffusion seems to be small compared with the velocity diffusion except in the outermost part of the layer it is likely that the same applies to the spectral densities, so we may take the difference term as a fair approximation to the energy transfer except at $\eta = 0{\cdot}1$ (where indeed the difference term appears implausibly large compared to the directly-measured part of the energy transfer). The scatter in the plotted points is almost entirely due to the behaviour of the terms representing spectral transfer due to inhomogeneity (Fig. 5): the factor $(1 + d \log\phi/d \log k_1 x)$ changes rapidly near $k_1 x = 10$ and is difficult to obtain accurately by graphical differentiation. The difference between the main terms shown in Fig. 4 is well-behaved.

The most striking feature is that the energy transfer goes positive at low wave numbers near $\eta = 0$, indicating that energy is being transferred from high wave numbers to low ones to make up for the diffusion of low-wave-number energy by the large eddies. The difference term also goes slightly negative at $\eta = 0{\cdot}1$,but this is most probably a result of approximating the diffusion part of the spectral transfer due to inhomogeneity by the velocity diffusion alone (Fig. 5(d)). Since the intensity increases very rapidly with wave number to reach a peak at the large eddy wave number it is entirely plausible that energy should be transferred towards low wave numbers, although the physical mechanism is not immediately clear. Another well-known example of reversed transfer is in the development of a continuous turbulence spectrum from a sinusoidal Tollmien-Schlichting wave, but in general vortex stretching by diffusion processes implies energy transfer to higher wave numbers. It is necessary to note that we are considering only the k_1 wave-number component so that we cannot rigorously prove that energy is being transferred to smaller wave-number magnitudes but this seems very likely a priori. Some of the directly-measured components of the energy transfer also go negative near $\eta = 0$ at low wave numbers (being necessarily zero at zero wave number) but this may be due to inaccuracy of measurement of the triple correlations at large separation. The u_1-component energy transfer (Fig. 6(e)) is the most reliable; the negative region is only noticeable for $\eta < 0{\cdot}05$, which is in line with the behaviour of the "difference" term.

The peak wave number of the plotted quantity, $k_1 x$ times the difference term, increases with increasing η because of the behaviour of the diffusion, which is discussed in Section 3.2: it is implied that the energy transferred is predominantly that of the u_1 component at $\eta = -0{\cdot}05$ and

of/

of the u_2 and u_3 components at $\eta = 0{\cdot}1$, but we cannot make any deductions about the isotropy or otherwise of the integrated energy transfer at the top end of the energy-containing range, because of the pressure-velocity correlations $\overline{p\,\partial u_i/\partial x_i}$ which exchange energy between the components at a given wave number. The directly-measured part of the energy transfer has a proportionately greater density in the high wave numbers at $\eta = 0{\cdot}1$ than at the other stations but the effect is much less noticeable than in the energy transfer obtained by difference, simply because the directly-measured part goes to zero at zero wave number. For the same reason, the general shape of the directly-measured part bears little resemblance to that of the difference term: this does not necessarily indicate a gross error in the measurement of either.

4. The Convection Velocity

It was shown in Ref. 5 that the convection velocities of the u_1 and u_2 components were different from each other as well as being different from the mean velocity of the fluid: the former effect was ascribed to the strong irrotational field, which is convected at the mean speed of the fluid in the high-intensity region and contributes a large part of the u_2 fluctuation near the edges of the layer, but it is certain that the convection velocity of the rotational fluctuations varies with wave number and, as remarked above, the dissipating eddies are not necessarily convected at the mean speed of the fluid. These effects are a considerable nuisance experimentally but do not require any modifications to our theoretical concepts: the most important consequences are in the calculation of the noise emitted by convected turbulence.

The differences between the frequency spectra and the transforms of the correlations with downstream separations, when compared on scales of $\omega x/U_c$ and $k_1 x$ where U_c is the overall convection velocity, are chiefly the results of inhomogeneity of the flow: in a boundary layer, which grows more slowly in the x_1 direction, the differences are much less. We cannot derive any useful information about the variation of convection velocity with wave number from the comparison, and indeed any detailed discussion requires care in the definition of "convection velocity" at a given wave number, for which there are several plausible but slightly different choices based on various integrals of the (k_1, ω) spectrum: these are discussed by Wills[20].

We have measured complete (k_1, ω) spectra only for the u_1 component which is much less interesting than the u_2 component. The (k_1, ω) spectrum at $\eta = -0{\cdot}05$, (Fig. 11), plotted as contours of spectral density in the $(\omega/k_1, k_1)$ plane to show the distribution of phase velocity ω/k_1 for each wave number, has a maximum at $\omega/k_1 U_m \simeq 0{\cdot}72$, $k_1 x \simeq 7$: the overall convection velocity is about $0{\cdot}82\ U_m$ and the mean velocity $0{\cdot}92\ U_m$. The position where $[\partial\phi/\partial\omega/k_1]_{k_1=\text{const}} = 0$ remains near $\omega/k_1 U_m = 0{\cdot}72$ until $k_1 x \simeq 20$ and then moves to higher values, reaching the approximate velocity of the fluid by $k_1 x \simeq 100$: this shows up the division of the turbulence into a group of strong large eddies and a nondescript "background" of more nearly isotropic turbulence (probably the peak in the (k_1, ω) spectrum, and also in the k_1 spectrum at $\eta = -0{\cdot}05$, occurs at a lower k_1 than the large eddy wave number - $k_1 x = 11$ - because the u_1 component of the large eddy motion is superimposed on a falling spectrum like $\phi_{11}(k_1 x)$ at $\eta = 0{\cdot}1$ where the large eddy motion has almost disappeared). The same features can be seen, less markedly, in the (k_1, ω) spectrum at $\eta = 0$ published by Wills[20].

5./

5. Conclusions

1. The loss of energy by diffusion from the high-intensity region of a mixing layer is nearly equal to the loss by dissipation, showing that the layer is far from a state of local energy equilibrium. The diffusion by pressure fluctuations, $\partial \overline{pu_2}/\partial x_2$, is much less, in most parts of the layer, than the non-linear diffusion $\frac{1}{2}\partial \overline{u_1^2 u_2}/\partial x_2$. The longitudinal diffusion $\frac{1}{2}\partial \overline{u_1^2 u_1}/\partial x_1$ is as much as 10 percent of the lateral diffusion near the edges of the flow.

2. The energy transfer through the spectrum has been obtained by difference from the wave-number spectra of the other terms in the energy balance equation, and some of its components have been measured directly. In the low-wave-number range, in the high-intensity region of the shear layer, the transfer is towards lower wave numbers because of the large energy losses by diffusion, for which the "large eddies" are chiefly responsible.

3. The diffusion spectrum goes to zero at high wave number no more quickly than the intensity spectrum, in contrast to the production spectrum: the concepts of local isotropy therefore require modification, but the effect on the dissipating eddies is very small at high Reynolds numbers.

4. The condition for isotropy of dissipating eddies in a turbulent shear flow can be written as $(\nu_e/\nu)^{\frac{3}{4}} \gg 1$ where ν_e is the effective eddy viscosity. $(\nu_e/\nu)^{\frac{3}{4}}$ is 200 in the present experiment, 50 in the wake where the components of $\overline{(\partial u_i/\partial t)^2}$ differed by up to 15 percent, 40 in the outer part of a turbulent boundary layer at $U_1\delta_1/\nu = 10^4$ and unity in the region of maximum production in a turbulent wall layer ($u_\tau y/\nu \doteq 12$). It follows that assumptions of some or all of the results of local isotropy are not very accurate in laboratory shear flows and become completely untenable near a wall. Consideration of the processes of energy transfer up the spectrum show that the locally isotropic part of the turbulence is not necessarily convected at the mean speed of the fluid.

5. The (lateral) "bulk convection velocity" at a given wave number, $\overline{u_1^2 u_2}(k)/\overline{u_1^2}(k)$ has a noticeable minimum in the range of wave numbers occupied by the large eddies, indicating that they are diffused less than the rest of the turbulence, although they are responsible for much of the diffusion of the rest of the turbulence.

6. The dissipation can be inferred from measurements of the energy transfer through a wave number at the top of the energy-containing range. In principle, this avoids the wire-length and frequency-response troubles encountered in attempts to measure the microscales, but measurements of the complete energy transfer would be very tedious.

7. Measurements of the pressure fluctuations within the flow would be of great help in understanding the turbulence structure.

6./

6. Acknowledgements

We are grateful to Dr. J. Laufer of J.P.L. for a helpful discussion, and to Dr. W. C. Reynolds of Stanford University for many useful comments on the draft manuscript of this paper. We are indebted to Dr. J. A. B. Wills for permission to reproduce Fig. 11. Mr. R. F. Johnson designed and maintained much of the electronic apparatus. Mr. G. K. Knight helped in the experimental work. Miss J. Dickerson operated the computer and Miss L. M. Esson performed further manual calculations, cross-plotting and graphical differentiation, of a tediousness second only to that of the experimental work.

7. Notation (infrequently-used symbols are defined in the text)

$E(k)$ wave-number-magnitude energy spectrum (see p.2)

i $\sqrt{-1}$

$\underset{\sim}{k}$ wave-number vector, components k_i, $i = 1, 2, 3$

k wave-number magnitude $(k_1^2 + k_2^2 + k_3^2)^{\frac{1}{2}}$

p static pressure

$\overline{q^2} \equiv \overline{u_i^2} \equiv \overline{u_1^2} + \overline{u_2^2} + \overline{u_3^2}$

$R_{ij}(\underset{\sim}{r})$ covariance $\overline{u_i(\underset{\sim}{x})\, u_j(\underset{\sim}{x} + \underset{\sim}{r})}$

$\underset{\sim}{r}$ separation vector, components r_i

$T_{\ell ii}(k_1)$ Fourier transform of $\left\{ \dfrac{\partial}{\partial r_\ell} \overline{[u_\ell(\underset{\sim}{x}+\underset{\sim}{r}) - u_\ell(\underset{\sim}{x})]u_i(\underset{\sim}{x}+\underset{\sim}{r})u_i(\underset{\sim}{x})} \right\}_{r=r_1}$ (see Appendix I)

U_c convection velocity

U_i x_i-component of mean velocity

U_m maximum value of U_1, 336 ft/sec nominal

u_i x_i-component of fluctuating velocity

$u_i(k_1) \equiv e^{ik_1 r_1} dZ_i(k_1)$ elementary wave: output of "wave-number filter" (see p.9)

x distance from nozzle to measurement station, 4 in.

$\underset{\sim}{x}$ position vector, components x_i. Origin at nozzle lip.

$dZ_i(k_1)$ Fourier amplitude increment: $\int_{-\infty}^{\infty} e^{ik_1 r_1} dZ_i(k_1) = u(r_1)$

δ/

δ shear layer thickness

ϵ dissipation

$\eta \equiv x_2/x$

ν kinematic viscosity

ρ density

τ shear stress

$\Phi_{ij}(\underset{\sim}{k})$ three-dimensional spectral density of $\overline{u_i u_j}$

$\phi_{ij}(k_1)$ one-dimensional spectral density of $\overline{u_i u_j}$, $\overline{u_i(k_1)\, u_j(k_1)}$:

$$\int_0^\infty \phi_{ij}(k_1)dk_1 = 1$$

$\phi_{ij,\ell m}$ $\overline{[u_i u_j](k_1)[u_\ell u_m](k_1)}$

ω frequency

Suffices i, j, ℓ, m. values 1, 2, 3. Repetition denotes summation except that multiple suffices to a single variable such as ϕ_{ii} are ignored, so that $\overline{u_i^2}\,\phi_{ii} = \overline{u_1^2}\,\phi_{11} + \overline{u_2^2}\,\phi_{22} + \overline{u_3^2}\,\phi_{33}$.

$\bar{F}$ time or ensemble average of F

$\underset{\sim}{F}$ vector F

F* complex conjugate of F

References/

References

No.	Author(s)	Title, etc.
1	G. K. Batchelor	Note on free turbulent flows, with special reference to the two-dimensional wake. J. Aero. Sci. 17, 441 (1950).
2	A. A. Townsend	Equilibrium layers and wall turbulence. J. Fluid Mech. 11, 97 (1961).
3	G. K. Batchelor	The theory of homogeneous turbulence. Cambridge (1956).
4	M. S. Uberoi	Energy transfer in isotropic turbulence. Phys. Fluids 6, 1048 (1963).
5	P. Bradshaw, D. H. Ferriss and R. F. Johnson	Turbulence in the noise-producing region of a circular jet. J. Fluid Mech. 19, 591 (1964).
6	J. L. Lumley and H. A. Panofsky	The structure of atmospheric turbulence. Wiley (1964).
7	F. O. Goodman	A summary of the theory of random processes. R.A.E. Tech. Note CPM.73 (1964).
8	A. A. Townsend	The structure of turbulent shear flow. Cambridge (1956).
9	H. W. Liepmann and J. Laufer	Investigation of free turbulent mixing. N A C A Tech. Note 1257 (1947).
10	C. E. Wooldridge and W. W. Willmarth	Measurements of the correlation between the fluctuating velocities and the fluctuating wall pressure in a thick turbulent boundary layer. AGARD Report 456 (1963).
11	G. M. Lilley and T. H. Hodgson	On surface pressure fluctuations in turbulent boundary layers. AGARD Report 276 (1960).
12	P. Bradshaw and M. T. Gee	Turbulent wall jets with and without an external stream. A.R.C. R.& M.3252 (1960).
13	J. O. Hinze	Turbulence. McGraw-Hill (1959).
14	V. A. Sandborn and W. H. Braun	Turbulent shear spectra and local isotropy in the low-speed boundary layer. N A C A. T.N.3761 (1956).

15/

No.	Author(s)	Title, etc.
15	R. W. Stewart and A. A. Townsend	Similarity and self-preservation in isotropic turbulence. Phil. Trans. Roy. Soc. A 243, 359 (1951).
16	H. L. Grant, R. W. Stewart and A. Moilliet	Turbulence spectra from a tidal channel. J. Fluid Mech. 12, 241 (1962).
17	A. A. Townsend	Local isotropy in the turbulent wake of a cylinder. Aust. J. Sci. Res. A 1, 161 (1948).
18	A. M. Oboukhov	Some specific features of atmospheric turbulence. J. Fluid Mech. 13, 77 (1962).
19	R. H. Kraichnan	Kolmogorov's hypotheses and Eulerian turbulence theory. Phys. Fluids 7, 1723 (1964).
20	J. A. B. Wills	On convection velocity in turbulent shear flows. J. Fluid Mech. 20, 417 (1964).
21	T. von Kármán and L. Howarth	On the statistical theory of isotropic turbulence. Proc. Roy. Soc. A 164, 192 (1938).
22	J. L. Lumley	Spectral energy balance in wall turbulence. Phys. Fluids 7, 190 (1964).

APPENDIX I/

APPENDIX I

Derivation of the Spectral Energy-Balance Equation

Von Kármán and Howarth[21] first derived the equation for the rate of change with respect to time of the covariance $\overline{u_i(\underset{\sim}{x})\, u_j(\underset{\sim}{x}+\underset{\sim}{r})}$ in decaying isotropic turbulence. The derivation for general homogeneous turbulence is given by Batchelor (Ref. 1, p.79) and others. For $\underset{\sim}{r} = 0$ the equation gives the time rate of decay of kinetic energy. In statistically stationary shear flow the rate of decay is zero and the dissipation is balanced by production: spatial diffusion and advection terms also appear. The derivation of the equation for $\overline{u_i(\underset{\sim}{x})\, u_j(\underset{\sim}{x}+\underset{\sim}{r})}$ is consequently more complicated than in the isotropic case.

Following Batchelor we write down the Navier-Stokes equation for $u_i(\underset{\sim}{x})$ and for $u_j(\underset{\sim}{x}+\underset{\sim}{r})$, multiply the first by $u_j(\underset{\sim}{x}+\underset{\sim}{r})$ and the second by $u_i(\underset{\sim}{x})$, and add to obtain an equation for $\dfrac{\partial\, \overline{u_i(\underset{\sim}{x})\, u_j(\underset{\sim}{x}+\underset{\sim}{r})}}{\partial t}$ (this being identical with $\overline{u_j(\underset{\sim}{x}+\underset{\sim}{r})\dfrac{\partial u_i(\underset{\sim}{x})}{\partial t}} + \overline{\dfrac{u_i(\underset{\sim}{x})\,\partial u_j(\underset{\sim}{x}+\underset{\sim}{r})}{\partial t}}$). Equating this term to zero, denoting $\underset{\sim}{x}+\underset{\sim}{r}$ by $\underset{\sim}{x}'$, $u_i(\underset{\sim}{x})$ by u_i and $u_j(\underset{\sim}{x}+\underset{\sim}{r})$ by u_j' for brevity, and noting that since u_i is independent of $\underset{\sim}{x}'$ then u_i can be taken inside any terms operated on by $\partial/\partial x'$, and so on, we obtain

$$0 = \frac{\partial\, \overline{u_i u_j'}}{\partial t} = -\frac{\partial}{\partial x_\ell'}\,\overline{(u_i u_j' u_\ell')} - \frac{\partial}{\partial x_\ell}\,\overline{(u_i' u_j u_\ell)} - \frac{1}{\rho}\left(\frac{\partial\, \overline{pu_j'}}{\partial x_i} + \frac{\partial\, \overline{p' u_i}}{\partial x_j'}\right)$$

$$+ \nu\,\left(\overline{u_i\, \nabla_{x'}^2\, u_j'} + \overline{u_j'\, \nabla_x^2\, u_i}\right) \qquad \ldots(A.1.1)$$

where the first two terms on the right are understood to be summed over $R = 1, 2, 3$ (we use suffix ℓ instead of the k used by Batchelor, to avoid confusion with wave number) and $\nabla_x^2 = \dfrac{\partial^2}{\partial x_\ell^2}$. It may be noted that this equation does not immediately reduce to the one-point energy equation if we put $j = i$ and $r = 0$, because $\partial/\partial x_\ell'$ is evaluated for $\underset{\sim}{x}$ = constant and not $\underset{\sim}{r}$ = constant. If we now put $j = i$ so as to obtain an energy equation for the covariance $\overline{u_i(\underset{\sim}{x})\, u_i(\underset{\sim}{x}+r_1)}$, the pressure terms simplify to

$$\frac{\partial\, \overline{pu_i'}}{\partial x_i} + \frac{\partial\, \overline{p' u_i}}{\partial x_i'}$$

and the viscous term becomes

2ν/

$$2\nu \left[\nabla^2 \overline{u_i(\underset{\sim}{x})\, u_i(\underset{\sim}{x} + \underset{\sim}{r})} \right]_{r=r_1} \neq 2\nu\nabla^2 \overline{u_i(\underset{\sim}{x})\, u_i(\underset{\sim}{x} + r_1)}$$

where $\nabla^2 = \dfrac{\partial^2}{\partial r^2}$. This is equal to the dissipation if the dissipating eddies are small compared with the width of the flow - that is, if the Reynolds number is high. Neither the pressure term nor the viscous term has been measured directly in the present experiment, but the qualitative behaviour of the dissipation spectrum is of some interest and is discussed below.

The triple products fall into several groups, since we see that

$$\frac{\partial}{\partial x'_\ell} \overline{u_i u'_i u'_\ell} + \frac{\partial}{\partial x_\ell} \overline{u_i u'_i u_\ell} = \left[\frac{\partial}{\partial r_\ell} \overline{u_i u'_i u'_\ell} \right]_{x_\ell = \text{constt.}} + \left[\frac{\partial}{\partial x_\ell} \overline{u_i u'_i u_\ell} \right]_{\substack{x'_\ell = \text{constt.} \\ r_\ell \neq \text{constt.}}}$$

$$= \left[\frac{\partial}{\partial r_\ell} \left(\overline{u_i u'_i u'_\ell} - \overline{u_i u'_i u_\ell} \right) \right]_{x_\ell = \text{constt.}} + \left[\frac{\partial}{\partial x_\ell} \overline{u_i u'_i u_\ell} \right]_{r_\ell = \text{constt.}} \qquad \ldots (A.1.2)$$

The first two terms in the final expression, which may be further simplified and reduced to dimensionless form as $\dfrac{x}{U_m^3} \dfrac{\partial}{\partial r_\ell} \overline{(u'_\ell - u_\ell) u_i u'_i}$, represent the energy transfer between eddies of different sizes and are of the same form as in homogeneous turbulence where one can make the simplifications $\dfrac{\partial}{\partial x_\ell} = -\dfrac{\partial}{\partial r_\ell}$ and $\dfrac{\partial}{\partial x'_\ell} = \dfrac{\partial}{\partial r_\ell}$ at once.

The last term in equation (A.1.2) represents the effects of inhomogeneity and, remembering that u_i includes the mean velocity as well as the fluctuation, we can see that it includes the production, advection and velocity-diffusion terms. It is written out in full, but not discussed, by Hinze (Ref. 13, p.257). The physical significance of the various terms, and the approximations it is legitimate to make, are seen more clearly by discussing the terms separately. The transformation from the correlation equation to the spectral energy balance for a given one-dimensional wave number k_1 is now performed by putting $\underset{\sim}{r} = r_1$ and taking the one-dimensional Fourier transform. This is straightforward and will not be written down explicitly. Because of the inhomogeneity of the flow the correlations are not exactly even functions of r_1, so the transforms have small imaginary parts. We choose to consider only the real part, which would appear alone in a homogeneous flow: the imaginary part does not include all the effects of inhomogeneity - the advection spectrum, for instance, is nearly real. Also, slight difficulties arise because the correlations are non-separable functions of k_1 and x_2 so

that/

that if $\phi(k_1, x_2) = \frac{2}{\pi}\int R(r_1, x_2) \cos k_1 r_1 \, dr_1$ then $\partial\phi/\partial x_2$ is not exactly equal to $\frac{2}{\pi}\int (\partial R/\partial x_2) \cos k_1 r_1 \, dr_1$. The approximations used in the numerical calculations should not have significantly affected the overall accuracy of the experimental results.

(a) Production

The shear production term, in dimensionless form, is $\frac{x}{U_m^3}\left[\frac{\partial U_1}{\partial x_2}\overline{u_1'u_2} + \frac{\partial U_1'}{\partial x_2'}\overline{u_1 u_2'}\right]$ but an adequate linear approximation to this is $\frac{1}{U_m^3}\frac{\partial U_1}{\partial \eta}(\overline{u_1'u_2} + \overline{u_1 u_2'})$. The normal-stress production term is $\frac{-2}{U_m^3}(\overline{u_1 u_1'} - \overline{u_2 u_2'})\,\eta\,\frac{\partial U_1}{\partial \eta}$ to the same approximation.

(b) Advection

It is simplest to deduce the advection spectrum from the overall advection term, by replacing $\overline{u_i^2}$ by its spectral density, defined as $\overline{u_i^2}\,\phi_{ii}\left(k_1 x_1, \frac{x_2}{x_1}\right)$: the advection spectrum in dimensionless form is then

$$\frac{x}{U_m^3}\left[U_1 \frac{\partial}{\partial x_1}\overline{u_i^2}\,\phi_{ii}\left(k_1 x_1, \frac{x_2}{x_1}\right) + U_2 \frac{\partial}{\partial x_2}\overline{u_i^2}\,\phi_{ii}\left(k_1 x_1, \frac{x_2}{x_1}\right)\right].$$

We must write the dimensionless wave number as $k_1 x_1$ rather than $k_1 x$ because we require $\partial\phi_{ii}/\partial x_1$: clearly x_1 is the correct non-dimensionalizing length for all quantities, including k_1. The advection spectrum can now be rearranged to contain only derivatives with respect to the similarity variables $k_1 x_1$ and $\eta \equiv x_2/x_1$, as

$$\left(\frac{U_2 - \eta U_1}{U_m}\right)\left(\frac{\overline{u_i^2}}{U_m^2}\frac{\partial \phi_{ii}}{\partial \eta} + \frac{\phi_{ii}}{U_m^2}\frac{\partial \overline{u_i^2}}{\partial \eta}\right) + \frac{U_1}{U_m}\frac{\overline{u_i^2}}{U_m^2}\left(\phi_{ii} + k_1 x_1 \frac{\partial \phi_{ii}}{\partial k_1 x_1}\right).$$

It is convenient to write the last factor as $\phi_{ii}(1 + \partial \log \phi_{ii}/\partial \log k_1 x_1)$. The second group of terms has an integral over all k_1 of zero: physically, it is a transfer of energy in a given element of fluid from high wave number to low wave number as x_1 increases, but it is better thought of as part of the advection spectrum than as a contribution to the spectral transfer, because it is a consequence of inhomogeneity. Another example of the effect of length-scale changes on the spectral energy balance is given by Lumley's analysis (Ref. 22) of wall turbulence with length scales proportional to distance from the wall.

A/

A further term should strictly be included to account for the variation of U_1/U_m over a typical correlation separation. It is nearly equal to $(\eta/U_1)\,\partial U_1/\partial\eta$ times the second group of terms above, and is small everywhere except in the outermost part of the flow ($\eta > 0{\cdot}1$ say).

(c) Diffusion

The velocity-diffusion spectra are the transforms of the spatial derivatives of $\overline{u_i(\underset{\sim}{x})\,u_i(\underset{\sim}{x}+\underset{\sim}{r}_1)\,u_j(\underset{\sim}{x})}/U_m^3$. In order to avoid a great deal of extra experimental work we have approximated them by the frequency spectra, using the convection velocities of u_i published in Ref. 5. This involves the assumption that the correlations or spectra are geometrically similar across the layer: actually an allowance has been made for the variation in shape. The overall longitudinal diffusion was found above to be very small, and negligible within the likely accuracy of the spectrum measurements. However, there is an appreciable extra term, with an integral over all k_1 of zero, analogous to the extra advection term. It is the contribution to rate of change, in the x_1 direction, of the spectral density of the triple products which arises from the change in the wave-number scale (so that the transform of the spatial derivative is not the spatial derivative of the transform). Exactly the same term arises in Lumley's analysis. In dimensional form it is

$$\frac{\overline{u_i^2 u_1}}{U_m^3}\,\phi_{11i}\left[1+\frac{\partial\,\log\,\phi_{11i}}{\partial\,\log\,k_1 x_1}\right]$$

where $\overline{u_i^2 u_1}\,\phi_{11i}$ is the spectrum of $\overline{u_i^2 u_1}$ and may be written $\overline{u_i u_1(k)\,u_i(k)}$. This is the cosine transform of the sum of the triple correlations, the sine transform of whose difference occurs in the energy-transfer spectrum, and has therefore been evaluated from these correlations as a matter of convenience. This extra term opposes the extra advection term on the high-velocity side of the layer but augments it on the low-velocity side.

(d) Dissipation

The dissipation spectrum is

$$\frac{2\nu x}{U_m^3}\left(k_1^2\,\overline{u_i^2}\,\phi_{ii}(k_1)+\frac{1}{\pi}\int_{-\infty}^{\infty}\left[\left(\frac{\partial^2}{\partial r_2^2}+\frac{\partial^2}{\partial r_3^2}\right)\overline{u_i(\underset{\sim}{x})\,u_i(\underset{\sim}{x}+\underset{\sim}{r})}\right]_{\underset{\sim}{r}=r_1}\cos\,k_1 r_1\,dr_1\right).$$

We observe that the spectral density at and near $k_1 = 0$ is non-zero, because a k_1 spectrum is obtained by integrating over all k_2, k_3. Isotropy of the dissipating eddies implies that dissipation occurs uniformly over the surface of spherical shells in wave-number space. If the three-dimensional spectral density of dissipation is $\phi_d(k)$, a function of wave-number magnitude only, then the one-dimensional spectral density, for k_1 small compared with the values of k at which the dissipation occurs (nearly equatorial slices of the spherical shells), is $2\int_0^\infty \phi_d(k)\,.\,2\pi k\,dk$, where

$\int_0^\infty$

$\int_0^\infty \phi_d(k) \cdot 4\pi k^2 dk = \epsilon = \int_0^\infty 2\nu k^2 e(k) dk$. The factor 2 in front of the integral arises because we are adding contributions from positive and negative k. This spectral density can be calculated from the universal form of the dissipation spectrum: according to Kolmogorov's theory, $\left(\frac{\nu}{\epsilon}\right)^{\frac{1}{2}} k^2 E(k)$ is a function of $k_1 \left(\frac{\nu^3}{\epsilon}\right)^{\frac{1}{4}}$. Using Uberoi's graphs of $k^2E(k)$ for convenience since most other experimenters have presented $k_1^2 \phi_{ii}(k_1)$, which is <u>not</u> the dissipation spectrum, we find that the spectral density at low k_1 is $4{\cdot}5\ (\nu\epsilon)^{\frac{3}{4}}$ or $0{\cdot}55\ (U_m\, x/\nu)^{-\frac{3}{4}}$ in dimensionless units at $\eta = 0$, so that as far as the energy-containing range of k_1 is concerned we may imagine the dissipation to take place on the surface of a sphere of radius $0{\cdot}22 \left(\frac{\epsilon}{\nu^3}\right)^{\frac{1}{4}}$ (or 2700 on the $k_1 x_1$ scale near $\eta = 0$) in three-dimensional wave-number space. This compares with about $0{\cdot}38 \left(\frac{\epsilon}{\nu^3}\right)^{\frac{1}{4}}$ for the centroid of Uberoi's wave-number <u>magnitude</u> spectrum of dissipation $(0{\cdot}5 \left(\frac{\epsilon}{\nu^3}\right)^{\frac{1}{4}}$ for the measurements of Stewart and Townsend[15] according to Townsend[8]). Since the spectral density of the production at $k_1 = 0$ and $\eta = 0$ is about 3×10^{-3} in dimensionless units whereas the spectral density of the dissipation is $2{\cdot}3 \times 10^{-5}$, we may neglect the effect of the dissipation on the energy balance at low wave numbers, although the effect on the integrated energy transfer at $k_1 x = 100$ is about five percent of the total dissipation so that an allowance would have to be made if the dissipation were to be calculated from the energy transfer across a plane $k_1 =$ constant in wave-number space. The dissipation becomes equal to the production at about $k_1 x = 130$ near $\eta = 0$ and at a lower wave number near the extremities of the shear layer, but this does <u>not</u> imply that the three-dimensional spectral densities of production and dissipation are equal at this wave-number magnitude: it is shown in Section 3.3 that the figure is more like $kx = 250$.

Finally we can write the real part of the spectral energy-balance equation for positive k_1 wave number as

$$\left(\frac{U_2 - \eta U_1}{U_m}\right) /$$

$$\left(\frac{U_2 - \eta U_1}{U_m}\right)\left(\frac{\overline{u_i^2}}{U_m^2}\cdot\frac{\partial\phi_{ii}}{\partial\eta} + \phi_{ii}\cdot\frac{1}{U_m^2}\cdot\frac{\partial\overline{u_i^2}}{\partial\eta}\right) + \frac{U_1}{U_m}\cdot\frac{\overline{u_i^2}}{U_m^2}\,\phi_{ii}\,(1 + \partial\log\phi_{ii}/\partial\log k_1 x_1)$$

advection — spectral transfer due to inhomogeneity

$$+\frac{1}{U_m}\frac{\partial U_1}{\partial\eta}\cdot\overline{u_1 u_2}\,(\phi_{12} + \phi_{21})$$

production

$$+\frac{\partial}{\partial\eta}\left(\overline{u_i^2 u_2}\,\phi_{i2i}\right) - \eta\frac{\partial}{\partial\eta}\left(\overline{u_i^2 u_1}\,\phi_{i1i}\right) + \frac{\overline{u_i^2 u_1}}{U_m^3}\,\phi_{i1i}\,(1 + \partial\log\phi_{i1i}/\partial\log k_1 x_1)$$

lateral diffusion — longitudinal diffusion — spectral transfer due to inhomogeneity

+ pressure diffusion spectrum

+ dissipation spectrum

$$= \frac{k_1}{\pi}\int_{-\infty}^{\infty}\frac{\overline{(u_1 - u_1')u_i u_i'}}{U_m^3}\sin k_1 r_1\, dr_1$$

measured part of spectral energy transfer T_{1ii}

$$+\frac{1}{\pi}\int_{-\infty}^{\infty}\frac{\partial}{\partial r_\ell}\frac{\overline{(u_\ell - u_\ell')u_i u_i'}}{U_m^3}\cos k_1 r_1\, dr_1 \qquad (\ell = 2, 3)$$

unmeasured part of spectral energy transfer $T_{\ell ii}$. ...(A.1.3)

APPENDIX II/

APPENDIX II

Measurement of the Triple Correlations

The correlations $\overline{u_1(\underset{\sim}{x})\, u_i(\underset{\sim}{x})\, u_i(\underset{\sim}{x}+\underset{\sim}{r}_1)}$ and $\overline{u_1(\underset{\sim}{x}+\underset{\sim}{r}_1)\, u_i(\underset{\sim}{x})\, u_i(\underset{\sim}{x}+\underset{\sim}{r}_1)}$ for $i = 1$ were measured at the same time, with two hot wires normal to the flow, and the results were generally satisfactory: in particular the two correlations tended to very nearly the same value at $r_1 = 0$ and as $r \to \infty$ (see Figs. 12(a) and (b), in which is plotted the correlation coefficient actually measured). The value at large r was in general different from zero by an amount sufficiently large to indicate some error of measurement (more than the likely error in the multiplier) but the quantity related to the energy transfer is the difference between the correlations, the sum being the Fourier transform of the wave-number spectrum of $\overline{u_1^2}$, one of the diffusion terms. The difference between the correlations was well-behaved, tending to zero at large r, and the Fourier transforms of the differences were also well-behaved except at the very low wave numbers corresponding to wavelengths of several times the width of the shear layer.

The correlations with $i = 2$ and $i = 3$ were measured with two cross-wire probes, which were used to obtain $u_1(\underset{\sim}{x})$ and $u_1(\underset{\sim}{x}+\underset{\sim}{r}_1)$ as well as the lateral components: this is a roundabout process, inherently less accurate than using single-wire probes for measuring u_1, but was forced on us by lack of sufficient constant-temperature anemometer channels to operate six wires simultaneously and by fears of the probe interference and liability to accidents resulting from the juxtaposition of an X probe and a U probe. The chief defect of the results was the failure of the two correlations to coincide for $r_1 = 0$. The measurements at $\eta = 0$ are shown in Figs. 12(c) to (f): if one were interested only in the sum of the correlations, which transform to give two more of the spatial diffusion terms, the results would be quite acceptable. Even at $\eta = 0$ where $\overline{u_1 u_2^2}$ and $\overline{u_1 u_3^2}$ are very small the discrepancy is only about 0·02 in correlation coefficient, but the effect on the difference is considerable. If the effect were really a bodily displacement of one correlation curve it would appear in an accurate Fourier transform of the difference as a delta function at the origin, which could be ignored. It is probable that unfaithful reproduction of the u_1-component fluctuation is chiefly to blame since the $u_2(\underset{\sim}{x})\, u_2(\underset{\sim}{x}+\underset{\sim}{r}_1)$ product is common to both correlations but probe interference may have had some effect. The downstream probe was aligned along the x_1 axis but the upstream probe was necessarily aligned along a radius with the prongs normal to the flow. The wires themselves were bent so that the active portions were at least 0·03 in. away from the plane of the longer pair of prongs, and the r.m.s. signal due to vibration or eddy shedding of the prongs of the radial probe was never more than 1 percent turbulence even at the highest speed of the jet, but possibly the prongs of the radial probe may have affected the downstream probe in some circumstances, although the problem is far less serious than in the less intense turbulence of a boundary layer. Certainly the correlations at $\eta = -0{\cdot}05$ were worse behaved than those in the high-intensity region, but the peculiarities sometimes found at small separation were generally attributable to the small separations between the probes in the x_2 and x_3 directions, necessary for mechanical reasons: it was usually easy enough to extrapolate the correlations to zero separation.

One/

One attempt was made to measure $\overline{[u_1(\underset{\sim}{x}) - u_1(\underset{\sim}{x} + r_1)]\, u_2(\underset{\sim}{x})\, u_2(\underset{\sim}{x} + r_1)}$ by subtracting the u_1 signals electrically. However the probe sensitivities found in practice were not in the same ratio as had been calculated from the calibrations, and the attempt was abandoned. This merely confirms the remarks above. In general it was felt to be more satisfactory to measure the correlations separately since the source of any errors would be more apparent than if one were merely confronted by an ill-behaved difference signal.

The measurements for $i = 2$ and $i = 3$ are therefore disappointing: fortunately, these terms are rather smaller than the $i = 1$ term so that a reasonable approximation to T_{1ii} can be obtained. It should be possible to do considerably better by using separate wires for u_1-component measurement, which would be possible for us if constant-current operation could be used without excessive distortion of the signals. It is unlikely that T_{2ii} and T_{3ii} could be measured with any accuracy because graphical differentiation of the correlations would be required: it is certainly not reasonable to attempt this in the present state of the art.

Table 1/

Table 1

Spectral Densities, per unit $k_1 x$, normalized by U_m and x

Production

η \ $k_1 x$	1	2	5	10	20	50	100
-0.05		0.000762	0.000872	0.00147	0.000578	0.0000888	0.0000153
0		0.00302	0.00338	0.00498	0.00192	0.000210	0.0000484
0.05		0.00326	0.00318	0.00244	0.000932	0.000146	0.0000342
0.10		0.00147	0.00117	0.000666	0.000288	0.0000582	0.0000122

Advection

-0.05	0.000467	0.000487	0.000950	0.00138	0.000735	0.000162	0.0000573
0	0.000143	0.0000975	0.000932	0.0000567	0.0000357	0.00000790	0.00000177
0.05	0.00000233	0.0000203	0.000122	0.000222	0.000115	0.0000244	0.00000723
0.10	0.000295	0.000244	0.000314	0.000367	0.000183	0.0000436	0.0000143

Normal-Stress Production

-0.05	-0.0000264	-0.0000316	-0.0000410	0.0000318	0.0000276	0.00000568	0.00000130
0	0	0	0	0	0	0	0
0.05	0.000172	0.000148	0.000159	0.0000246	-0.00000320	-0.00000536	-0.00000271
0.10	0.000250	0.000178	0.000115	0.0000239	0.00000386	-0.00000358	-0.00000174

Lateral Diffusion

-0.05	-0.00337	-0.00374	-0.00336	-0.001241	-0.000455	-0.000111	-0.0000675
0	0.00406	0.00427	0.00431	0.00275	0.000130	0.000411	0.000160
0.05	0.000146	-0.0000003	-0.0000850	0.000246	0.000284	0.0000962	0.0000128
0.10	-0.00150	-0.00151	-0.00149	-0.00141	-0.000870	-0.000284	-0.0000904

Spectral Transfer due to Inhomogeneity: Advection

-0.05	0.000379	0.000381	0.000769	+0.00101	-0.000190	-0.0000585	-0.0000207
0	0.000723	0.000723	0.00104	+0.00106	-0.000271	-0.0000843	-0.0000282
0.05	0.000503	0.000511	0.000446	+0.000376	-0.0000489	-0.0000342	-0.0000117
0.10	0.000107	0.000107	0.0000902	+0.0000475	-0.0000143	-0.00000756	-0.00000233

Contd./

Spectral Transfer due to Inhomogeneity: Longitudinal Diffusion

-0·05	-0·000378	-0·000381	-0·000644	-0·000453	+0·0000454	0·0000349	0·0000090
0	-0·0000771	-0·000200	-0·000950	-0·000366	+0·0000152	0·0000156	0·0000020
0·05	0·00150	0·00145	0·00100	+0·000969	-0·000417	-0·0000602	-0·0000045
0·10	0·00327	0·00311	0·00177	+0·000410	-0·000272	-0·000192	-0·000080

T_{iii} Energy Transfer

-0·05	+0·00000400	+0·0000140	+0·00000300	-0·000102	-0·0000690	+0·00000900	+0·0000110
0	+0·0000200	+0·0000360	-0·0000310	-0·000203	-0·000134	+0·00000100	+0·0000110
0·05	-0·00000100	-0·0000130	-0·000104	-0·000223	-0·000147	-0·0000170	-0·00000100
0·10	-0·0000120	-0·0000310	-0·0000820	-0·0000970	-0·000082	-0·0000221	-0·00000530

T_{iii} Energy·Transfer

-0·05	+0·0000128	+0·0000404	+0·0000480	+0·00000800	-0·0000434	-0·000016	+0·00000650
0	+0·0000238	+0·0000410	+0·0000615	-0·000156	-0·000402	-0·0000328	-0·0000520
0·05	-0·0000422	-0·0000505	-0·000172	-0·0000874	-0·000121	+0·0000168	+0·0000634

26 743

FIG. 1(a)

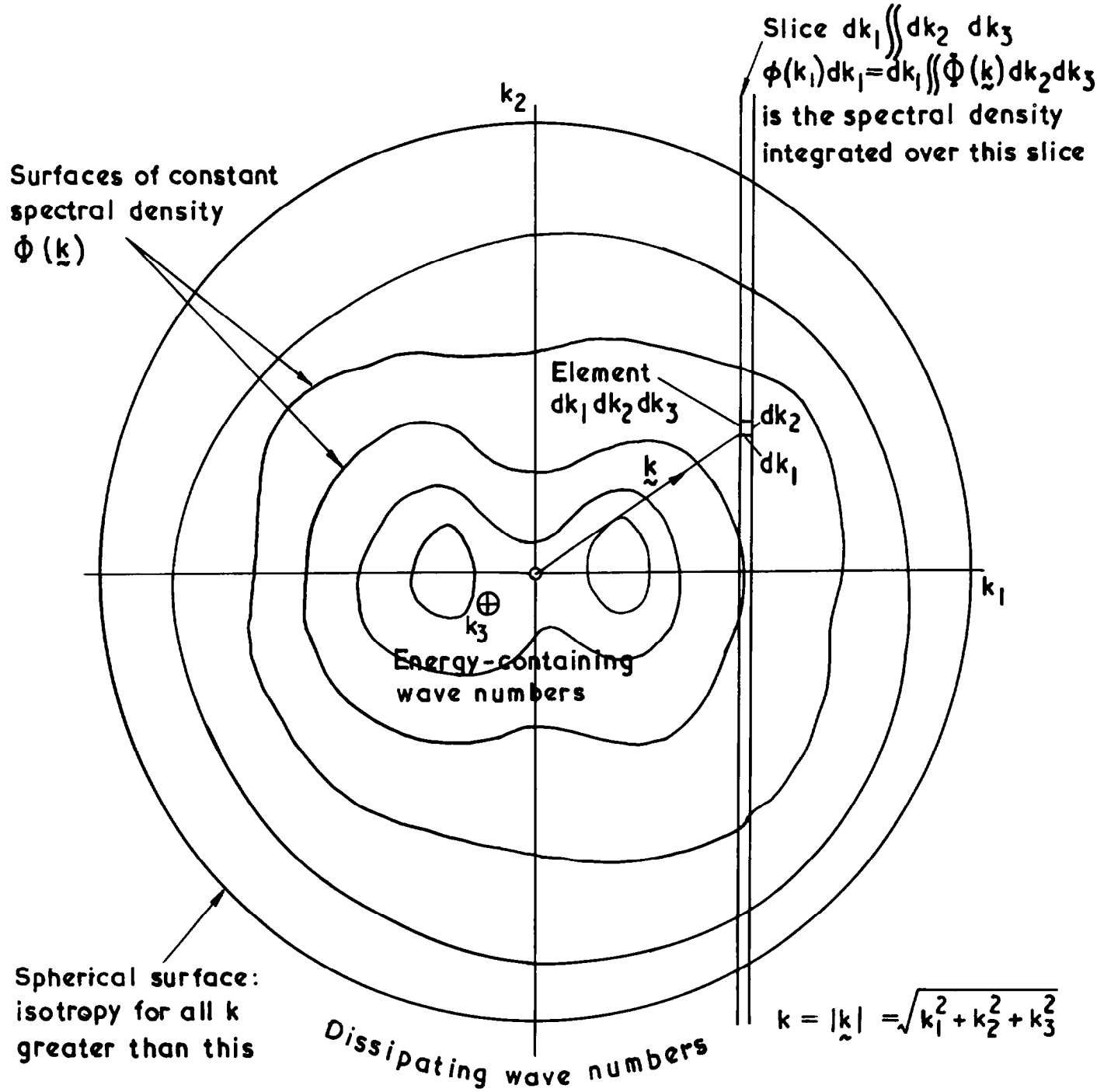

Sketch of the plane $k_3 = 0$ in wave-number space (The k_1 axis may be thought of roughly as an axis of rotational symmetry)

26 743
FIG. 1(b)

Energy content of cube $= \Phi(\underset{\sim}{k})\, dk_1\, dk_2\, dk_3$

Energy content of slice $= dk_1 \iint \Phi(\underset{\sim}{k})\, dk_2\, dk_3 = \Phi(k_1)\, dk_1$

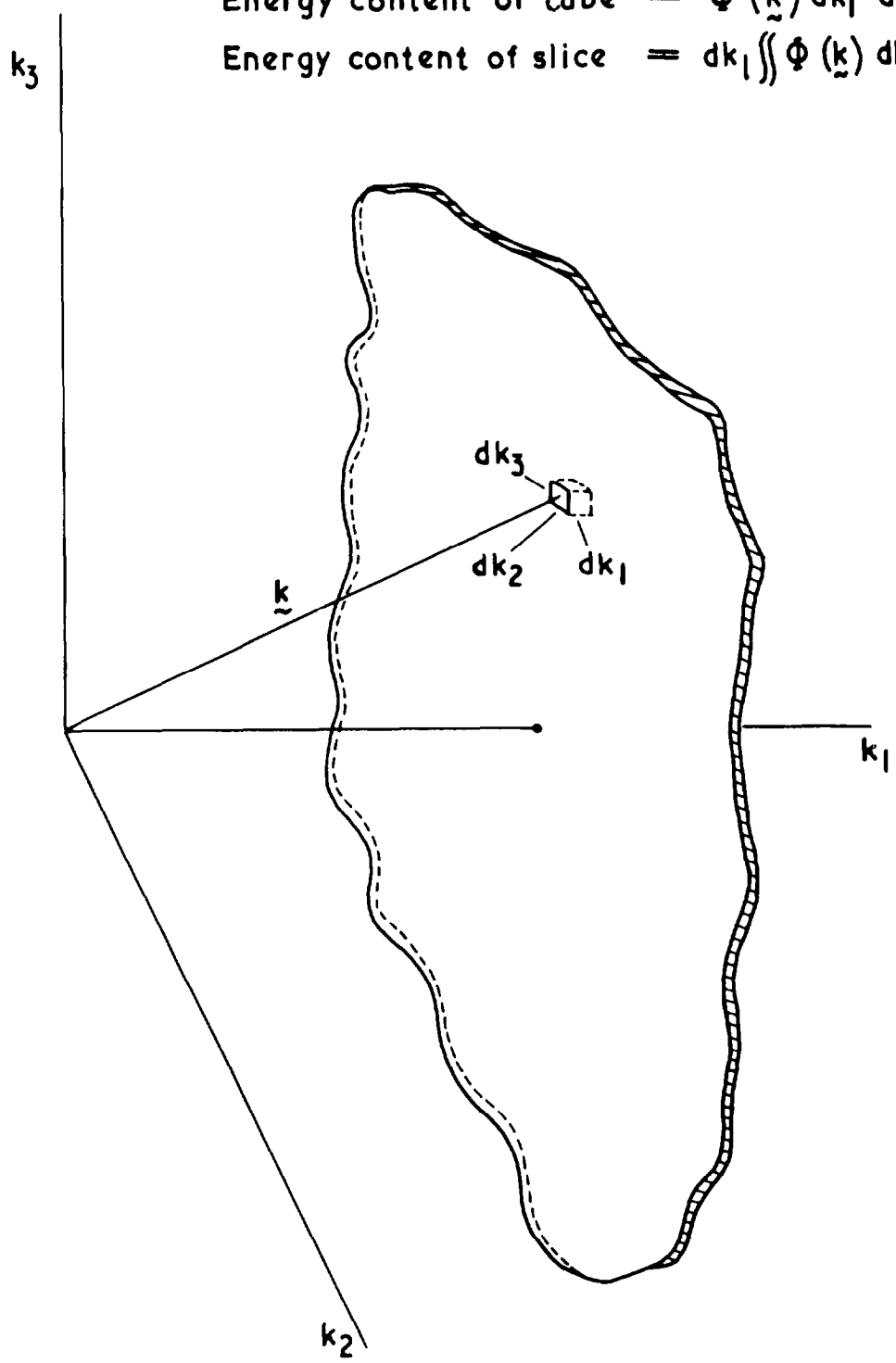

One-dimensional and three-dimensional spectra

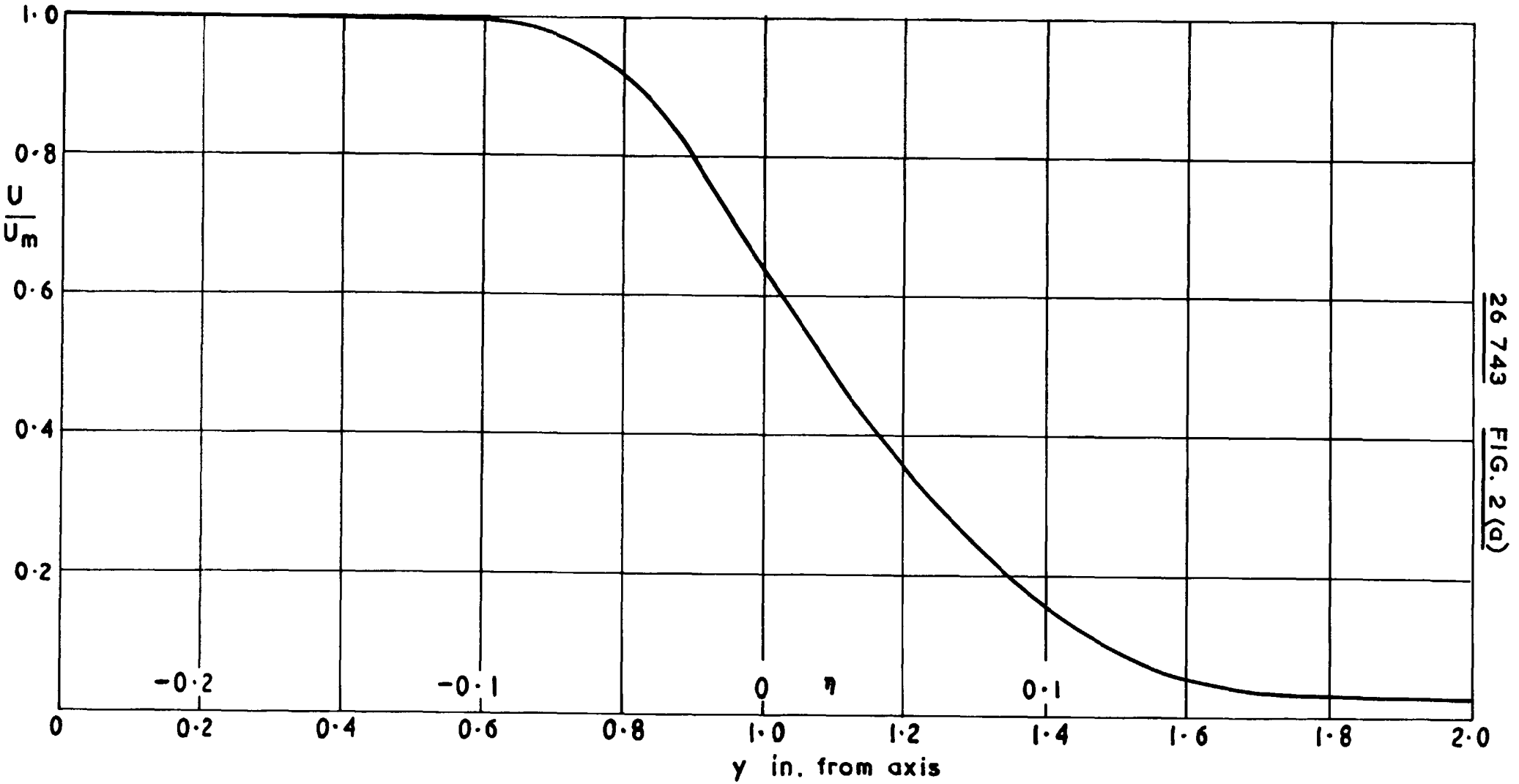

26 743 FIG. 2(a)

Mean velocity: x = 4 in.

26 743

FIG. 2(b)

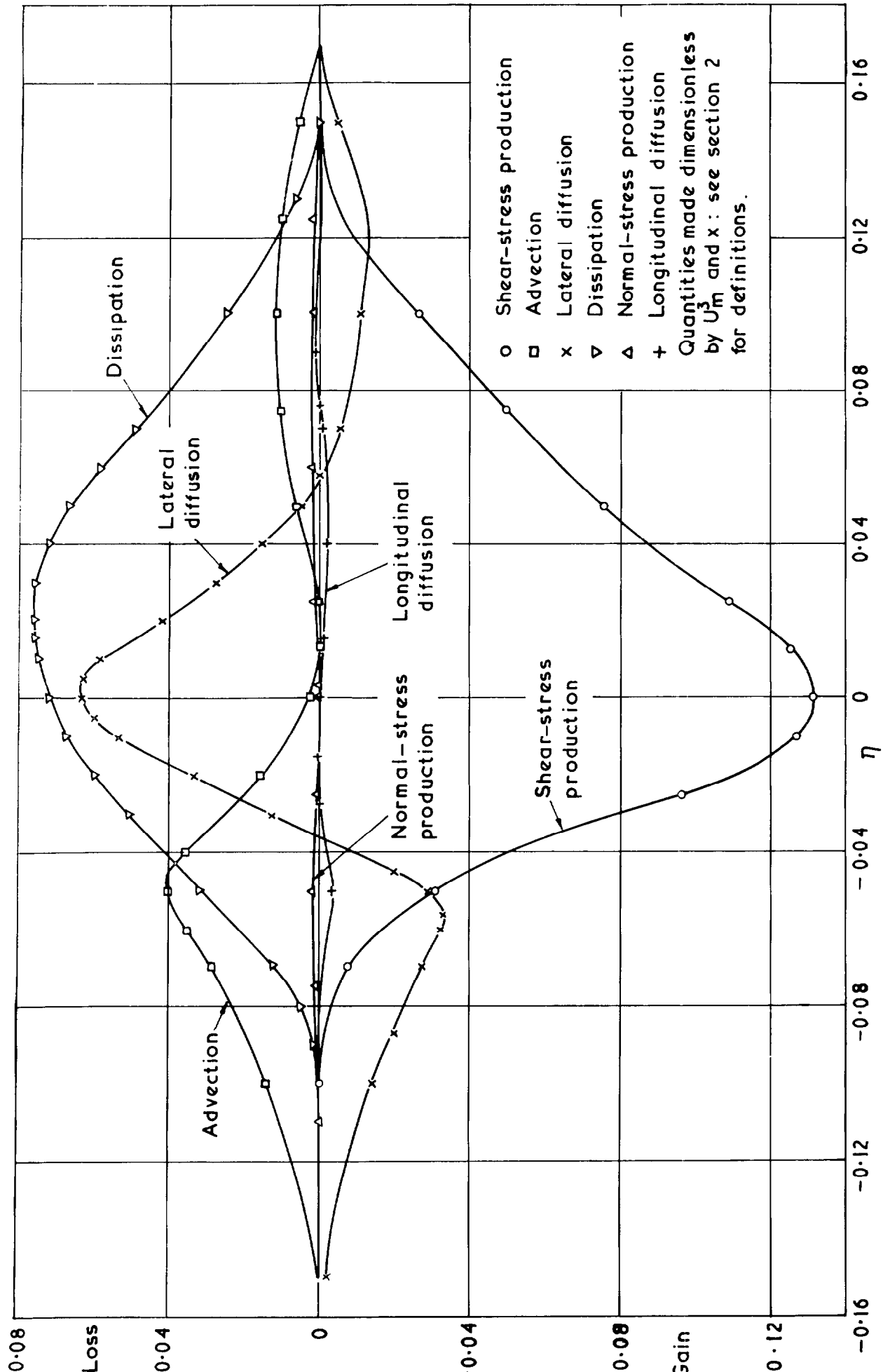

Overall energy balance

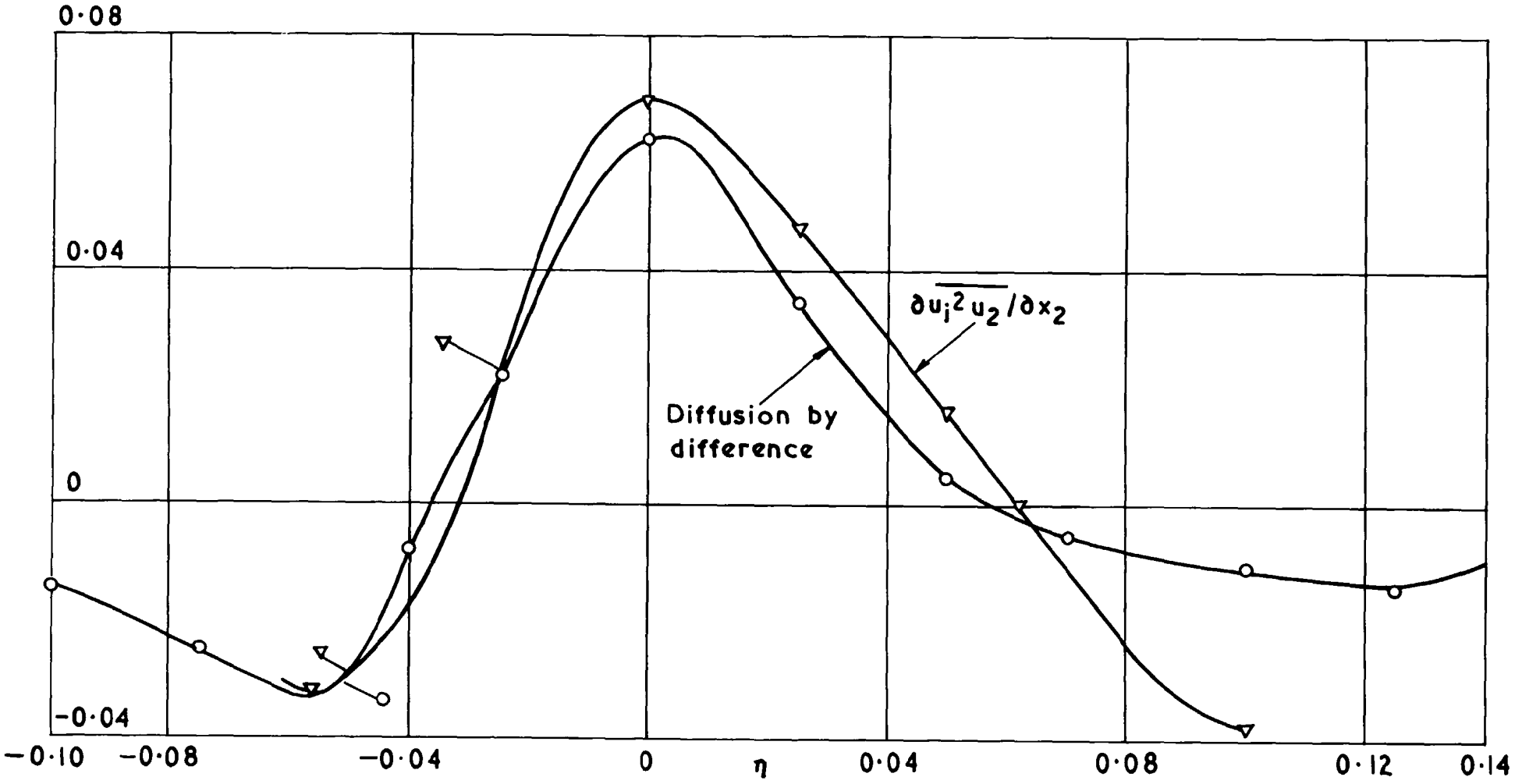

26 743
FIG. 2(c)

Comparison between triple-product lateral diffusion (measured) and total lateral diffusion (by difference)

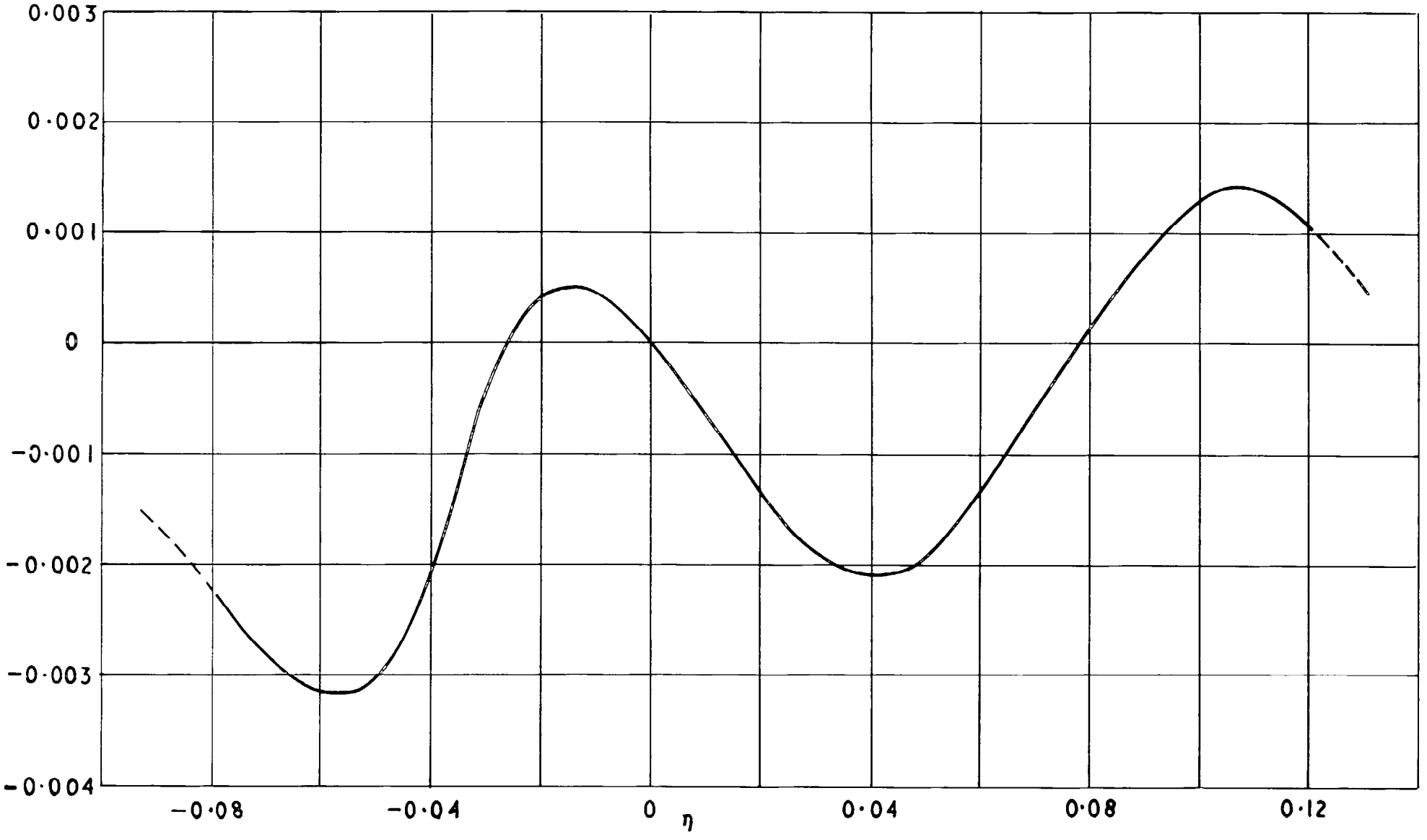

26 743
FIG. 2(d)

Triple-product longitudinal diffusion

26 743

FIG. 2(e)

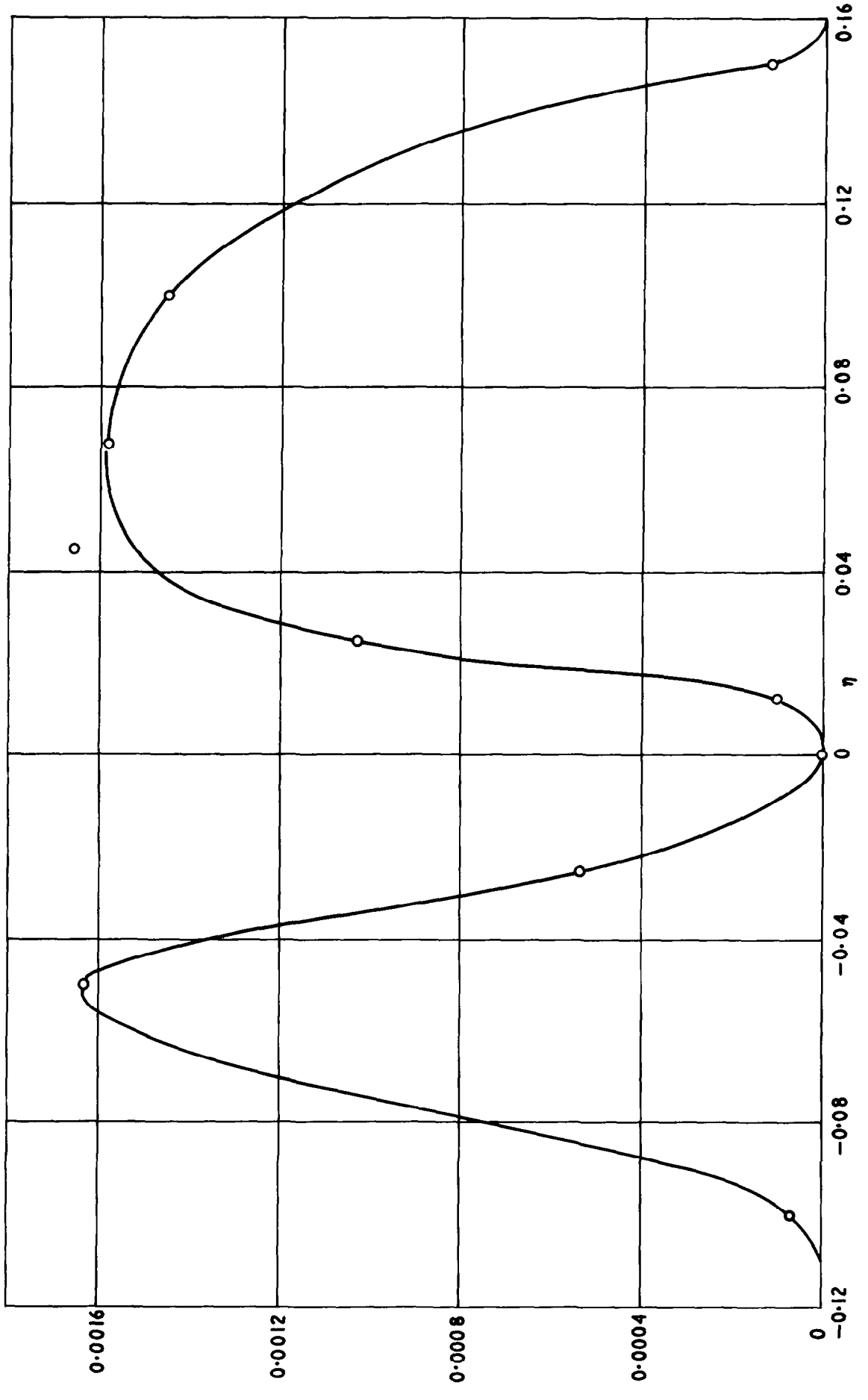

Production by normal stresses

26 743
FIG. 3(a)

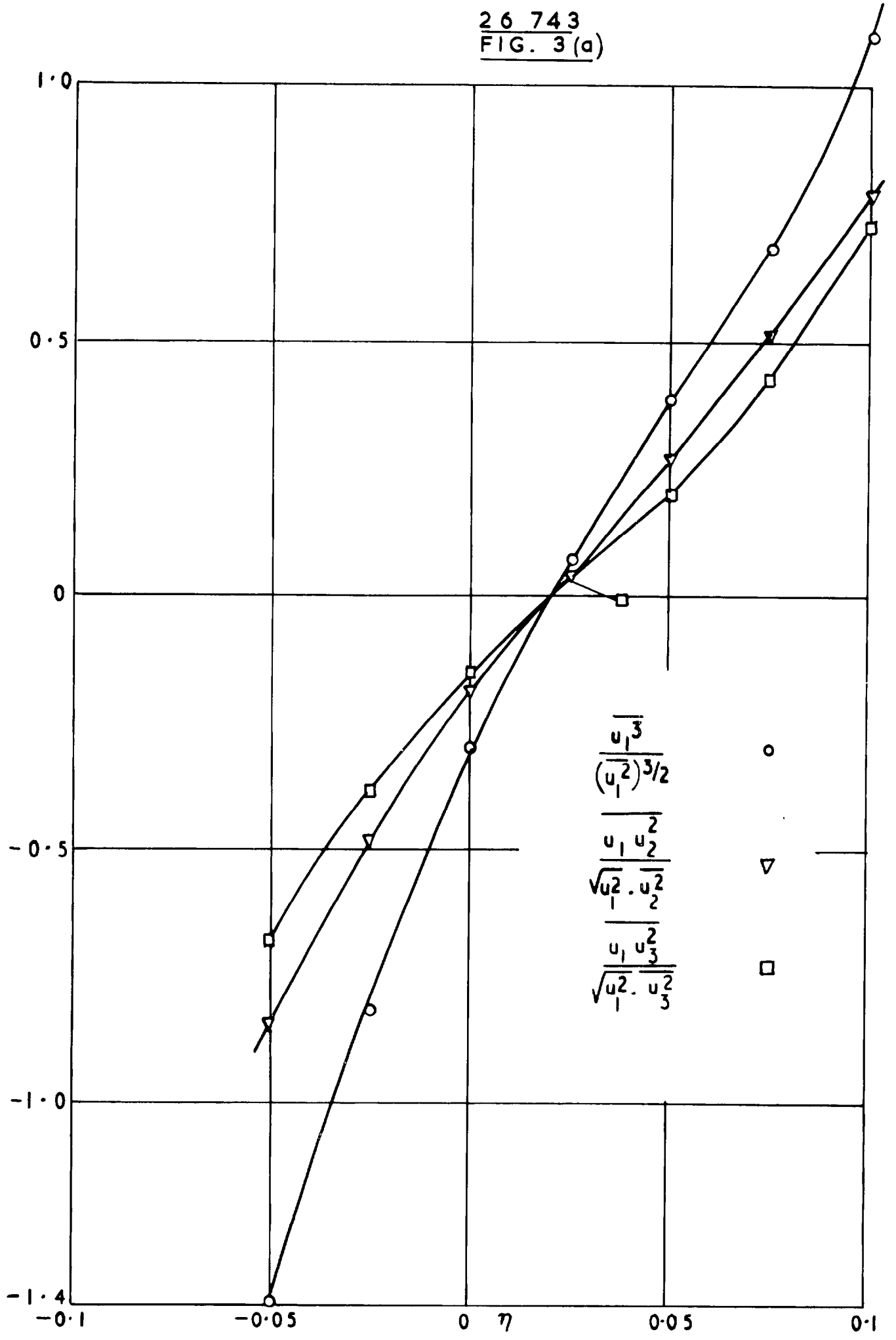

Components of $\overline{u_i^2 u_1}$

26 743
FIG. 3(b)

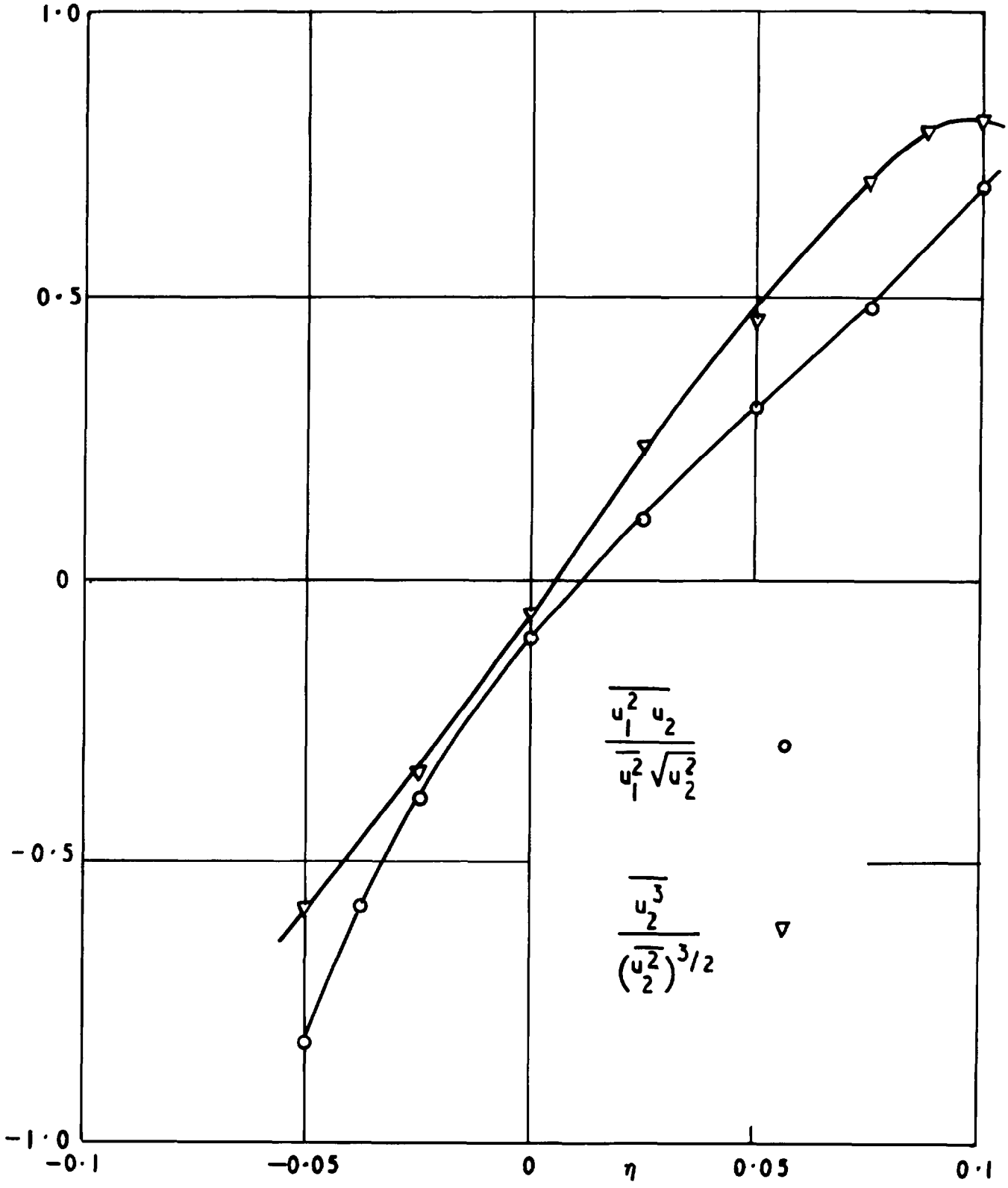

Components of $\overline{u_i^2 u_2}$

26 743
FIG. 3(c)

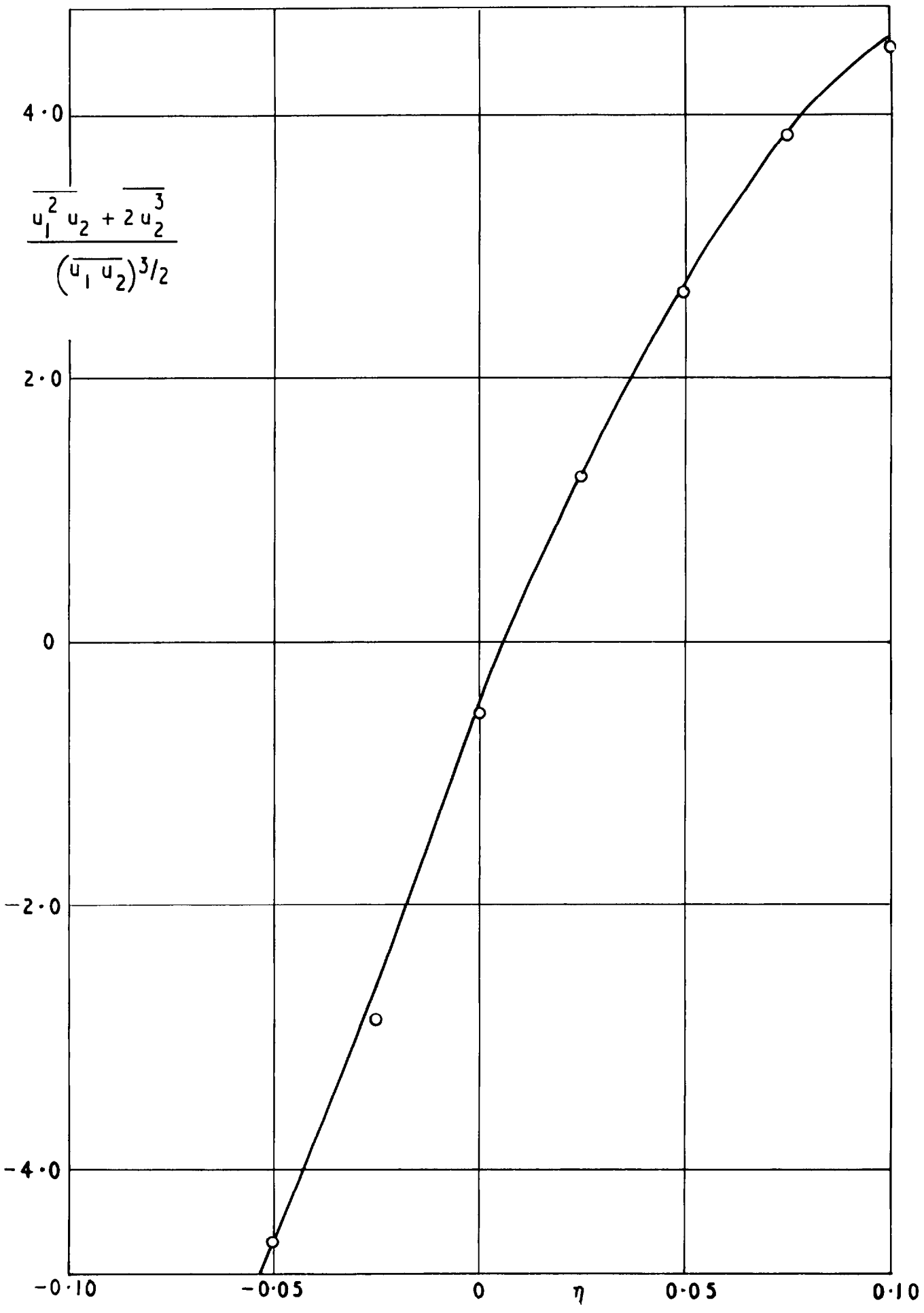

Approximation to $\overline{u_1^2 u_2}$, normalized by shear stress

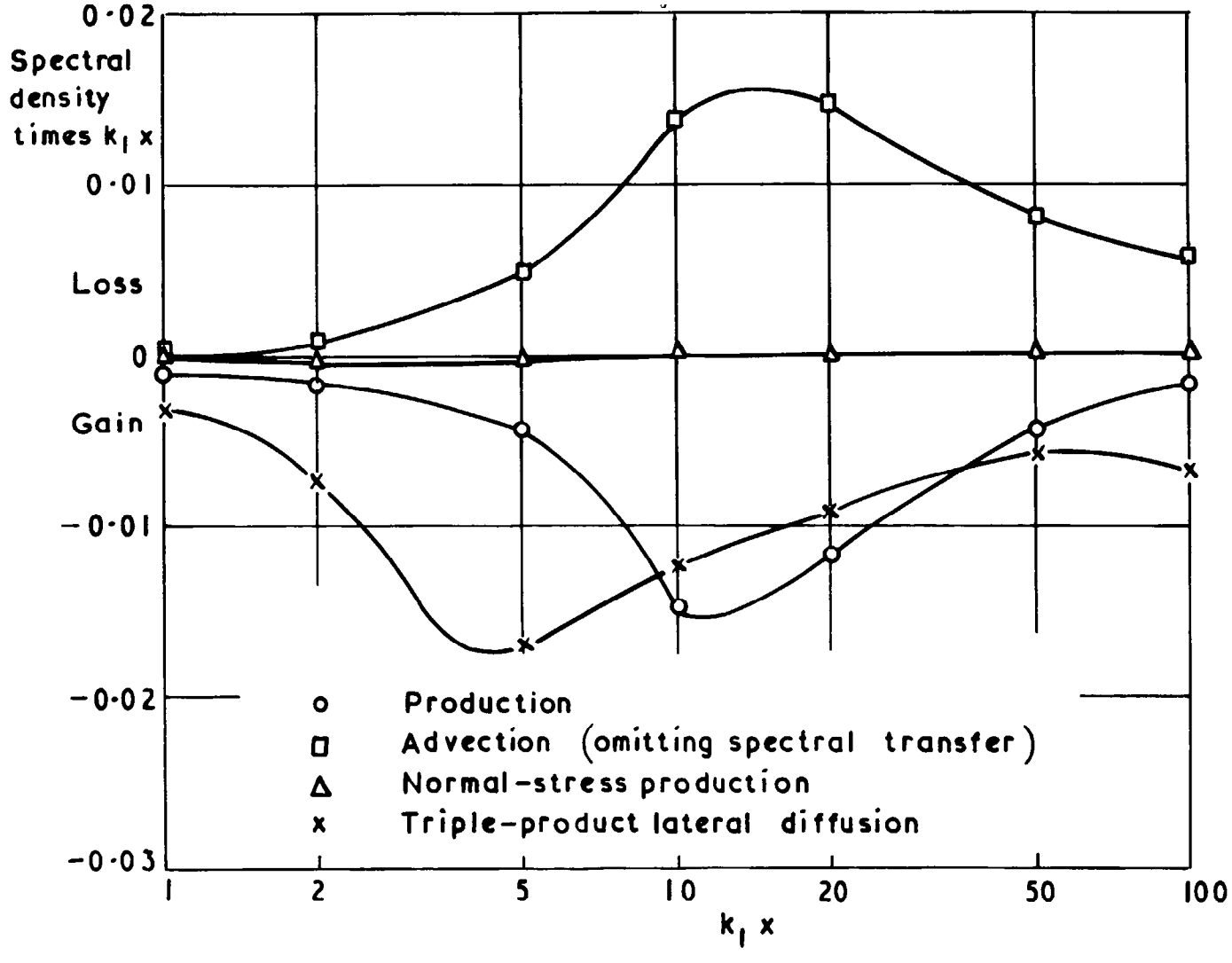

Energy-balance spectrum: $\eta = -0{\cdot}05$

26 743
FIG. 4(a)

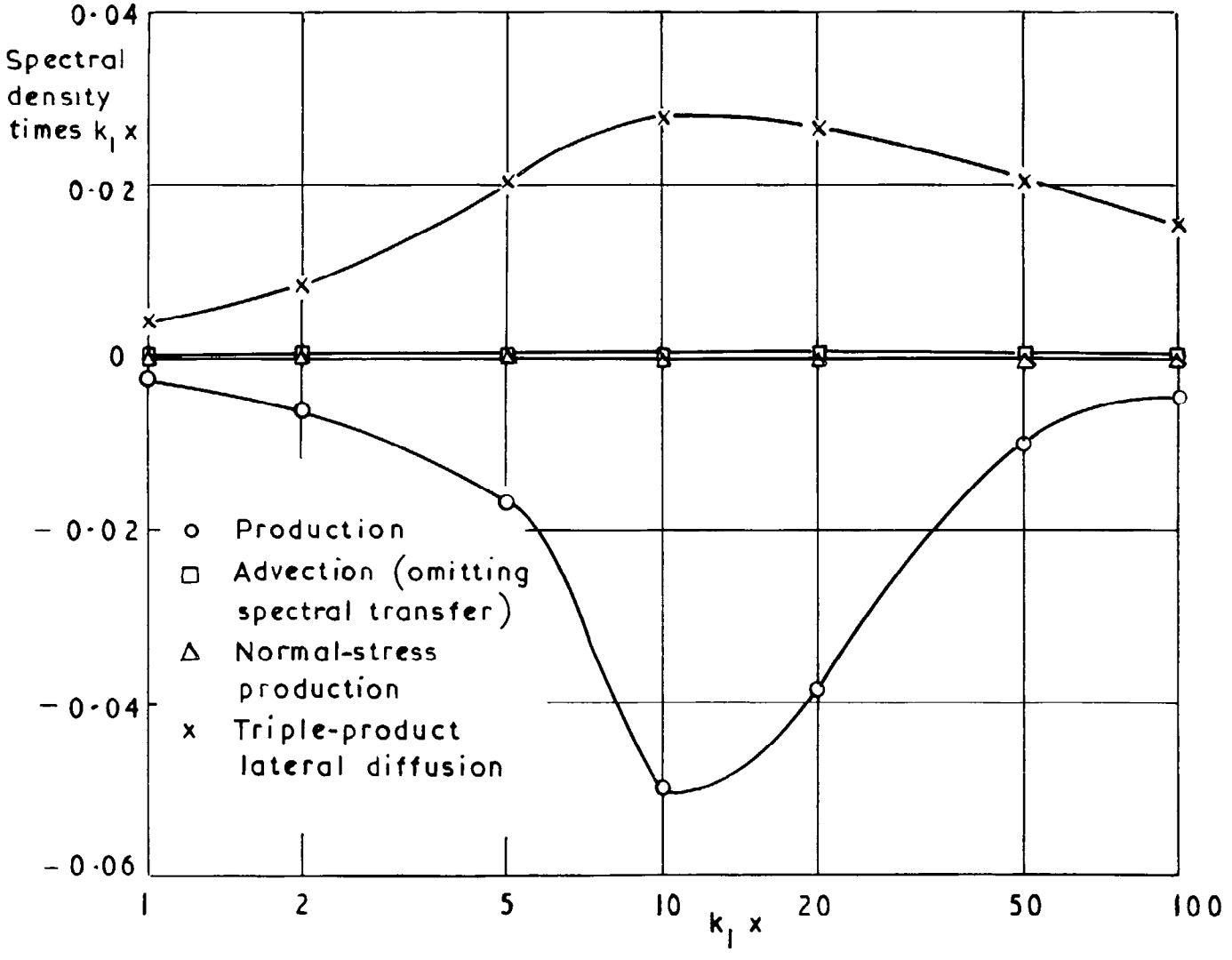

Energy-balance spectrum : $\eta = 0$

26 743
FIG. 4(b)

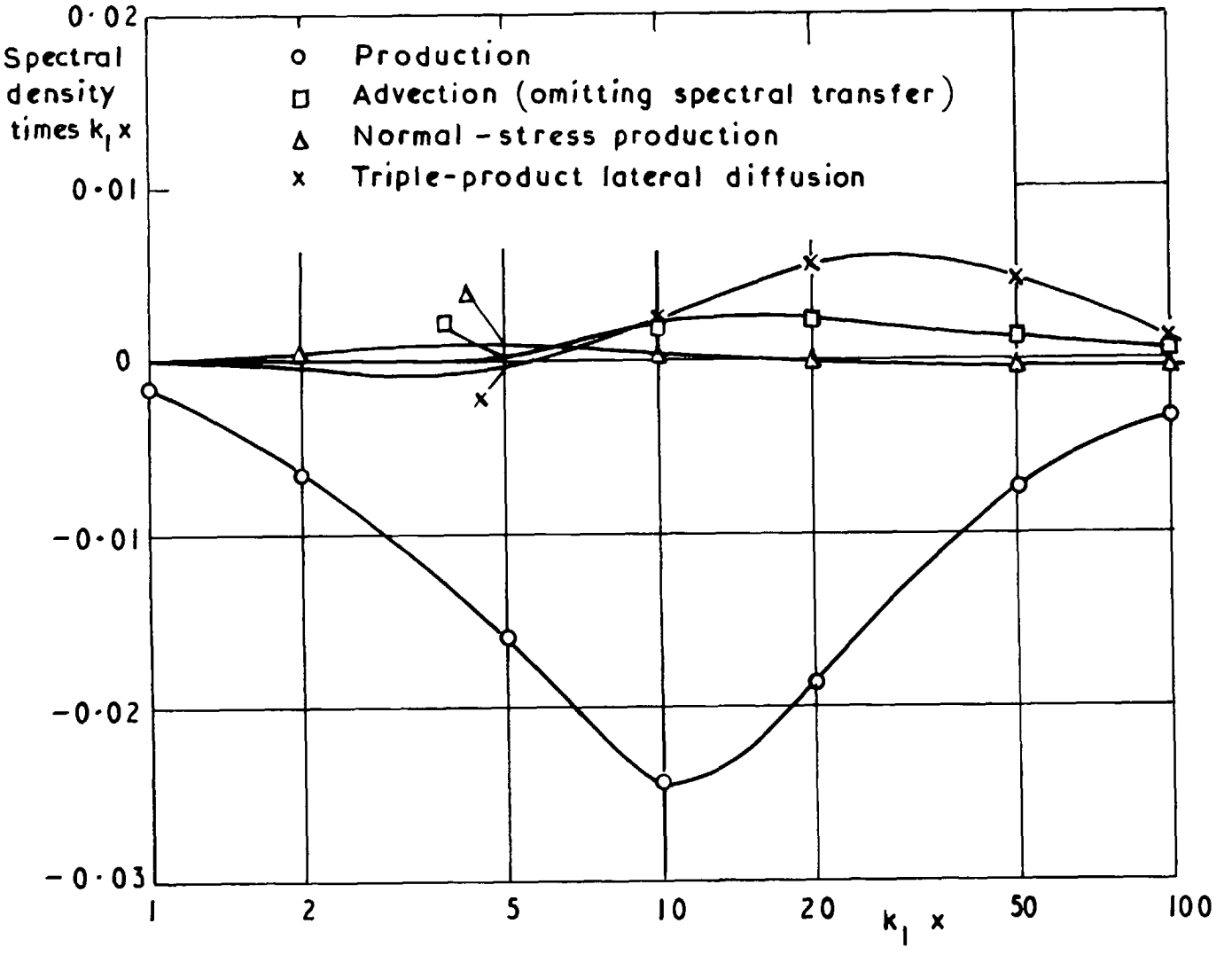

Energy-balance spectrum : $\eta = 0{\cdot}05$

26 743
FIG. 4 (c)

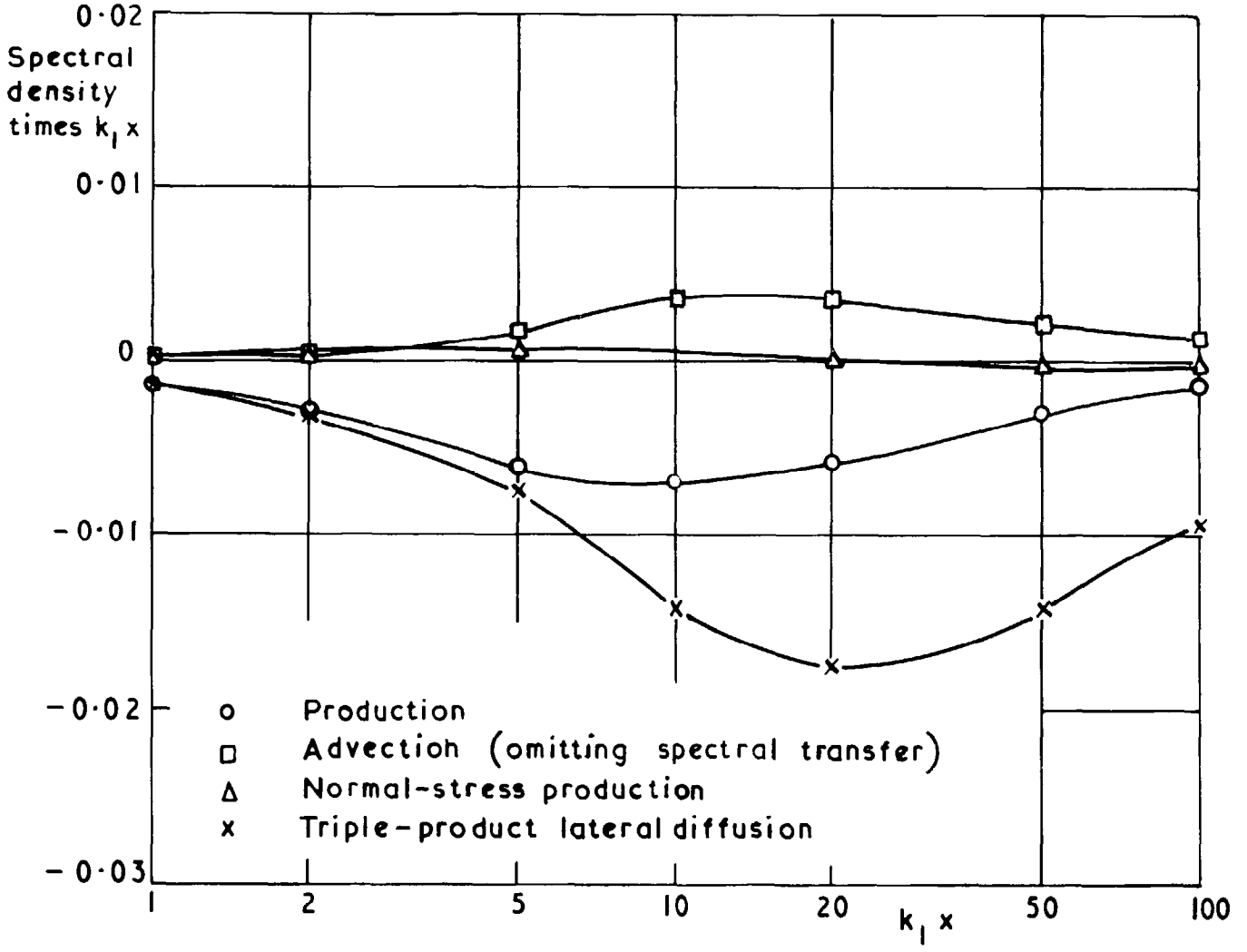

Energy-balance spectrum: $\eta = 0 \cdot 1$

26 743
FIG. 4(d)

26 743
FIG. 5 (a)

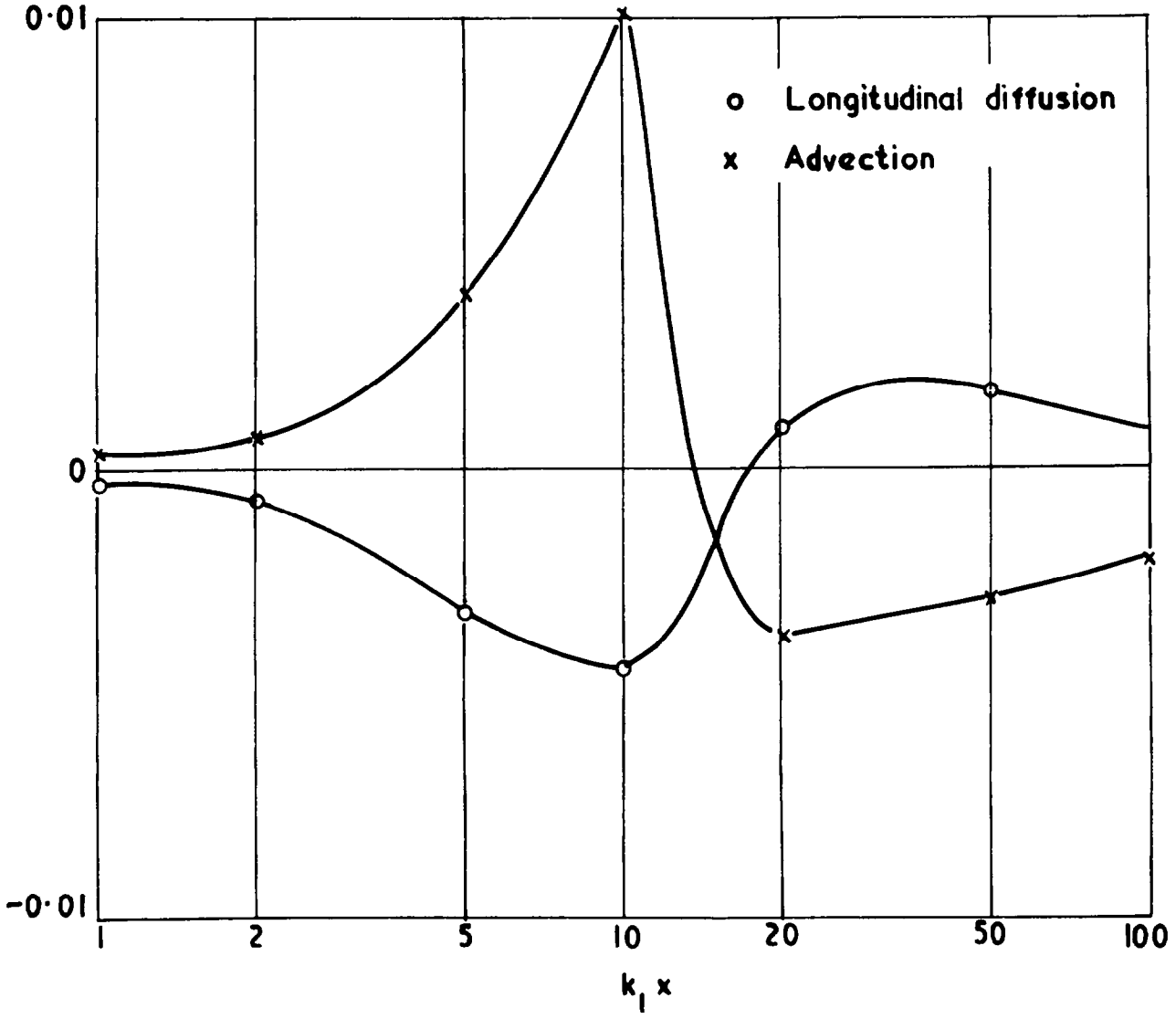

Spectral transfer due to inhomogeneity $\eta = -0{\cdot}05$

26 743
FIG.5(b)

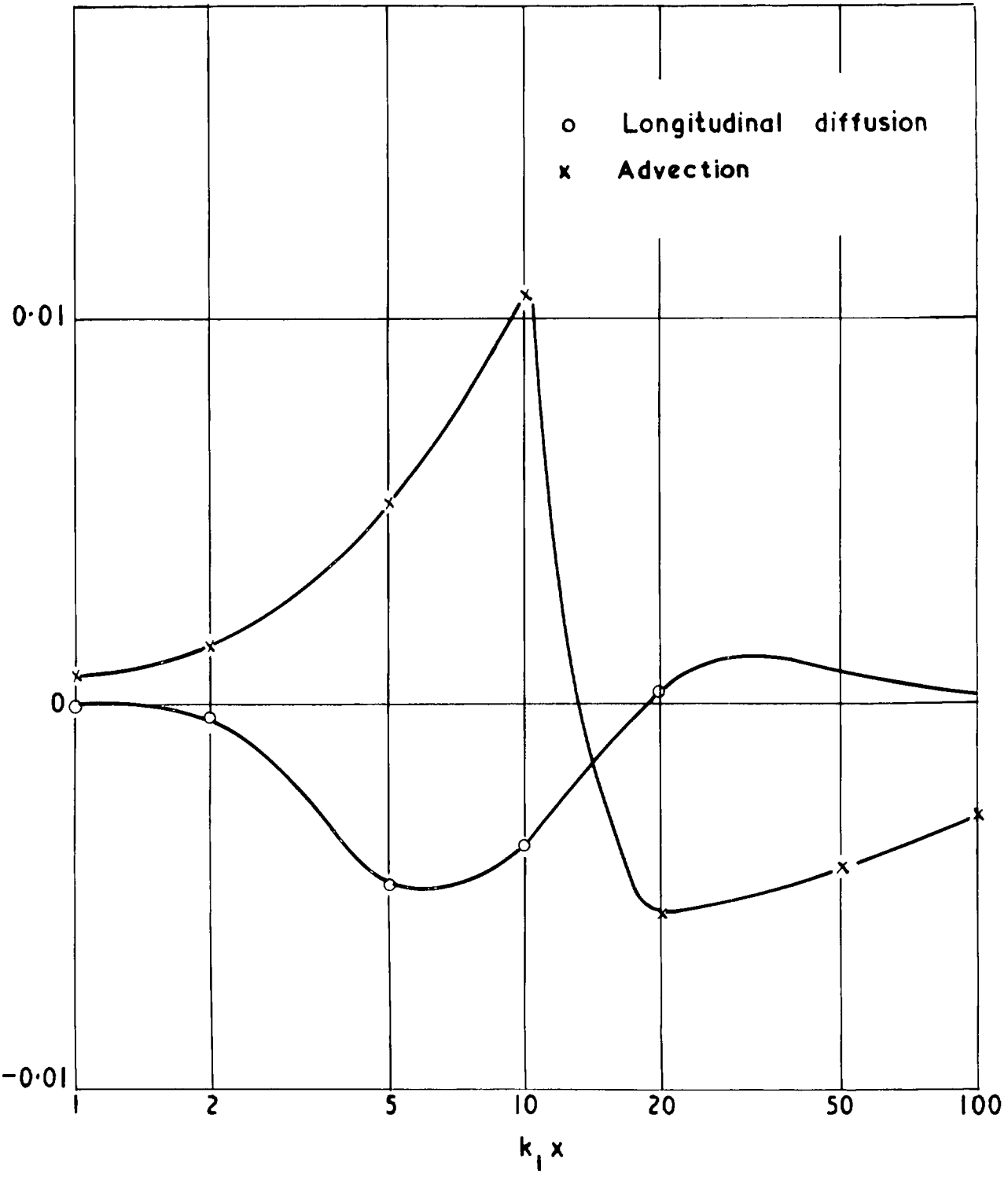

Spectral transfer due to inhomogeneity $\eta = 0$

26 743
FIG. 5 (c)

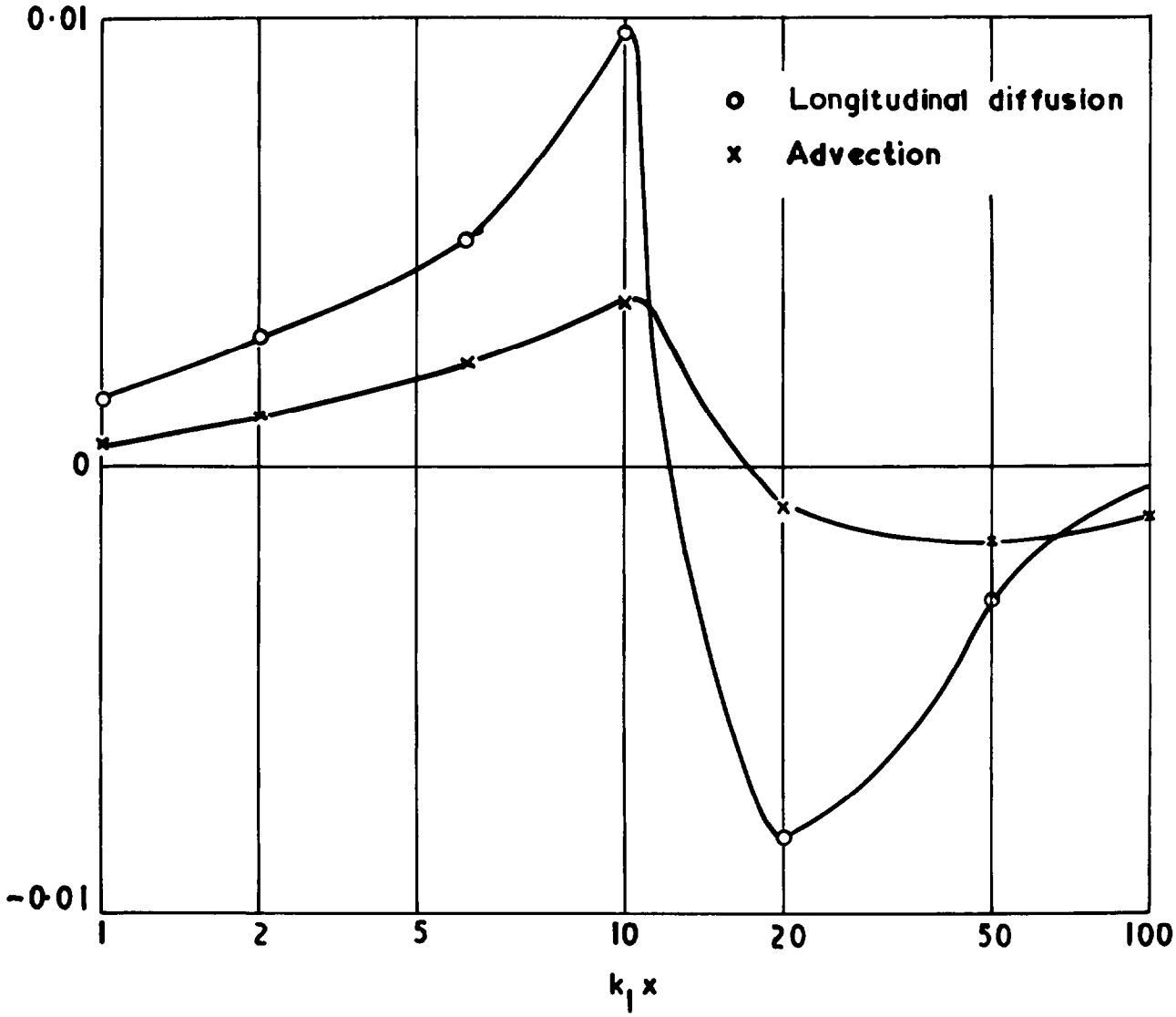

Spectral transfer due to inhomogeneity $\eta = 0{\cdot}05$

26 743
FIG. 5 (d)

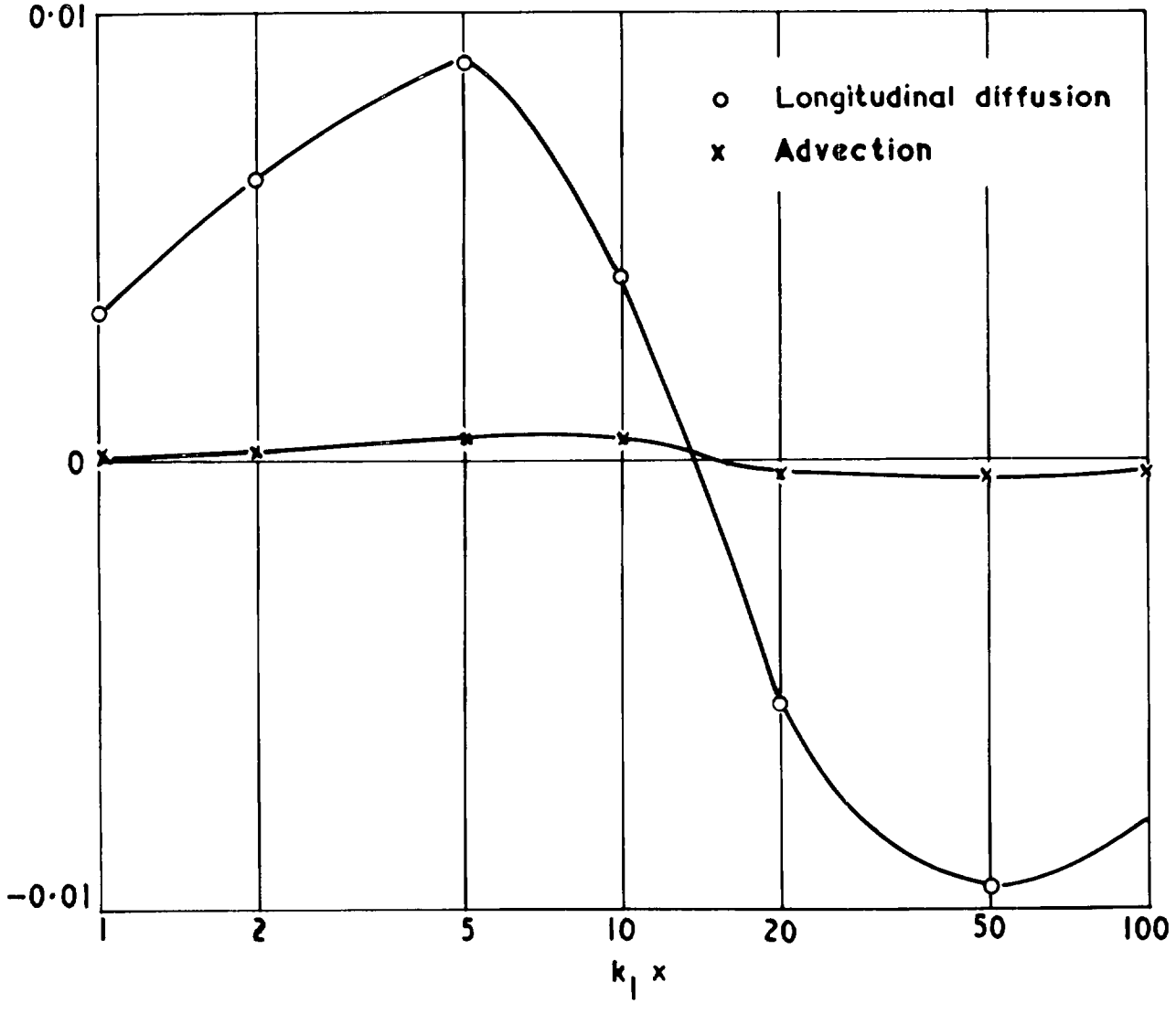

Spectral transfer due to inhomogeneity $\eta = 0{\cdot}1$

26 743
FIG. 6(a)

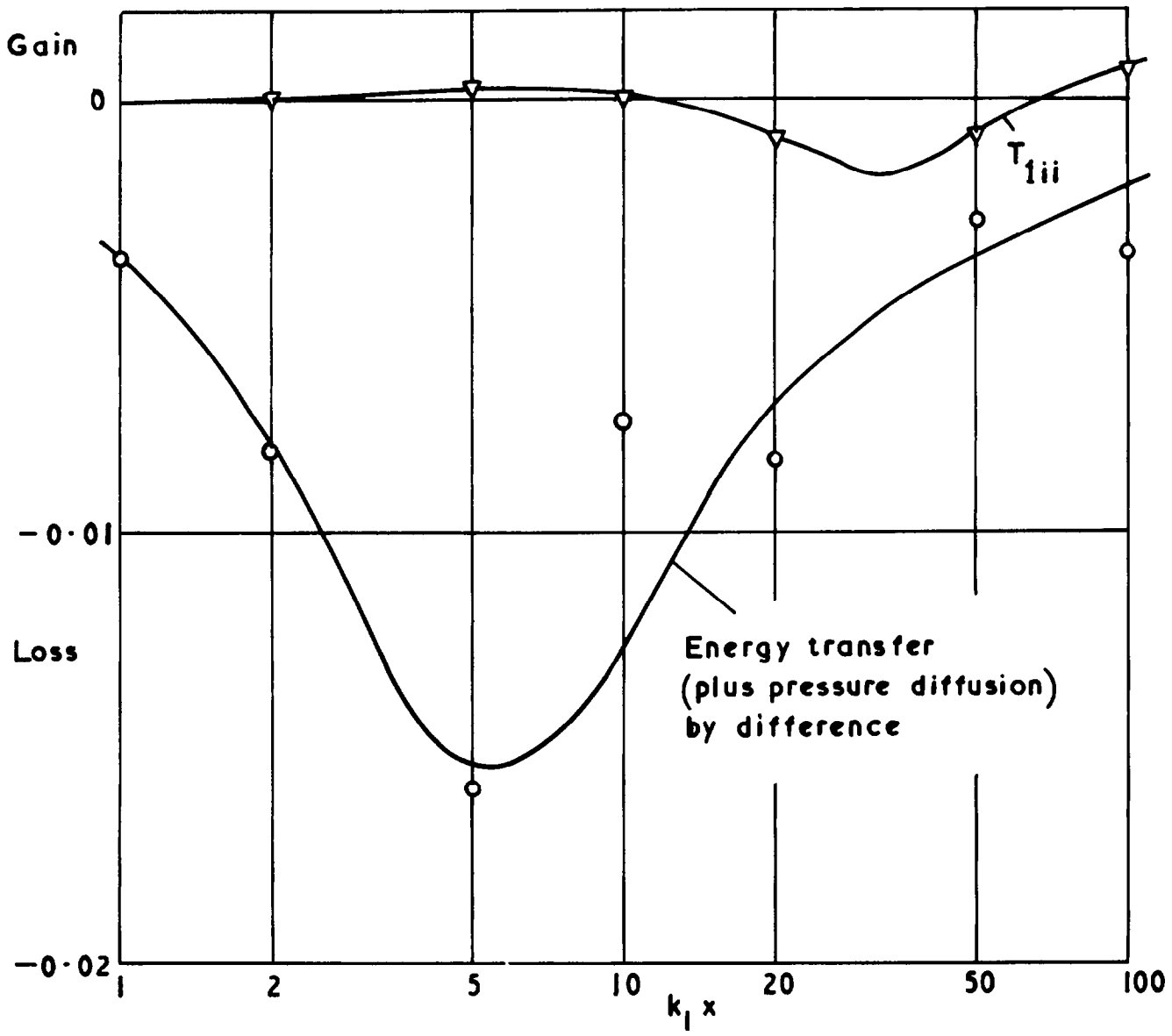

Energy transfer : $\eta = -0{\cdot}05$

26 743
FIG. 6(b)

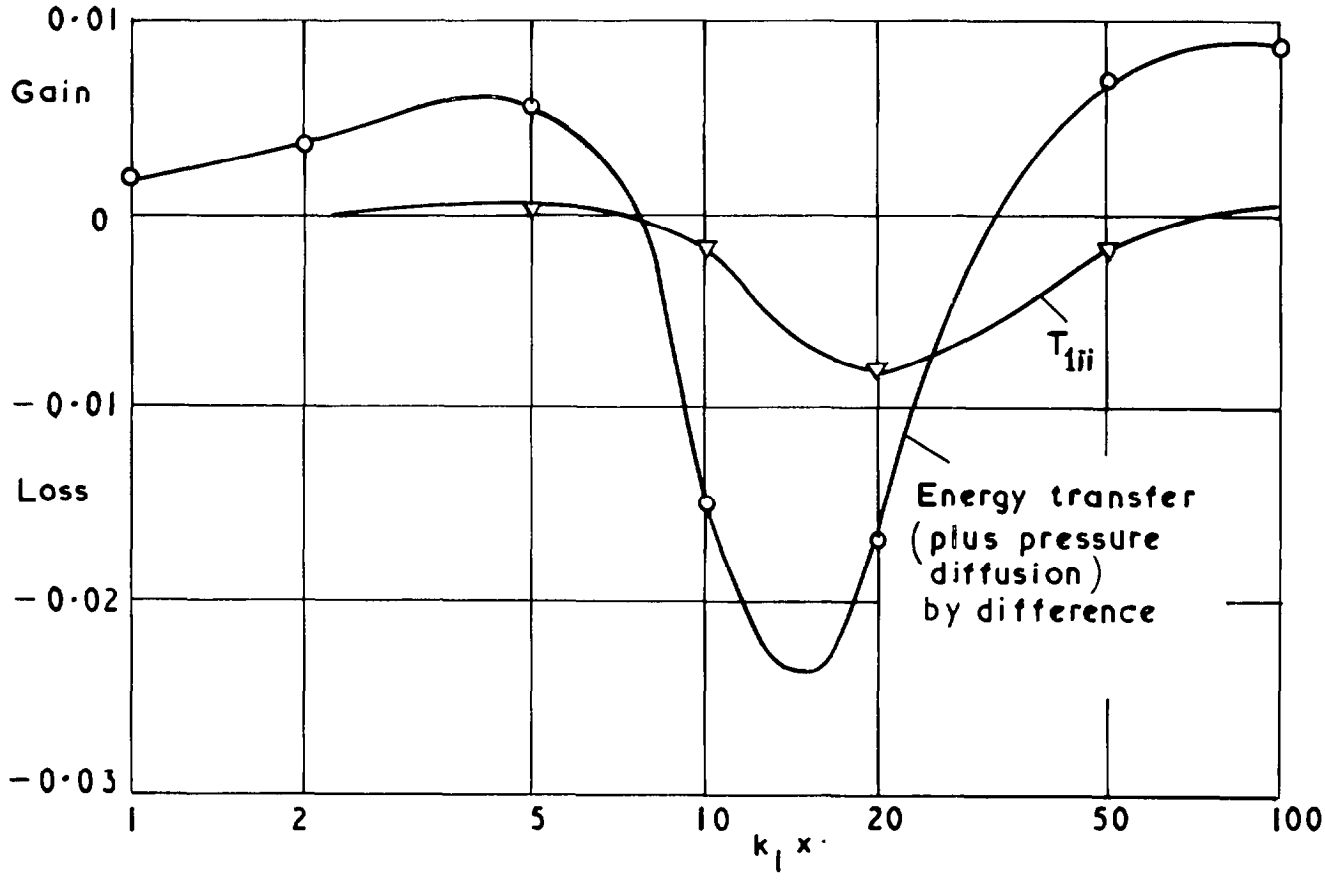

Energy transfer : $\eta = 0$

26 743
FIG. 6(d)

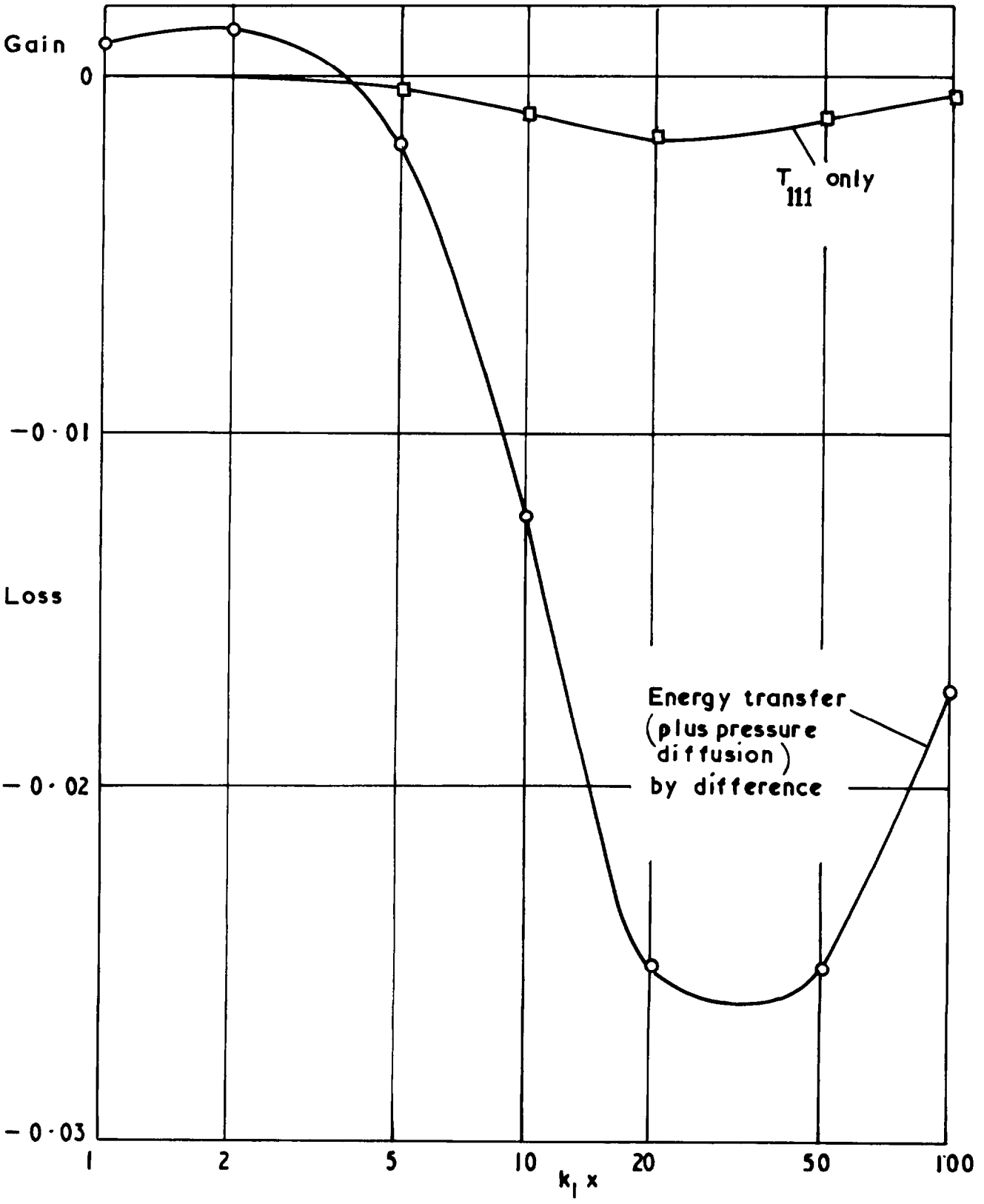

Energy transfer : $\eta = 0{\cdot}1$

26 743
FIG. 6(c)

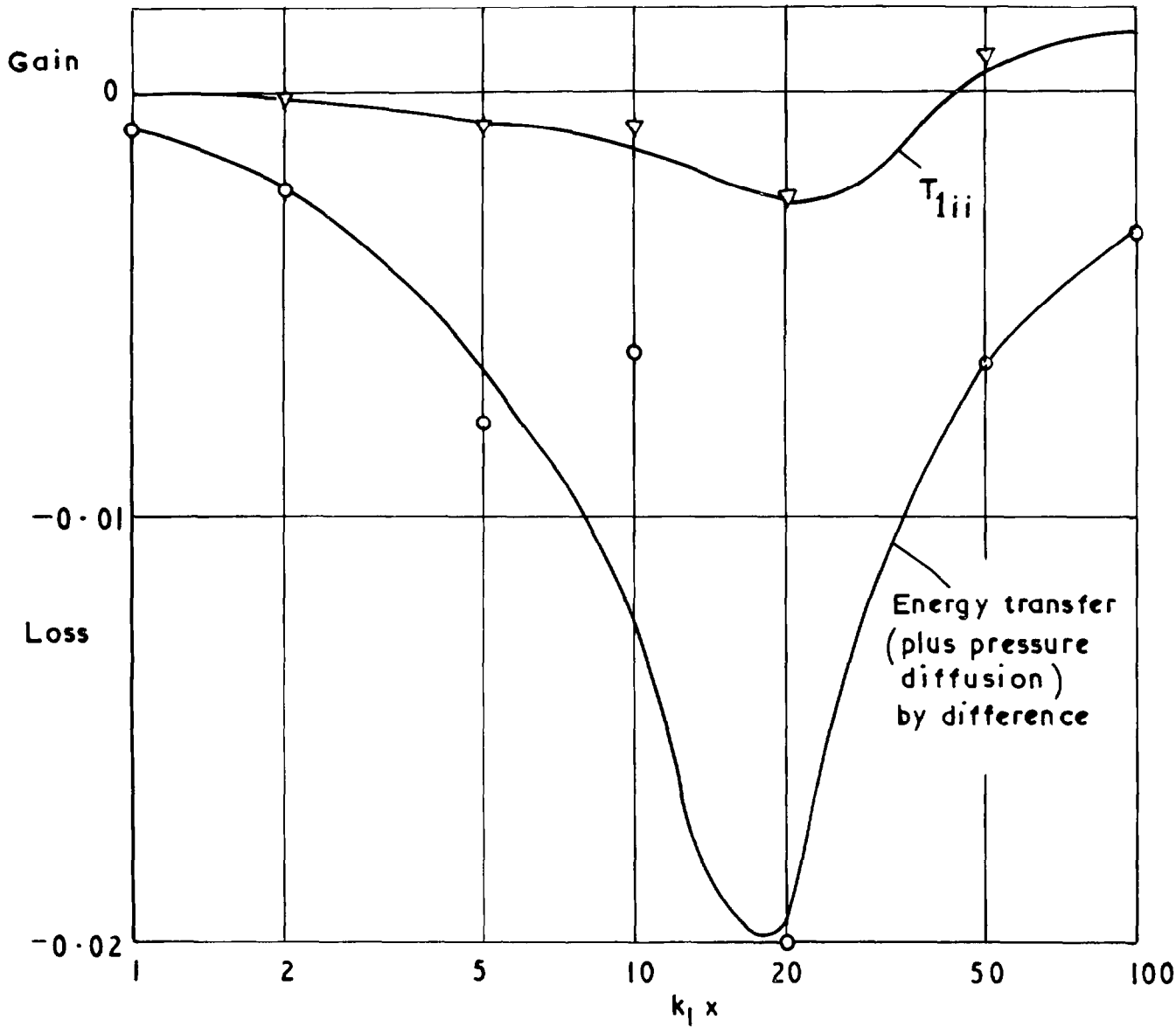

Energy transfer: $\eta = 0{\cdot}05$

26 743
FIG. 7

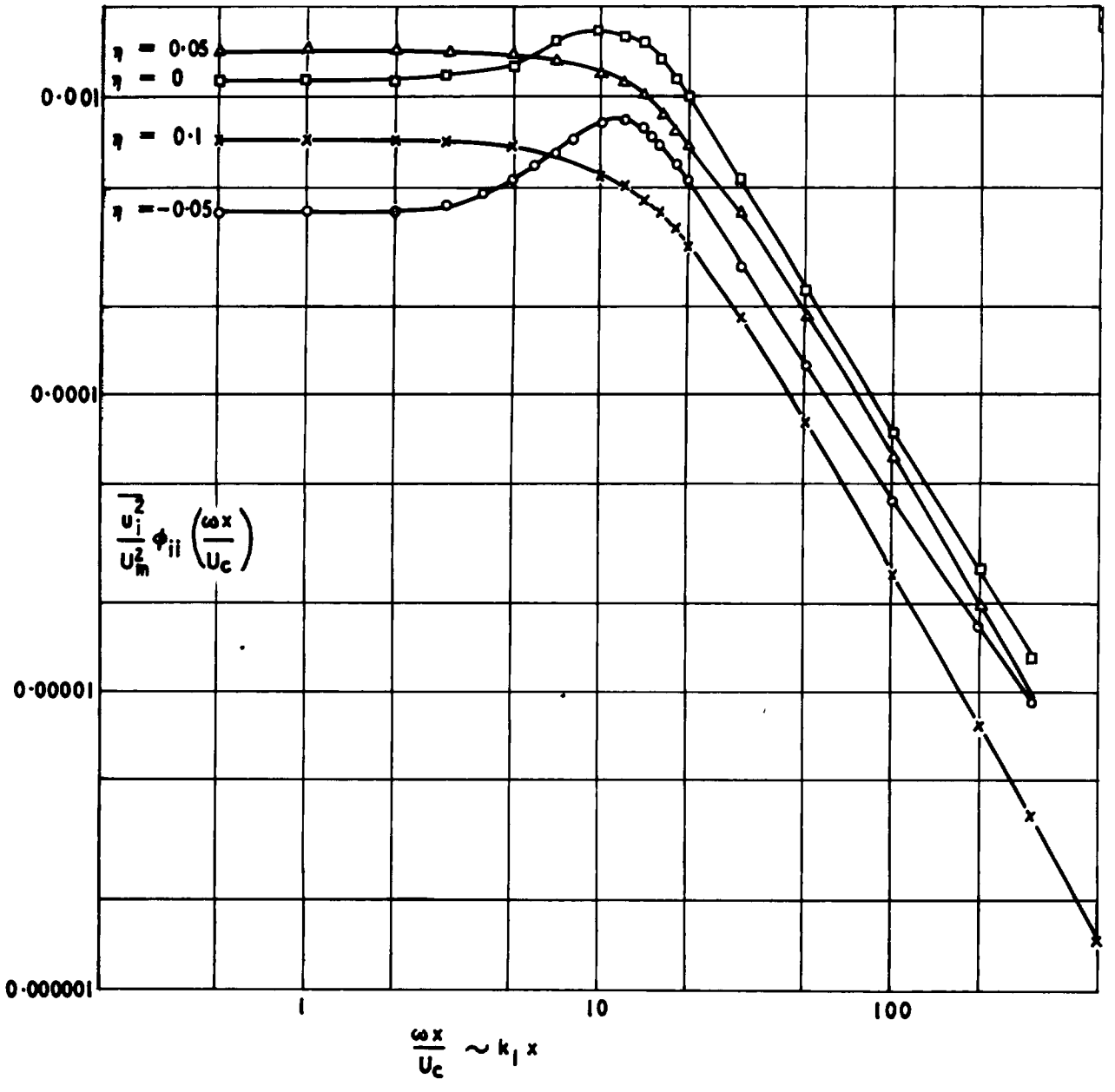

Frequency spectra of turbulent intensity $q^2 \equiv u_i^2$

26743
FIG. 6(e)

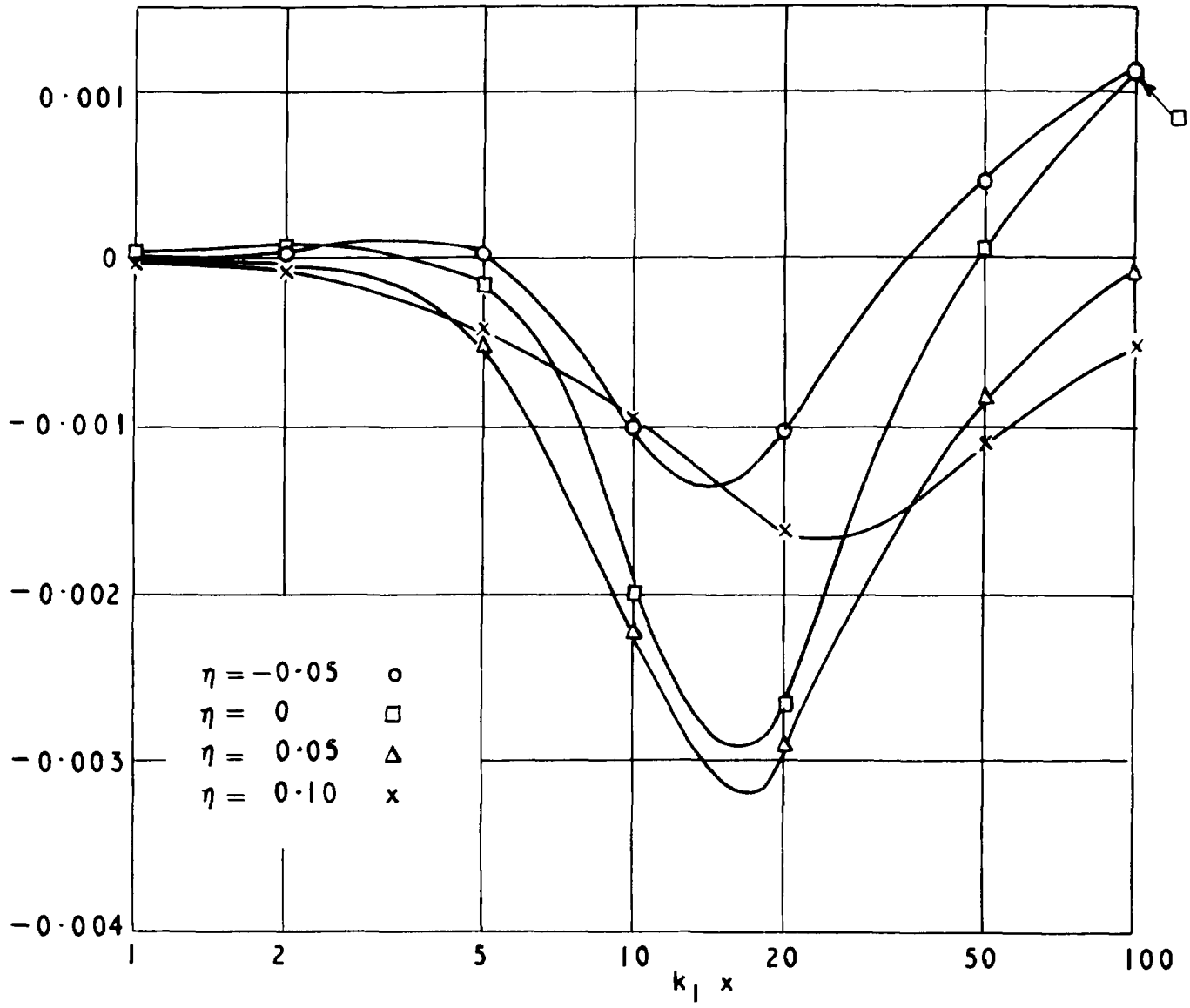

Energy transfer: T_{1ii}

26 743

FIG. 8 (a)

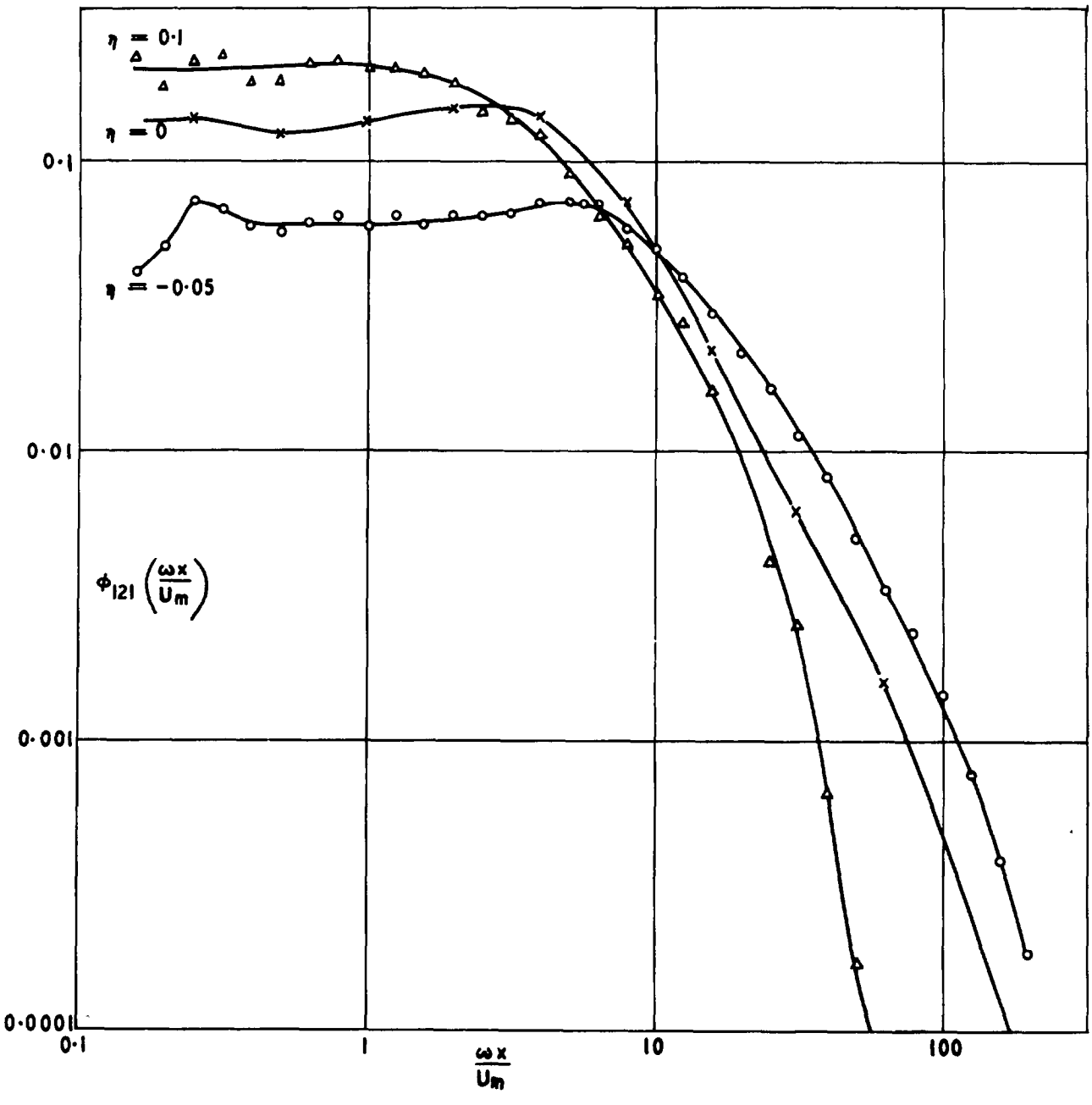

Frequency spectrum $\overline{u_1(\omega)\, u_1 u_2(\omega)}$

26 743

FIG. 8 (b)

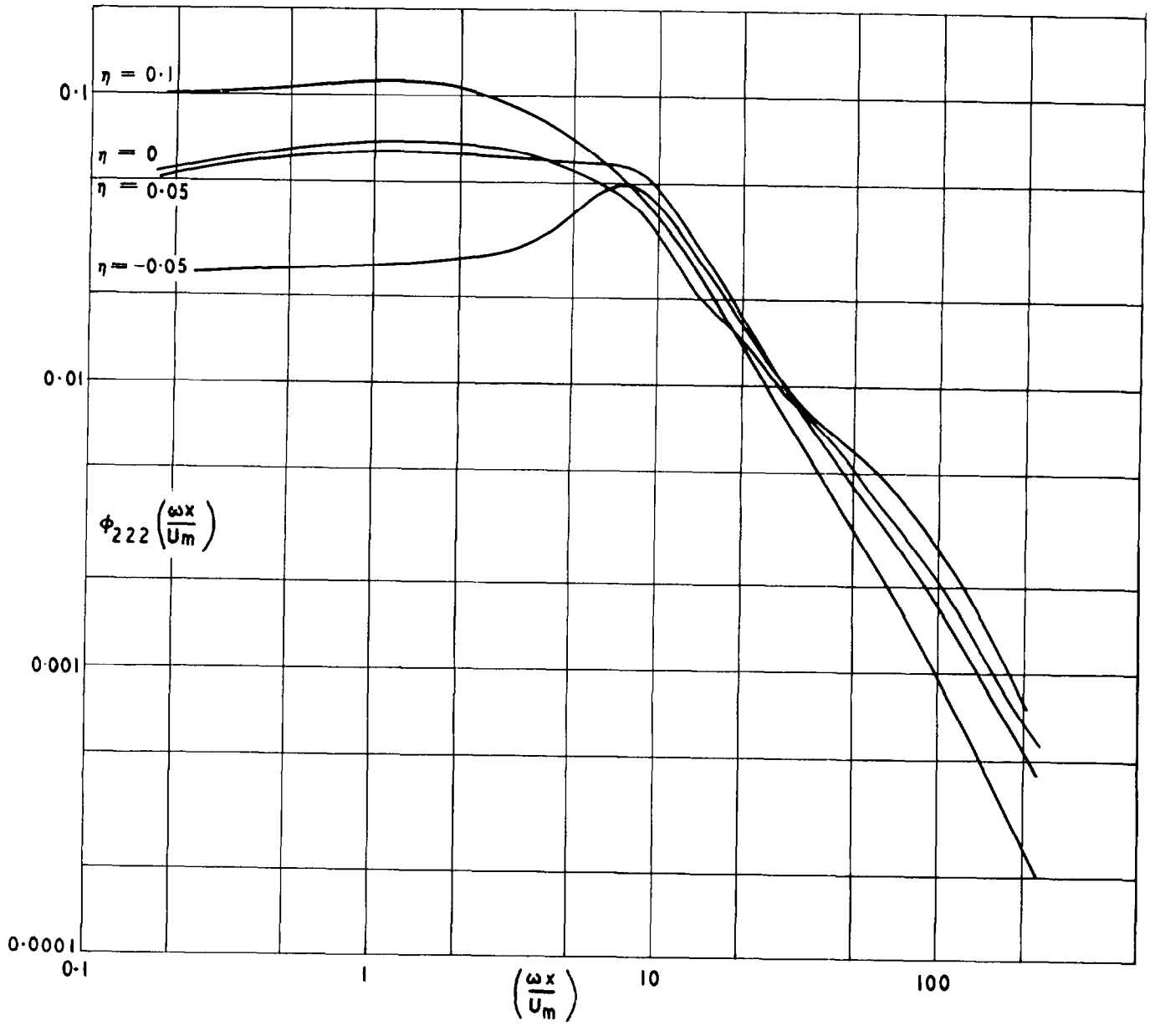

Frequency spectrum $\overline{u_2(\omega)\, u_2^2(\omega)}$

26 743

FIG. 9

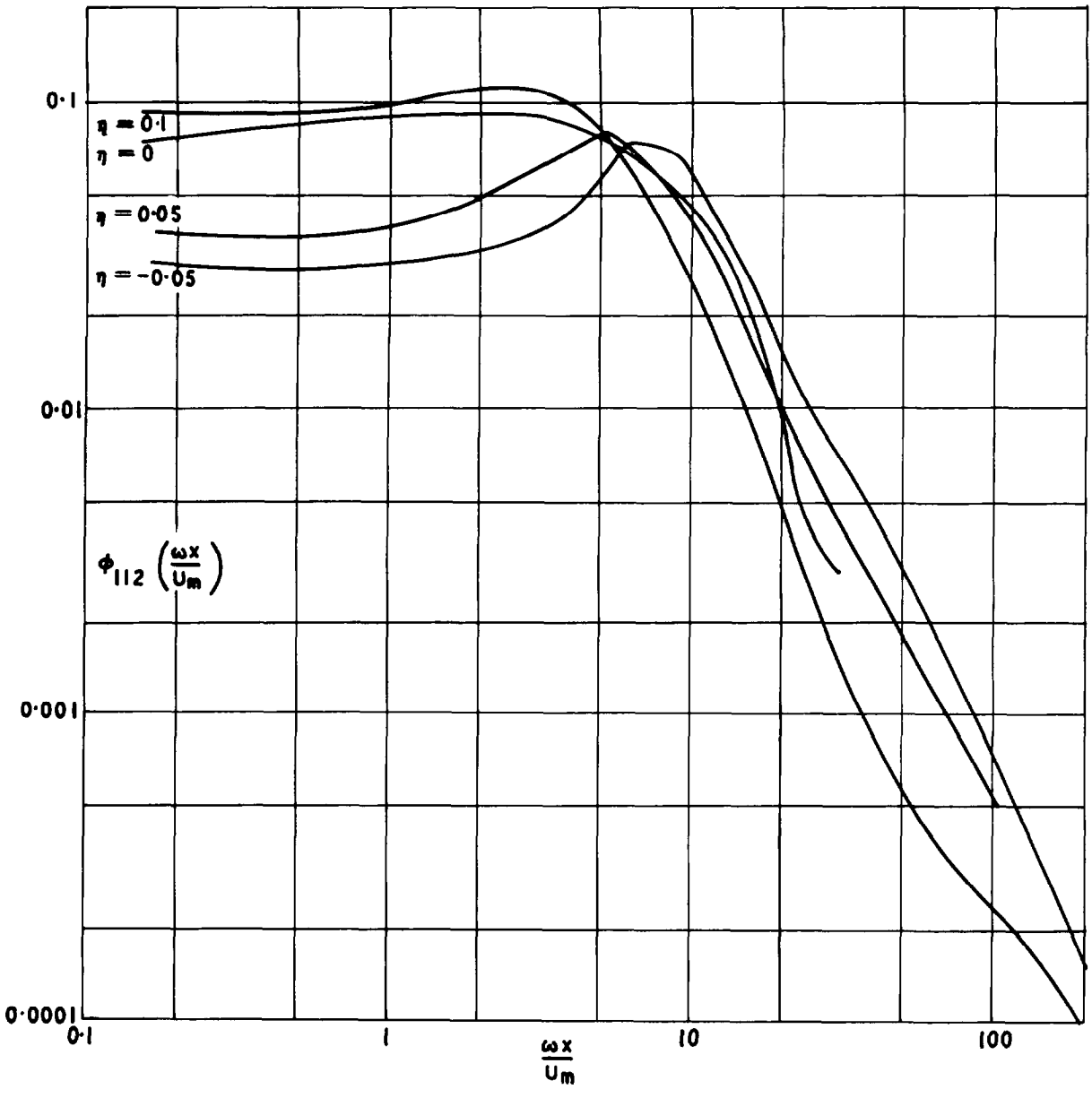

Frequency spectrum $\overline{u_1^2(\omega)\, u_2(\omega)}$

26 743
FIG.10

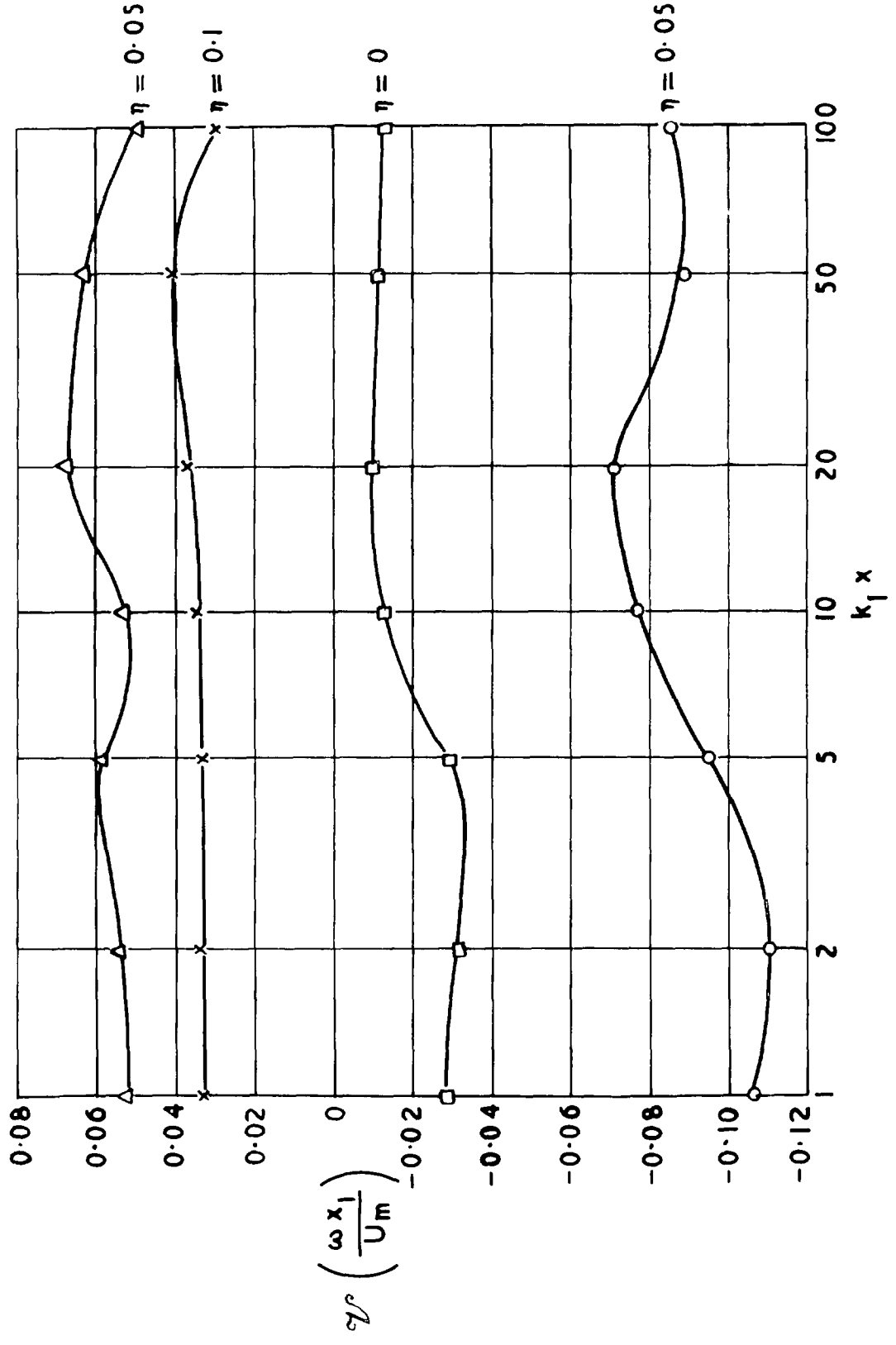

$$\frac{\mathcal{P}}{U_m} = \frac{\overline{2\,u_2^3}\,\phi_{222} + \overline{u_1^2\,u_2}\,\phi_{121}}{U_m\,\overline{u_1^2}\,\phi_{11}}$$

26 743

FIG. 11

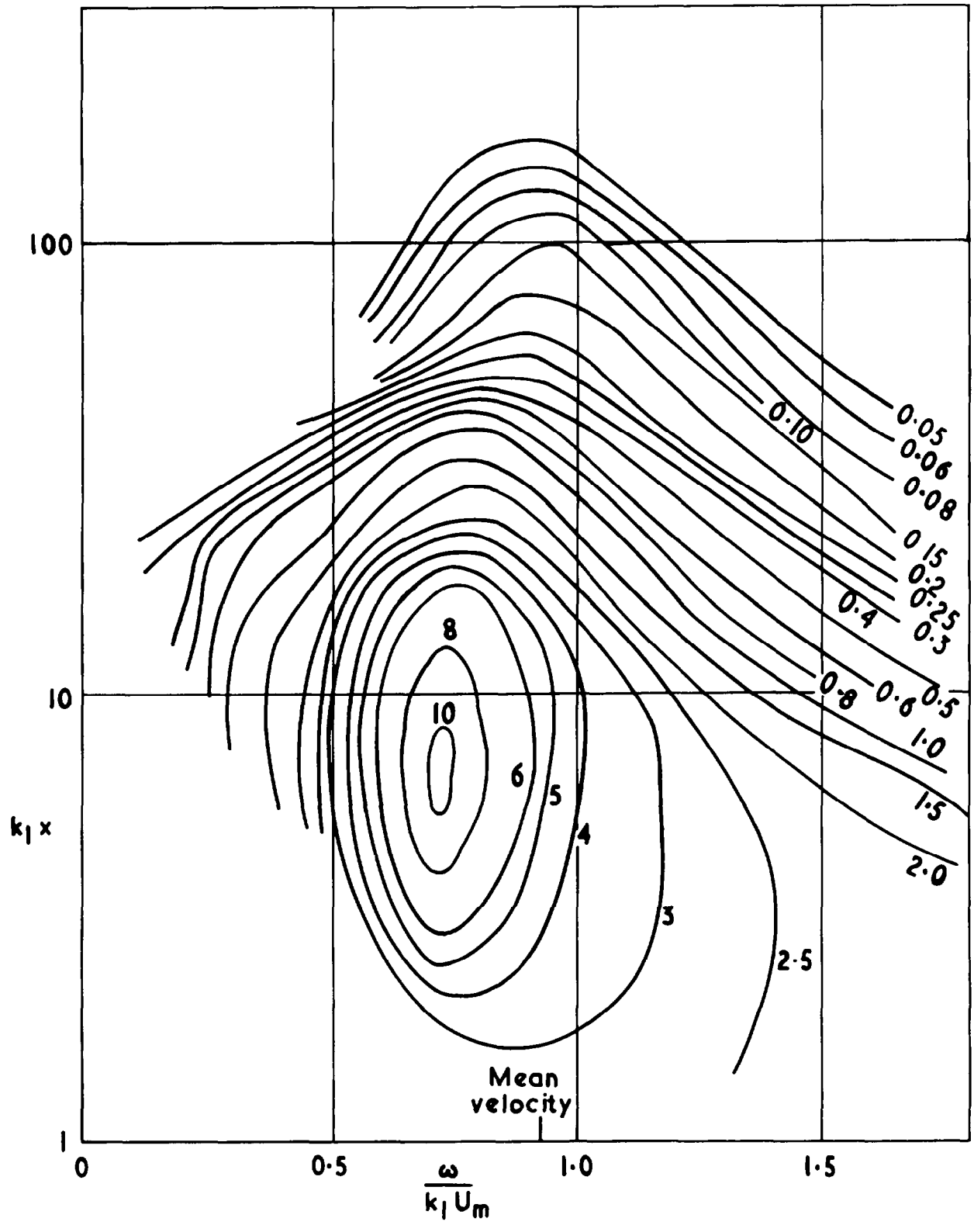

Convection velocity: Energy contours in phase-velocity / wave number plane. $\eta = -0{\cdot}05$

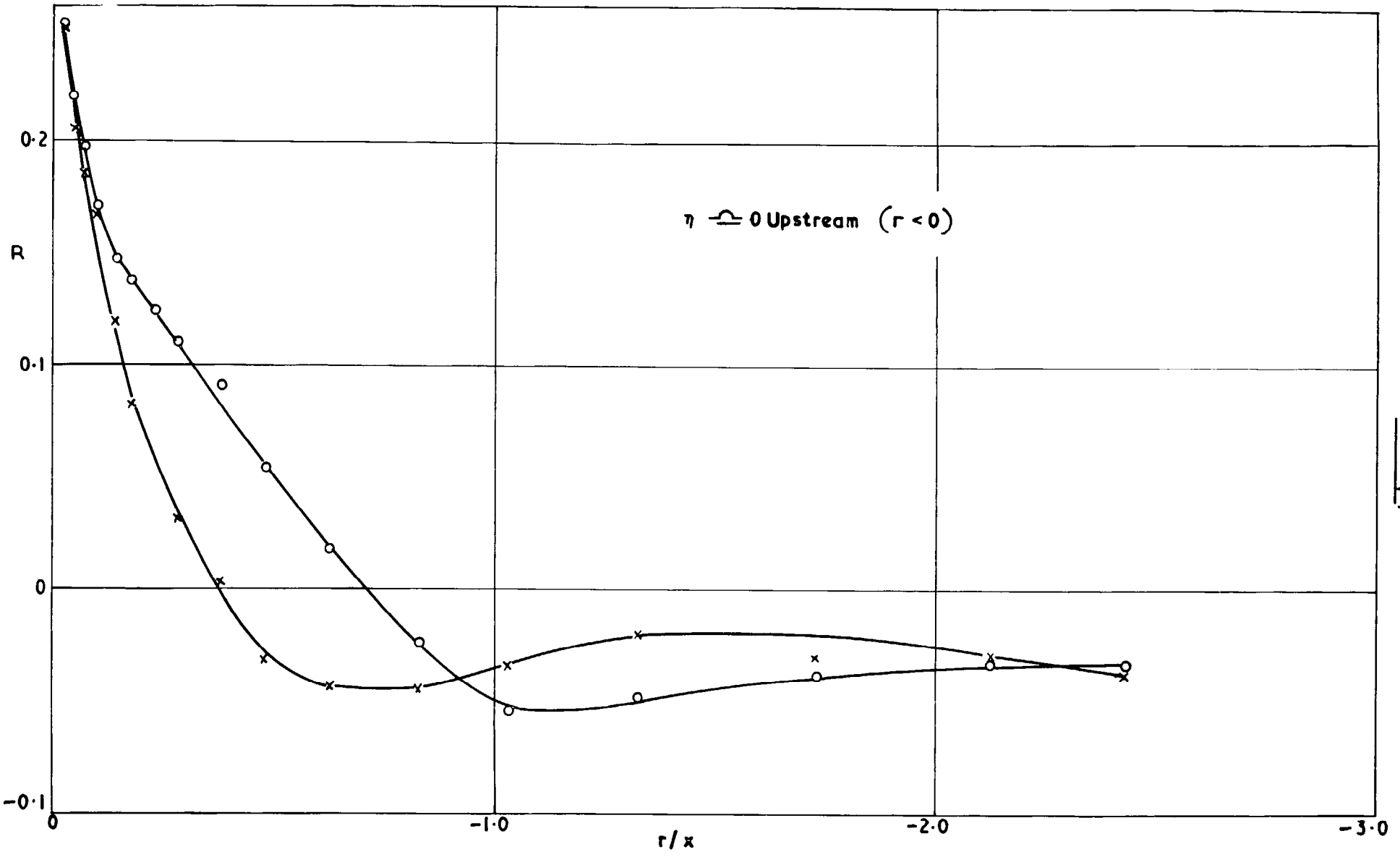

26 743
FIG. 12(a)

Correlation coefficients $R_{111} = \dfrac{\overline{u_1(o)\,u_1^2(r)}}{\sqrt{\overline{u_1^2(o)}\cdot\overline{u_1^2(r)}}}$ and $\dfrac{\overline{u_1^2(o)\,u_1(r)}}{\overline{u_1^2(o)}\cdot\sqrt{\overline{u_1^2(r)}}}$

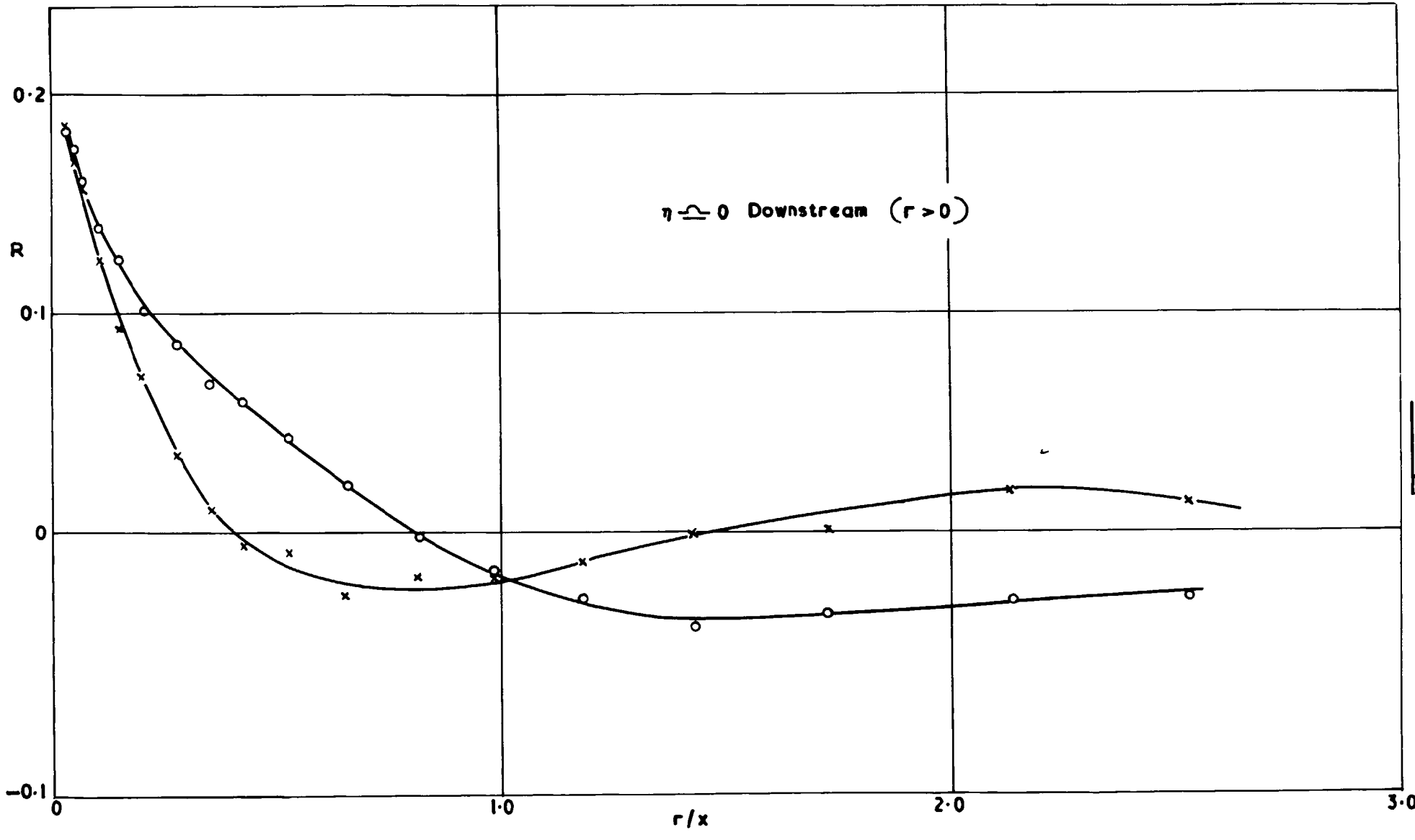

26 743
FIG.12(b)

Correlation coefficients $R_{III} = \dfrac{\overline{u_1(o)\,u_1^2(r)}}{\sqrt{\overline{u_1^2}(o).\overline{u_1^2}(r)}}$ and $\dfrac{\overline{u_1^2(o)\,u_1(r)}}{\overline{u_1^2}(o)\,\sqrt{\overline{u_1^2}(r)}}$

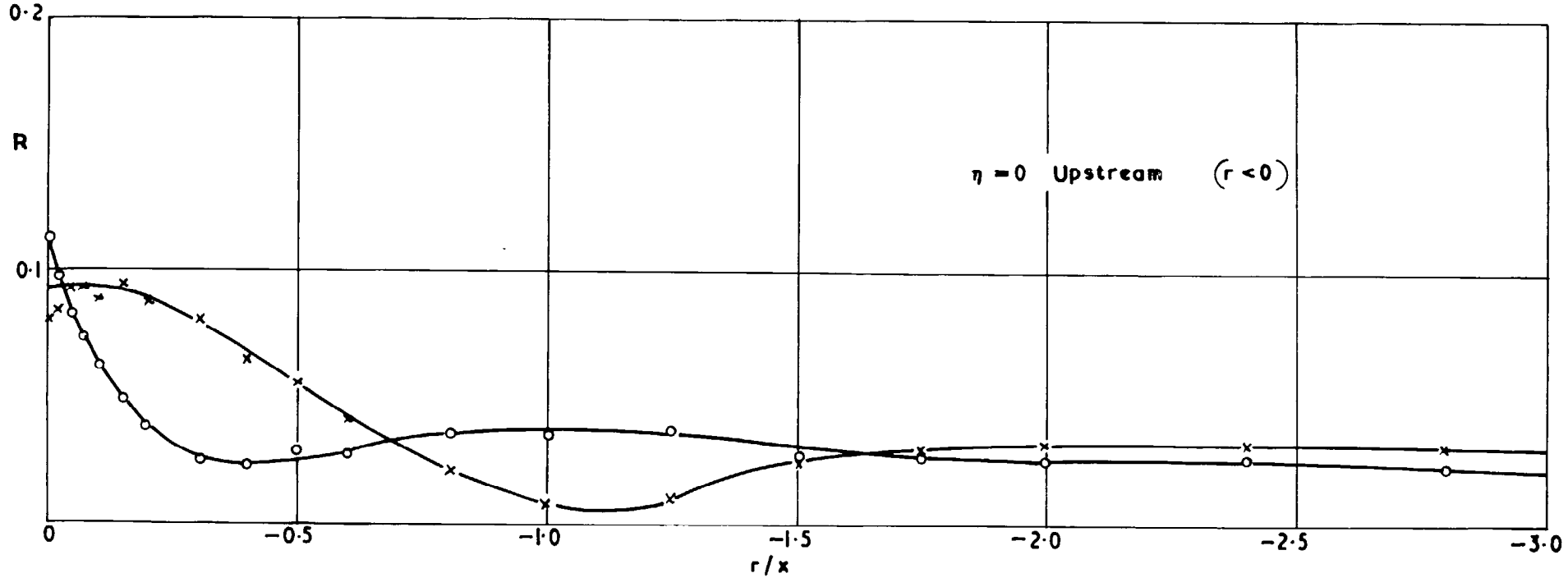

26 743
FIG.12 (c)

Correlation coefficients $R_{122} = \dfrac{\overline{u_1(o)\,u_2(o)u_2(r)}}{\sqrt{\overline{u_1^2}(o).\overline{u_2^2}(o).\overline{u_2^2}(r)}}$ and $\dfrac{\overline{u_1(r)\,u_2(o)\,u_2(r)}}{\sqrt{\overline{u_1^2}(r).\overline{u_2^2}(o).\overline{u_2^2}(r)}}$

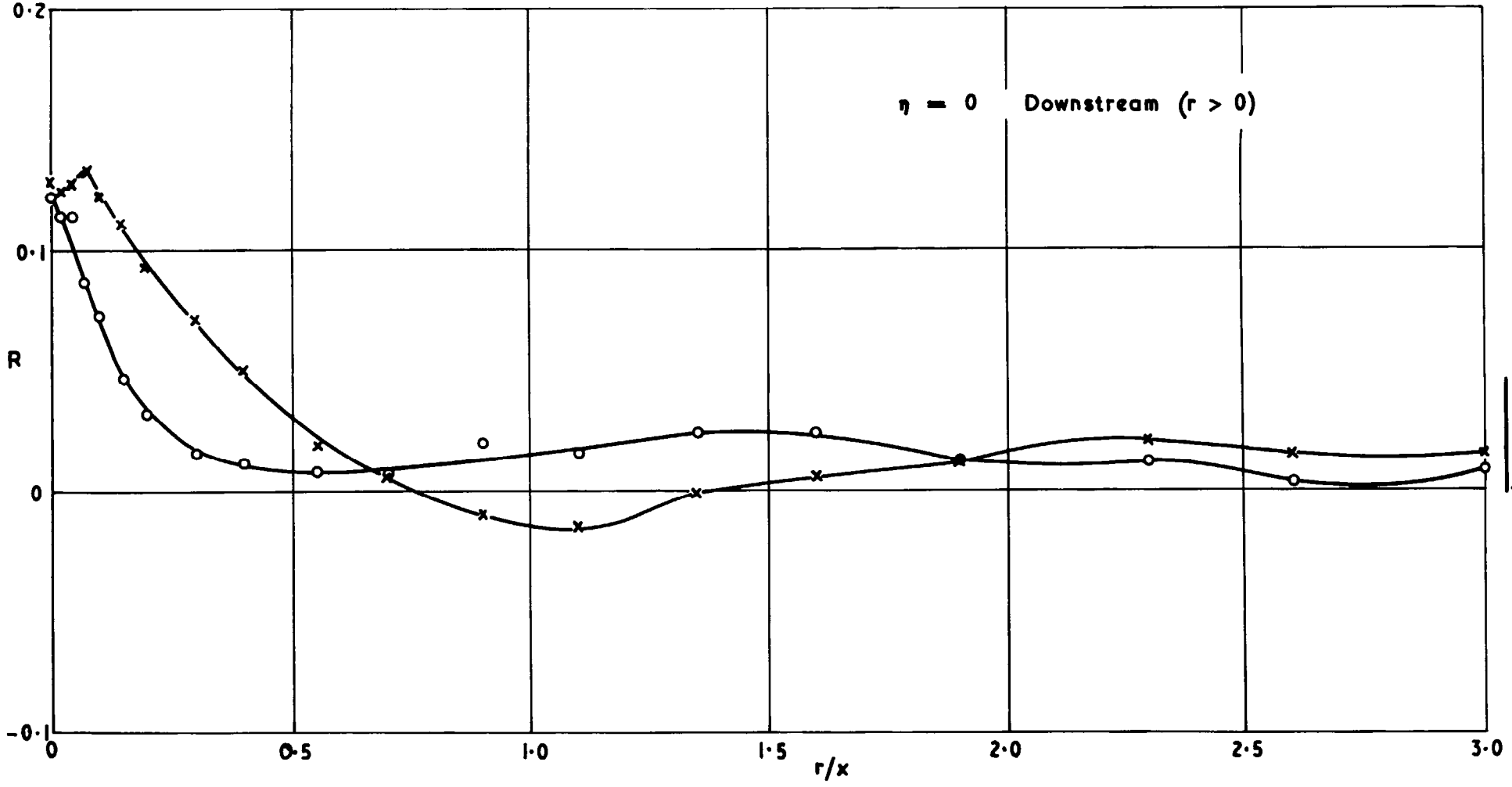

26 743
FIG. 12 (d)

Correlation coefficients $R_{122} = \dfrac{\overline{u_1(o)\,u_2(o)\,u_2(r)}}{\sqrt{\overline{u_1^2(o)}.\overline{u_2^2(o)}.\overline{u_2^2(r)}}}$ and $\dfrac{\overline{u_1(r)\,u_2(o)\,u_2(r)}}{\sqrt{\overline{u_1^2(r)}.\overline{u_2^2(o)}.\overline{u_2^2(r)}}}$

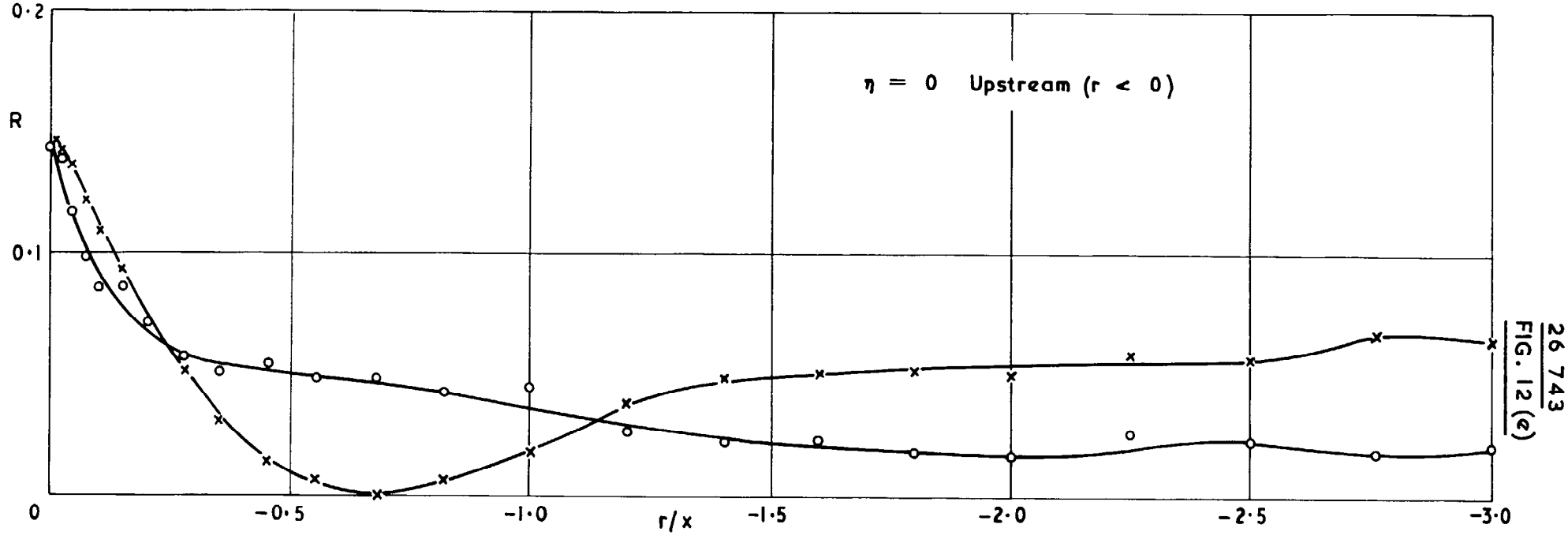

26 743
FIG. 12 (e)

Correlation coefficients $R_{133} = \dfrac{\overline{u_1(o)\,u_3(o)\,u_3(r)}}{\sqrt{\overline{u_1^2(o)}.\overline{u_3^2(o)}.\overline{u_3^2(r)}}}$ and $\dfrac{\overline{u_1(r)\,u_3(o)\,u_3(r)}}{\sqrt{\overline{u_1^2(r)}.\overline{u_3^2(o)}.\overline{u_3^2(r)}}}$

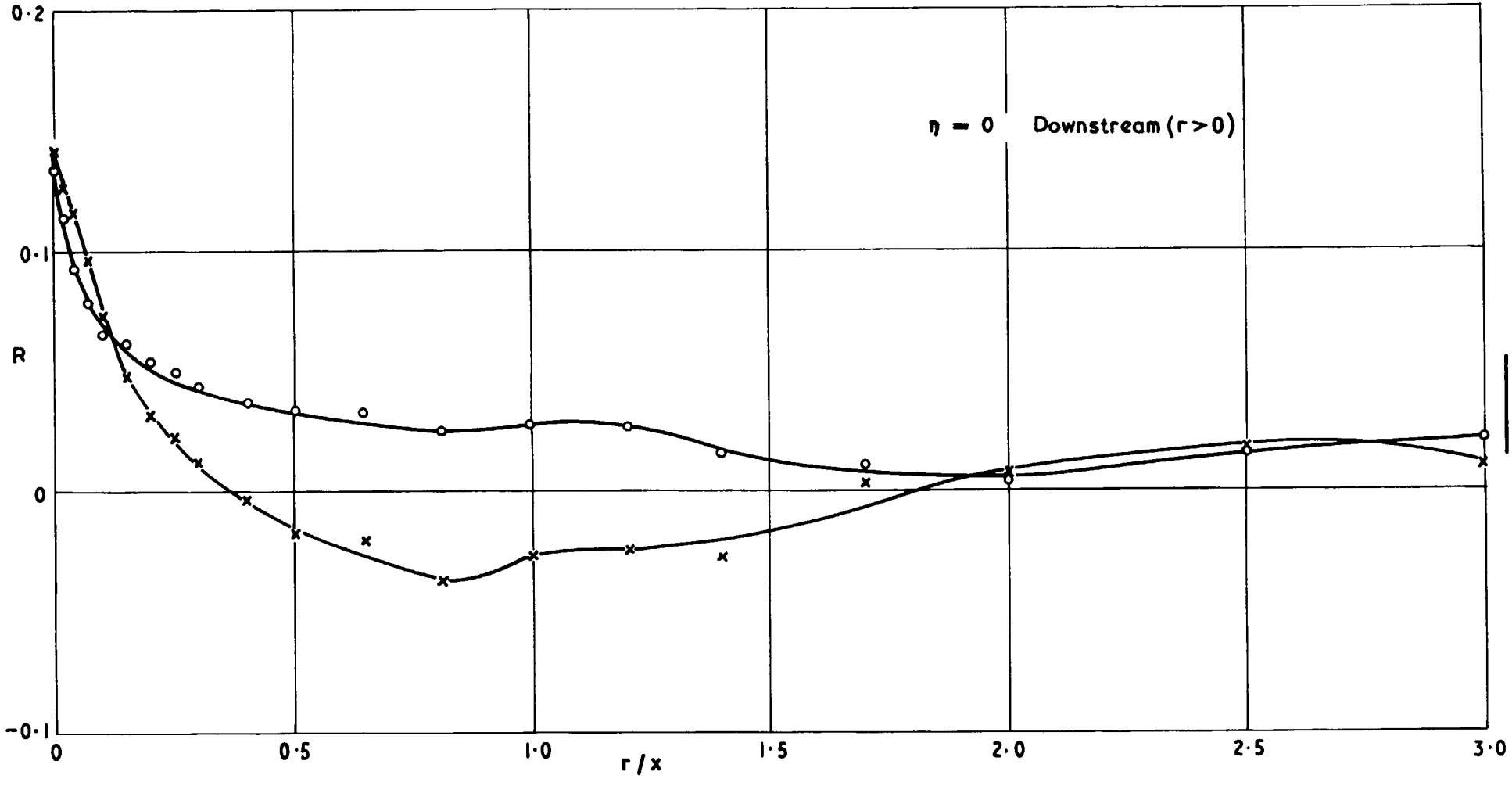

26 743
FIG. 12(f)

Correlation coefficients $R_{133} = \dfrac{\overline{u_1(o)\,u_3(o)\,u_3(r)}}{\sqrt{\overline{u_1^2(o)}.\overline{u_3^2(o)}.\overline{u_3^2(r)}}}$ and $\dfrac{\overline{u_1(r)\,u_3(o)\,u_3(r)}}{\sqrt{\overline{u_1^2(r)}.\overline{u_3^2(o)}.\overline{u_3^2(r)}}}$

A.R.C. C.P. No. 899
March, 1965
Bradshaw, P. and Ferriss, D. H.

THE SPECTRAL ENERGY BALANCE IN A TURBULENT MIXING LAYER

Measurements are presented of the spectral density of contributions to the turbulent energy balance as a function of longitudinal wave number. The energy transfer through the spectrum has been deduced, and some of its components have been measured directly: transfer in the direction of decreasing wave number occurs in some parts of the flow.

A.R.C. C.P. No. 899
March, 1965
Bradshaw, P. and Ferriss, D. H.

THE SPECTRAL ENERGY BALANCE IN A TURBULENT MIXING LAYER

Measurements are presented of the spectral density of contributions to the turbulent energy balance as a function of longitudinal wave number. The energy transfer through the spectrum has been deduced, and some of its components have been measured directly: transfer in the direction of decreasing wave number occurs in some parts of the flow.

A.R.C. C.P. No. 899
March, 1965
Bradshaw, P. and Ferriss, D. H.

THE SPECTRAL ENERGY BALANCE IN A TURBULENT MIXING LAYER

Measurements are presented of the spectral density of contributions to the turbulent energy balance as a function of longitudinal wave number. The energy transfer through the spectrum has been deduced, and some of its components have been measured directly: transfer in the direction of decreasing wave number occurs in some parts of the flow.

A.R.C. C.P. No. 899
March, 1965
Bradshaw, P. and Ferriss, D. H.

THE SPECTRAL ENERGY BALANCE IN A TURBULENT MIXING LAYER

Measurements are presented of the spectral density of contributions to the turbulent energy balance as a function of longitudinal wave number. The energy transfer through the spectrum has been deduced, and some of its components have been measured directly: transfer in the direction of decreasing wave number occurs in some parts of the flow.

DETACHABLE ABSTRACT CARDS

Printed and published by
HER MAJESTY'S STATIONERY OFFICE
To be purchased from
49 High Holborn, London W.C.1
423 Oxford Street, London W.1
13A Castle Street, Edinburgh 2
109 St. Mary Street, Cardiff
Brazennose Street, Manchester 2
50 Fairfax Street, Bristol 1
35 Smallbrook, Ringway, Birmingham 5
80 Chichester Street, Belfast 1
or through any bookseller

Printed in England

C.P. No. 899

S O Code No 23-9016-99